Biological Cycling of Carbon, Nitrogen and Silicon in Arctic and sub-Arctic Marine Waters: Insights from Phytoplankton Studies in the Laboratory and the Field

by

Brianne Kelly
B.Sc., University of Waterloo, 2005

A Thesis Submitted in Partial Fulfillment of the Requirements for the Degree of

MASTER OF SCIENCE

in the Department of Biology

Biological Cycling of Carbon, Nitrogen and Silicon in Arctic and sub-Arctic Marine Waters: Insights from Phytoplankton Studies in the Laboratory and the Field

by

Brianne Kelly
B.Sc., University of Waterloo, 2005

Supervisory Committee

Dr. Diana E. Varela, Supervisor
(Department of Biology and School of Earth and Ocean Sciences)

Dr. John Dower, Departmental Member
(Department of Biology)

Dr. Kevin Telmer, Outside Member
(School of Earth and Ocean Sciences)

Supervisory Committee

Dr. Diana E. Varela, Supervisor
(Department of Biology and School of Earth and Ocean Sciences)

Dr. John Dower, Departmental Member
(Department of Biology)

Dr. Kevin Telmer, Outside Member
(School of Earth and Ocean Sciences)

ABSTRACT

This thesis characterizes the cycling of carbon, nitrogen and silicon by marine polar diatoms through the aid of a field study and a laboratory study. Field studies were conducted along a transect from Victoria, Canada to Barrow, Alaska and particulate carbon, nitrogen and silicon, chlorophyll a, nitrate, phosphate, silicic acid, and carbon and nitrogen incorporation, along with biogenic silica net incorporation were measured. Total primary production was lowest in the NE Pacific (0.3 to 1.0 mmol m^{-3} day^{-1}), with new production contributing 17 to 38% of total production. Biogenic silica net incorporation in the upper 250 m of the water column in the NE Pacific was relatively low (0 to 0.12 mmol m^{-3} day^{-1}), but positive, indicating the opportunity for export from the euphotic zone. Total primary, new production and production by siliceous plankton was highest in the Chukchi Sea, due to the influence of nutrient influx from the Anadyr Stream. Total primary production ranged from 1.0 to 3.2 mmol m^{-3} day^{-1}, new production contributed as much as 56% of total production, and the production by siliceous phytoplankton was as high as 5.6 mmol m^{-3} day^{-1}. Siliceous biomass was usually recycled in the upper water column of the Bering and the Chukchi Seas, in contrast to the NE Pacific.

The interference of lithogenic material on the measurement of biogenic silica was explored using data from the Bering and Chukchi Seas. Results show that lithogenic interference is location specific. Sediment clay composition data should be considered when high concentrations of lithogenic silica are present.

The laboratory study examined the effects of different irradiance and temperature conditions on two polar diatom species: *Thalassiosira antarctica* and *Porosira glacialis*. Temperature and irradiance had species-specific effects on the cellular content of carbon, nitrogen and silicon. The relationship between growth rate and silicon content for *T. antarctica* showed that silicon content increased as growth rate decreased, which is in agreement with previous studies. However, this relationship did not hold for *P. glacialis* at low temperatures. These species-specific effects complicate the understanding of how environmental change will influence phytoplankton populations in Arctic and sub-Arctic marine areas.

In general, primary production was lower in the Bering and Chukchi Seas when compared to previous studies, however it is unknown whether differences are due to interannual variability or a trend of decreasing production. Data from both the field and laboratory component indicate a high amount of biological silicon cycling in polar environments. This study represents the first time net silicon incorporation has been measured as far north as the Chukchi Sea.

TABLE OF CONTENTS

LIST OF TABLES

LIST OF FIGURES

ACKNOWLEDGEMENTS

I would like to acknowledge my supervisor, Dr. Diana Varela for her guidance and support as well as financial funding (NSERC Discovery grant). I would also like to acknowledge my committee members Dr. John Dower and Dr. Kevin Telmer for their support and expertise. My lab mates Damian, Emma, Ian, and Valeria were instrumental in their assistance, as well as our lab technician, Samantha Robbins. The University of Victoria Outdoor Aquatics Facility, specifically Michael James, Simon Grant and Brian Ringwood, were enormously helpful with my laboratory experiments. The Biology Department at the University of Victoria provided me with funding in the form of a fellowship, scholarships, teaching assistant positions and income supplements.

My field work would not have been conducted without the support and help of the Institute of Ocean Sciences, specifically Eddy Carmack and the captain and crew of the Sir Wilfrid Laurier CCGS. The work which supplied me with temperature and salinity data for Chapter 3 was conducted as part of the Canada/US/Japan Joint Western Arctic Climate Study program, funded by Fisheries and Oceans Canada, the U.S. National Science Foundation and the Japan Agency for Marine-Earth Science and Technology. Program leaders were E.C. Carmack and F. McLaughlin from the Institute of Ocean Sciences, Fisheries and Oceans Canada, Sidney, B.C., co coordinator for the Laurier science program was B. van Hardenberg, shipboard chief scientists were W. Williams and J. Nelson, and data were processed by G. Gatien.

And of course I could not have completed this thesis without my mother, Marianne Kelly, and the support of my family and friends, specifically my roommate, Chloeann Golinsky.

Chapter 1
Introduction

Marine phytoplankton play an important role in biogeochemical cycling. Phytoplankton have such a strong connection to nutrient cycling in the ocean, that average dissolved nutrient concentrations in ocean bottom waters have been found to be the same as phytoplankton average cellular composition (carbon:nitrogen:phosphorus 106:16:1) (Redfield, 1958). This relationship between phytoplankton cellular quotas and deep ocean chemistry is generally agreed upon in the oceanographic community, and yet no one has been able to provide the biological basis for this ratio (Falkowski, 2000). Many deviations from this ratio exist in phytoplankton communities in the surface of the ocean, depending on the location of the community and the environmental variables to which the community is exposed (e.g. Franck et al., 2000; Hutchins and Bruland, 1998; Takeda, 1998). These deviations are important for regional nutrient cycling and can provide us with information for the biological basis of these nutrient ratios.

The objective of this chapter is to serve as an introduction for the topics discussed in this thesis. The macronutrients carbon, nitrogen and silicon will be introduced and background information on the most important taxonomic group responsible for biological silicon cycling (the diatoms) will be provided. Two important environmental factors affecting diatom production will be introduced: irradiance and temperature. The cycling of the macronutrients carbon, nitrogen and silicon in the Northeastern Pacific Ocean and Bering and Chukchi Seas, and the hydrography of these regions will be briefly described.

1.1 Diatom Physiology

1.1.1 Nutrient Requirements and Stoichiometry

In 1958, Alfred C. Redfield published a paper detailing how, on average, deep sea water chemistry matched the nutrient stoichiometry of phytoplankton living in surface waters. This average ratio of carbon:nitrogen:phosphorus (C:N:P) equaling 106:16:1 became a canonical value referred to as the Redfield ratio and has since shaped much of marine biogeochemical research. In 1985, Brzezinski published a paper expanding the Redfield ratio to include silicon (Si) values from laboratory cultures of diatoms. The relationship of Si to the Redfield ratio was found to be 106:16:15:1 (C:N:Si:P) (Brzezinski, 1985). However, since the Redfield ratio is an average, there is wide variation in the world oceans due to different environmental conditions (Redfield, 1958; Sambrotto et al., 1993). For example, under iron limiting conditions, the silicate:nitrate uptake ratio is higher then under iron replete conditions (Hutchins and Bruland, 1998; Takeda, 1998). Iron limitation can lead to more heavily silicified frustules in diatom populations (Hutchins and Bruland, 1998), while an addition of iron to iron limited areas can increase the rate of nitrate uptake (Franck et al., 2000). Deviations from the Redfield ratio are a point of interest when studying an ecosystem as they can provide clues to the metabolic processes of phytoplankton community members.

The nutrients included in the Redfield/Brzezinski ratio are important macronutrients for diatoms. Nitrogen, in the form of nitrate, ammonium or urea, can become a limiting factor for the growth of diatoms in the marine environment (e.g. Ryther and Dunstan, 1971). Nitrogen is used by diatoms mainly as a component of nucleic acids and proteins (Geider and Laroche, 2002). Nitrate (NO_3^-) is especially useful

as an indicator in phytoplankton studies as it is a 'new' nutrient; it enters an ecosystem from "outside", either through upwelling, lateral or vertical advection, etc. Nitrate uptake is used to estimate new production, which represents the amount of primary production that is available to sink out of the euphotic zone and contribute to carbon sequestration in deep waters, or transfer up the food web over time scales of a season or longer (Dugdale and Goering, 1967). Accurate knowledge of the amount and distribution of NO_3^- in the natural environment, coupled with quantification of its uptake rate by phytoplankton can help characterize nutrient cycling and energy pathways in a given system.

Silicic acid ($Si(OH)_4$) is another macronutrient which can be used to elucidate nutrient cycling in an ecosystem. This nutrient is used by diatoms to construct their frustules, although a significant portion (up to 70%) of the $Si(OH)_4$ which is taken up by diatoms can be stored intracellularly (Martin-Jezequel et al., 2000). Silicic acid can be considered a new nutrient, or a recycled nutrient (Brzezinski et al., 2003), as $Si(OH)_4$ may be supplied to a system from the outside, or may be recycled back to its dissolved form through remineralization (i.e. dissolution) within a system. A higher proportion of biogenic silica (BSi), in the form of diatom frustules, sinks out of the water column than particulate carbon (PC) or particulate nitrogen (PN). This is due to a difference in regeneration mechanisms between BSi (see section 1.2.1) and PC and PN. Higher sinking rates of BSi out of the euphotic zone compared to PC and PN can influence phytoplankton community dynamics by causing the drawdown of $Si(OH)_4$ in surface waters to concentrations limiting to diatoms (Dugdale et al., 1995).

The profound affect that phytoplankton have on nutrient cycling in the marine environment necessitates a better understanding of their physiology in order to elucidate

marine biogeochemical cycles. Determining the effect of different environmental variables on the uptake of nutrients by phytoplankton and deviations from the Redfield ratio is one approach to understanding marine nutrient cycles. The following section introduces two environmental variables and the way in which they influence diatom physiology.

1.1.2 Effects of Temperature and Irradiance on Diatom Physiology

Temperature and irradiance are two environmental factors that can influence the growth rate and nutrient stoichiometry of marine diatoms (e.g. Mortain-Bertrand, 1989; Suzuki and Takahashi, 1995). Low irradiance can limit phytoplankton growth (e.g. Boyd et al., 1999; Mortain-Bertrand 1989), however high irradiance can photoinhibit phytoplankton growth (e.g. Hoffman et al., 2007). In addition to the irradiance level, phytoplankton are also affected by factors such as day length and irradiance fluctuations (e.g. Mortain-Bertrand, 1989).

Temperature is a major factor influencing phytoplankton photosynthesis (Raven and Geider, 1988) and affects the rate of growth of phytoplankton in marine environments (Eppley, 1972). The relationship between diatom growth rates and temperature has been demonstrated by Suzuki and Takahashi (1995) who measured the growth rates of eight diatom species from temperate and polar regions over the entire temperature range of each species. Growth rates increased with increasing temperature up to a maximum point, after which the growth rate decreased until it ceased completely. The effect of temperature on phytoplankton growth rates (Berges et al., 2002) can limit the distribution of diatom species and may ultimately affect community composition in a given environment (Suzuki and Takahashi, 1995).

Temperature and irradiance also affect the nutrient stoichiometry of diatom cells (e.g. Thompson, 1999). Carbon, silicon and chlorophyll *a* (chl *a*) cellular quotas change with temperature, whereas nitrogen quotas usually do not (e.g. Furnas, 1978; Berges et al., 2002). Irradiance mainly has an effect on chl *a* concentrations in phytoplankton. For example, diatoms will adjust cellular concentrations of phytopigments to adapt to low light levels (e.g. Beardall and Morris, 1976). However irradiance can indirectly affect other cellular quotas, such as BSi concentrations, which are affected by a change in growth rate resulting from a change in irradiance (Martin-Jezequel et al., 2000).

Phytoplankton species respond differently to changes in environmental conditions. This was described by Hutchinson in 1961 and is termed 'the paradox of the phytoplankton'. In order for a number of species with similar physiological requirements to survive in the same environment without succumbing to predictions inspired by the principle of competitive exclusion (Hardin, 1960), each species must be competitively superior under a given set of environmental conditions; however, as conditions fluctuate, the superiority of any one species does not lead to the local extinction of any other species. Thus changes in temperature and irradiance will have varying affects on different species of phytoplankton.

In chapter four of this thesis, the combined effect of irradiance and temperature are discussed for two ecologically important diatom species from polar regions, *Thalassiosira antarctica* and *Porosira glacialis*. Both species are capable of forming large blooms in polar environments (von Quillfeldt, 2000) and have been used as palaeoindicators (e.g. Maddison et al., 2006). As temperatures in Arctic waters warm (e.g. Karcher et al., 2003; Johannessen et al., 2004) and ice levels decrease (e.g. Serreze

et al., 2003), the composition of the phytoplankton communities could change as individual species best adapted to the new environmental conditions out-compete others. Nutrient cycling by phytoplankton may change depending on the nutrient stoichiometry of newly successful species. Chapter four will address species-specific cellular stoichiometry differences and possible ecological implications.

1.2 Nutrient Cycling

1.2.1 Silicon Cycling

Silicon is delivered to the ocean in the form of silicate minerals via rivers, hydrothermal vents and aeolian transport. The concentration of the dissolved form of silicon, $Si(OH)_4$), is thought to remain constant on time scales of ~10,000 years, but may vary over longer periods of time (Basile-Doeslch, 2005). Net inputs of Si into the world's oceans are estimated at 6.1 ± 2.0 Tmol yr^{-1} (Treguer et al., 1995). The average $Si(OH)_4$ concentration in the ocean is approximately 70 μmol L^{-1}, however it can range from <2 μM in oligotrophic gyres to as high as 100 μmol L^{-1} in the Southern Ocean (Treguer et al., 1995). The major Si sink from the oceans consists of deposition and diagenesis of biosiliceous material and is estimated at 7.1 ± 1.8 Tmol yr^{-1} (Treguer et al., 1995). The amount of Si present in the ocean is estimated at 10^{17} mol (Treguer, 1995). As a global average, approximately 3% of BSi produced in surface waters is preserved through sedimentation. However, rates of preservation differ regionally with higher rates occurring at high latitudes (Treguer et al., 1995). Although quantitative estimates are continually being revised, it is thought that in general the inputs and outputs of Si in the

marine cycle are balanced (DeMaster, 2002). More detailed estimates of Si cycling on a regional scale will help to better constrain our knowledge of the Si budget.

Diatoms, radiolarians, sponges, silicoflagellates and ebriids all incorporate Si into their shells, although diatoms dominate the biological cycling of Si in marine environments (Nelson et al., 1995). Diatoms have an absolute requirement for silicon (Lewin, 1962) and incorporate silicon into their frustules (their shells) as hydrated amorphous silica ($Si_nO_{2n-(nx/2)}(OH)_{nx}$) (Martin-Jezequel et al., 2000). As a result, diatom production can be limited in areas of the ocean that have low $Si(OH)_4$ concentrations. Diatoms are important members of the phytoplankton community due to their abundance, influence on nutrient cycles (Nelson et al., 1995), and as food for higher trophic levels (Fry and Wainright, 1991). In the marine environment diatoms are capable of growing in large aggregates (e.g. Kiorboe et al., 1998) and outcompeting other phytoplankton taxa for nutrients under certain conditions. Diatoms are strong competitors when concentrations of nitrate, silicic acid and iron are high (Bruland et al., 2001), which is usually at the beginning of the growing season in the spring.

Silicic acid is under-saturated in sea water (Lewin, 1961) and the basic pH of seawater is slightly corrosive to BSi (Martin-Jezequel et al., 2000). The rate of the physico-chemical dissolution of exposed BSi is temperature dependent (Kamatani, 1982; Kamatani and Riley, 1979); however, diatoms produce an organic coating which covers their frustules, and protects them from dissolution (Lewin, 1961). Bacteria actively attack and degrade this coating in lysed diatom cells, exposing the BSi to the corrosive effects of saltwater and facilitating the dissolution of diatom frustules (Bidle and Azam, 2001; Bidle and Azam, 1999). Bacterial metabolism is influenced by temperature, therefore

lower bacterial metabolic rates in colder environments diminishes the degradation of the organic coating and dissolution of frustules, facilitating preservation (Bidle et al., 2002). The temperature dependence of bacterial metabolism can explain the higher preservation rates of BSi in sediments of cold water regions such as polar and sub-polar environments (Bidle et al., 2002).

The magnitude of BSi production and dissolution can differ by 10-fold between regions, indicating a large degree of variability in surface water Si cycling (Brzezinski et al., 2003). Few studies have been conducted on BSi in the NE Pacific Ocean or Bering and Chukchi Seas; these areas will be the focus of the field work reported in Chapters 2 and 3 of this thesis.

1.2.2 Nitrogen Cycling

Various aspects of the marine nitrogen (N) cycle have been studied intensely and a number of reviews have been written summarizing our current knowledge (e.g. Codispoti et al., 2001; Herbert, 1999; Hulth et al., 2005; Ward, 2000; Zehr and Ward, 2002). Nitrogen is available for uptake in the water column in the forms of NO_3^-, nitrite, urea and ammonia. Since Martin and Fitzwater published their seminal paper in 1988 on high nitrate low chlorophyll (HNLC) areas being limited by iron, the relationship between iron availability and nitrate uptake has been more intensively studied (e.g. Hutchins and Bruland, 1998; Takeda, 1998). Nitrogen is supplied to the ocean through atmospheric deposition, riverine flow and biological fixation of dissolved N_2, and is removed through denitrification, gaseous evasion, sedimentation, and biomass harvest. The biological cycling of N differs from Si in that N is transferred up the food web, whereas Si is not (Dugdale et al., 1995).

1.2.3 Carbon Cycling

Carbon cycles through all living organisms, including marine phytoplankton. Autotrophic phytoplankton take up dissolved carbon dioxide (CO_2) and convert it into organic carbon. This organic carbon can be transferred up the food web, remineralized by bacteria in the water column or buried in marine sediments. The uptake of C by phytoplankton has received a great deal of attention for the way in which high uptake rates of C by phytoplankton can draw down atmospheric CO_2 levels. The drawdown of CO_2 from the atmosphere and its incorporation into phytoplankton cells, followed by sinking through the water column and eventual burial in ocean floor sediments is known as the "biological carbon pump" (e.g. Ducklow et al., 2001). The activity of the ocean's biological pump has the potential to reduce CO_2 concentrations in the atmosphere, which is especially important as scientists work to understand and predict global climate change.

1.3 Physical Setting of Field Work

1.3.1 The Northeast Pacific Ocean

The NE Pacific Ocean contains several different water masses, the main ones being the sub-Arctic current, the Alaska gyre and the Alaskan Stream. The sub-Arctic current travels east at approximately the 45°N line (Favorite et al., 1976) and is the southern bound of the Alaska gyre. As the sub-Arctic current approaches the western Coast of Canada, it bifurcates into the Alaska Stream to the north, and the California current to the south. The Alaska Stream follows the western coast of Canada to the north and curves around alongside the chain of Aleutian Islands. It is the northern bound of the Alaska Gyre. The middle of the Alaska gyre is at approximately 52°N and 155°W (Favorite et al., 1976).

The open sector of the NE Pacific Ocean (Fig. 1.1) is a high-nitrate, low-chlorophyll (HNLC) area (Martin and Fitzwater, 1988) where NO_3^- concentrations can remain as high as 5 μM during the summer months (Varela and Harrison, 1999). However, low $Si(OH)_4$ availability can limit primary production in this area, with concentrations in the Alaska gyre of less than 1 μM in some years (Wong and Matear, 1999; Whitney et al., 2005). Primary productivity is >3 g C m^{-2} d^{-1} during the summer (Boyd and Harrison, 1999), with carbon removal from the upper surface waters in the sub-Arctic NE Pacific estimated at 0.577 Gt C yr^{-1} (Wong et al., 2002). New production rates were 21% of total production on average in the NE Pacific (Varela and Harrison, 1999).

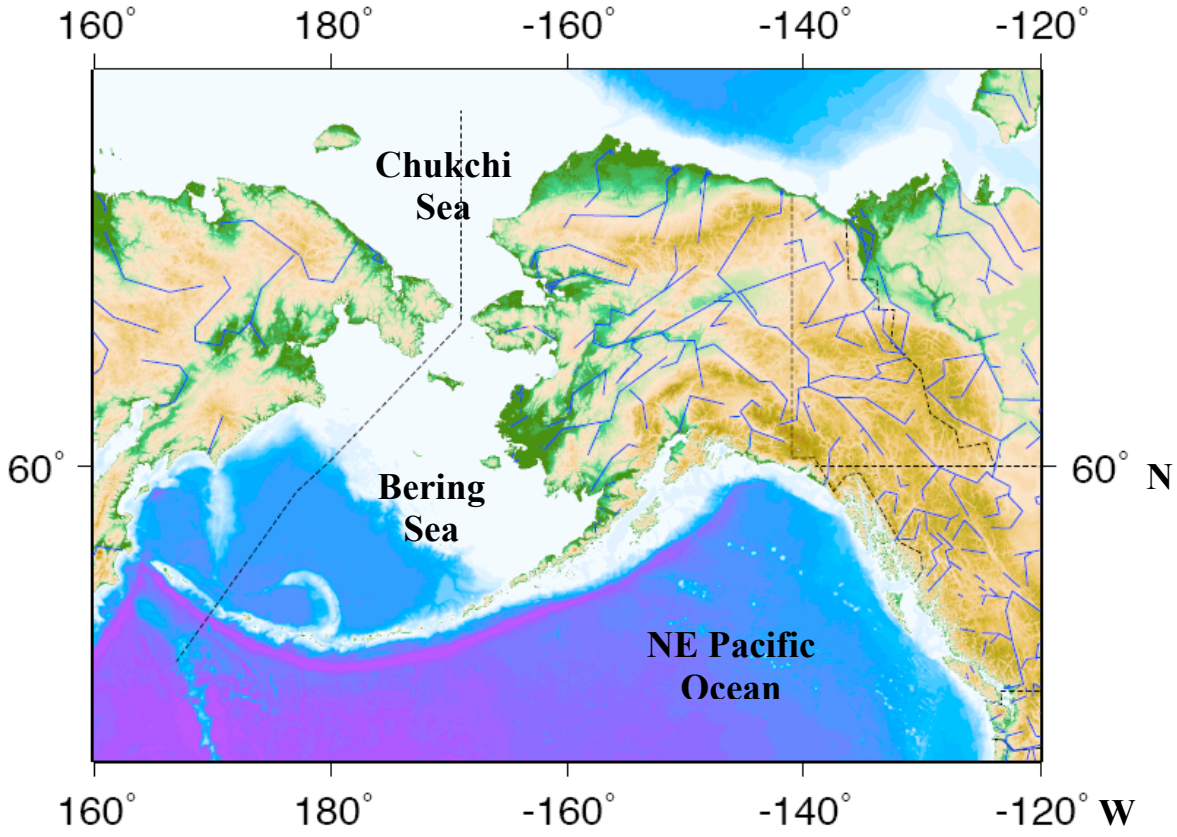

Figure 2.1. Location of sampling stations in the Bering and Chukchi Seas on board the CCGS Sir Wilfrid Laurier from July 11th to July 21st of 2006: Central Bering (A), Anadyr Stream (B), Alaska Coastal Current (C), Chukchi 1 (D) and Chukchi 2(E). Map of area studied in chapters 2 and 3, specifically the NE Pacific Ocean, Bering Sea and Chukchi Sea.

Diatom species indicative of the sub-Arctic North Pacific (east and west) include *Fragilariopsis oceanica, Fragilariopsis pseudonana, Neodenticula seminae, Proboscia eumorpha, Rhizosolenia hebetate, Thalassiosira conferta*, and *Thalassiosira gravida* (Aizawa et al., 2005). Sub-Arctic oceanic and coastal samples contained up to 10^4-10^5 cells L^{-1}, with peaks in diatom abundance found near the Aleutian Islands. These elevated concentrations of diatoms were the result of nutrient enrichment from upwelling around the shallow shelf (Aizawa et al., 2005). In general, centric diatoms are more numerous in coastal and upwelling areas where nutrient concentrations are higher in contrast to open

oligotrophic ocean areas where nutrient concentrations are lower and pennate diatoms are more numerous (Aizawa et al., 2005).

1.3.2 The Bering Sea and the Chukchi Sea

The Bering Sea contains the largest continental shelf outside the Arctic Ocean and is approximately 400 by 500 km (Coachman, 1986). Transport of water across the shelf is driven mainly by tidal forcing (Coachman, 1986). Water transport through the Bering Strait is mainly northwards, as a result of a difference in bottom elevation (Coachman, 1986). Two main water masses flow along the South Eastern Bering Sea Shelf: Alaskan Coastal water along the inner shelf and Central Shelf water along the middle domain (Coachman, 1986). Alaskan Coastal water is a mixture of freshwater runoff from land and saltwater advected across the shelf and its temperature can reach up to 10°C in the summer (Coachman, 1986). Warming of coastal and middle domains begins in March, and by May there is enough of a difference in temperature between surface water and lower water layers to overcome tidal mixing and form a thermocline (Coachman, 1986). This thermocline persists until the end of September. The outer domain is an area of lateral mixing between upwelled water from the deep Bering Sea basin and water from the middle domain (Coachman, 1986).

Another important hydrographic feature of the Bering Sea is the Anadyr Stream, which is created by upwelled waters in the Gulf of Anadyr along the Siberian coast (Nihoul et al., 1993). Anadyr Stream water flows through the Bering Strait alongside the Alaskan Coastal water and Central Bering water, creating a frontal zone where primary production may be enhanced (Nihoul et al., 1993). The nutrient-rich waters which flow

through the Bering Strait fuel productivity on the Chukchi Sea shelf (Carmack and Wassmann, 2006).

The Bering Sea is influenced by the drainage from three major rivers, the Kuskokwim, the Yukon and the Anadyr rivers (Hood, 1983). The surface waters of the Bering Sea deep basin have high $Si(OH)_4$ concentrations (5.6-15.9 μmol L^{-1}) but are limited by the trace metals iron and zinc for which concentrations are below 0.2 nmol L^{-1} (Leblanc et al., 2005). Silicic acid concentrations on the shallow shelf of the Bering Sea are also high, exceeding 10 μmol L^{-1} (Hood, 1983). The Bering Sea is known as the "sea of silicate" due to its high concentrations of $Si(OH)_4$, relative to other areas of the world's oceans (Tsunogai et al., 1979). Nitrate, in contrast, becomes depleted on the continental shelf of the Bering Sea throughout the growing season to less then 0.2 μmol L^{-1} (Bates et al., 2005). Nitrogen is subsequently re-supplied in autumn and winter through cross-shelf and vertical diffusion, vertical mixing by storms, benthic release and possibly nitrification (Whitledge et al., 1986). Primary productivity on the Bering Sea shelf can be as high as 16 g C m^{-2} day^{-1} in nutrient-rich Anadyr Stream water, but is normally about 0.5 g C m^{-2} day^{-1} (Springer and McRoy, 1993). Similar to the Bering Sea, in the Chukchi Sea, $Si(OH)_4$ concentrations are relatively high (10 μmol L^{-1}) even when other macronutrients are depleted (Hood, 1983). Primary production on the shelf of the Chukchi Sea is ~0.34 g C m^2 day^{-1} in the summer (Bates et al., 2005). New production in the Anadyr Stream water mass in the Bering Sea was as high as 80% of total production (Walsh et al., 1989). However, new production in the front between the Anadyr Stream and the Central Bering water was between 30 and 50% of total production, while in the Alaska Coastal current new production was 10% (Walsh et al., 1989). The dominant diatom species vary

between locations in the Bering Sea, but include *Nitzschia spp., Detonula spp., Chaetoceros laciniosus, Rhizosolenia spp.* and *Thalassiosira nordenskioeldii* (Schandelmeier and Alexander, 1981). No diatom species composition studies are available for the Chukchi Sea. The Bering and Chukchi Seas are important ecological areas for higher trophic levels, as they support numerous marine mammal and sea bird populations (Hood, 1983).

1.4 Sub-Arctic and Arctic Ecosystem Shifts

Global climate change is predicted to have larger effects at high latitudes compared to low latitudes (IPCC, 2007). Effects on the biology of sub-Arctic and Arctic systems resulting from global climate change have already been documented by long-term studies in the Northern hemisphere**.** Examples include a steady decrease in benthic production in the Bering Sea from the 1990's to the present (Grebmeier et al., 2006; Grebmeier et al., 2005) and a change in foraging patterns of migrating gray whales (Moore et al., 2003). Physical effects include ice cover reduction (Serreze et al., 2003) and temperature increases (Karcher et al., 2003). As ice cover in the Arctic is reduced each year (Stroeve et al., 2005), areas of the Bering and Chukchi Seas will be exposed to higher irradiance levels for longer periods of time. Arctic waters will continue to warm if the heat flux flowing through the Bering Strait continues to increase as it has in recent years (Woodgate 2006, personal communication).

An ecosystem shift from Arctic to sub-Arctic characteristics due to increasing water temperatures has been identified on the shelf of the Northern Bering Sea. Grebmeier et al. (2006) documented that the warmer waters favor a pelagic fish-based ecosystem as opposed to the previously existing tightly-coupled benthic-pelagic

ecosystem. Reasons for this ecosystem change may include the expansion of fish habitat north, following warmer temperatures. As well, a change in habitat selection by marine mammals has occurred recently concomitant with a reduction in benthic prey organisms. A decrease in water column productivity and organic carbon flux to the ocean floor has been hypothesized as a possible cause for the decrease in benthic animals (Grebmeier et al., 2006). Therefore, it is crucial to better understand the role that water column primary productivity and the biological pump play in these areas.

A few key studies have quantified carbon and nitrogen fluxes and dissolved nutrients in the Bering and Chukchi Seas (e.g. Lee et al., 2007; Walsh et al., 1989; Springer and McRoy, 1993). However, little is known regarding the cycling of Si in these environments. Diatoms are known to dominate Bering Sea spring blooms (Springer et al., 1996), however to date only one study has been conducted on BSi cycling in the Bering Sea (Banahan and Goering, 1986) and none on BSi cycling in the Chukchi Sea. Characterizing BSi cycling in the Bering and Chukchi Seas would help to better understand the impact of nutrient cycling by phytoplankton in these two highly productive areas.

1.5 Thesis Objectives

My Masters' research project was comprised of both a laboratory and a field component. Chapters 2 and 3 of this thesis are part of the field study. The objective of chapter 2 is to quantify the concentrations of BSi in the Bering and Chukchi Seas while accounting for lithogenic interference on BSi measurements. The objective of chapter 3 is to quantify C, N and Si cycling, and total and new production along with the production

of siliceous organisms on a transect which extended from the southwest corner of Vancouver Island, Canada, to Barrow, Alaska.

Chapter 4 focuses on the laboratory experiments. The objective of chapter 4 is to quantify the effect of temperature and irradiance on C, N and Si cycling in two polar diatom species *Thalassiosira antarctica* and *Porosira glacialis*.

Finally, Chapter 5 presents the general conclusions of this thesis. Findings from the field and laboratory studies will be combined to suggest implications for marine ecosystems in Arctic and sub-Arctic environments. Ideas for future studies will be presented.

Chapter 2

Particulate Silica in Surface Waters of the Bering and Chukchi Seas: Accounting for the Interference of Lithogenic Silica during Biogenic Silica Determinations

2.1 Introduction

Little is known regarding silicon cycling in the waters of the Bering and Chukchi Seas, despite extensive studies in these areas on primary production involving carbon and nitrogen (e.g. Springer and McRoy, 1993). Diatoms are members of the phytoplankton community, and have an absolute requirement for Si (Lewin, 1962) which they use for the construction of their frustules. Diatoms are important primary producers that dominate spring (Springer et al., 1996) and summer (Sukhanova et al., 2006) phytoplankton blooms in these areas of the world's oceans. Only one study has been conducted to assess BSi production and dissolution in the Bering Sea (Banahan and Goering 1986), and no studies of this nature have been conducted in the Chukchi Sea. A full understanding of primary production in the Bering and Chukchi Seas requires knowledge of diatom production and Si cycling, considering the important contribution of diatoms to total primary production during the spring bloom and throughout the growing season.

The Bering and Chukchi Sea shelves, together, are one of the largest continental shelves in the world (Coachman, 1986). The Bering Sea is known for its high concentrations of $Si(OH)_4$, not just during the spring when concentrations of all nutrients are high, but throughout the entire summer period when the Bering Shelf is free of ice cover. The high concentrations of $Si(OH)_4$ are derived not only from nutrient rich Pacific Ocean waters, but from the input of several rivers that feed into the Bering Sea. The three major rivers in this area are the Kuskokwim and the Yukon Rivers which drain into the

eastern Bering Shelf, while the Anadyr River drains into the Gulf of Anadyr on the western side of the Bering Sea (Hood, 1983). The southern Chukchi Sea is less influenced by large rivers, but heavily influenced by the inflow of Bering Sea water through the Bering Strait. There are two major water masses which flow through the Bering Strait: the Anadyr Stream to the West, and the Alaskan Coastal Current to the East (Coachman, 1986). The amount of $Si(OH)_4$ input and circulation patterns make the Bering and Chukchi shelves a unique place to examine Si cycling.

The major rivers flowing into the Bering Sea are a source not only of $Si(OH)_4$, but also of particulate silica (PSi; PSi = LSi + BSi). Both lithogenic silica (LSi) in the form of clay minerals, and potentially BSi from riverine siliceous phytoplankton populations can be added to the adjacent marine areas. The rivers flowing into the Bering and Chukchi Seas contribute lithogenic material of slightly different compositions. For example, the Yukon and Kuskokwim rivers are rich in illite but low in smectite and chlorite, while the Anadyr River is rich in chlorite but low in smectite and kaolinite (Naidu et al., 1995). Seawater BSi and LSi concentrations both can be measured from the same sample using a digestion method involving NaOH and HF (Brzezinski and Nelson, 1989). The assumption is that digestion with NaOH dissolves the BSi component of the sample only, while digestion with HF dissolves the LSi component.

Analysis of seawater BSi concentrations using the NaOH digestion method (Brzezinski and Nelson,1989) is convenient for measuring BSi due to its high yield and high precision (98% and 5% measurement range, respectively according to Ragueneau and Treguer (1994)). In general, the quantification of BSi involves digesting the PSi material using 0.2 M NaOH, and the resulting dissolved fraction in the form of $Si(OH)_4$ is

measured spectrophotometrically. However, lithogenic interference is a potential complication in areas where high amounts of LSi are present (Ragueneau and Treguer, 1994), as NaOH can digest small amounts of some types of LSi caught on the filter (Krausse et al., 1983). The amount of LSi interference in the BSi measurement is dependent not only on the quantity of clay minerals but on the type, grain size and surface area of the clay particles (Krausse et al., 1983). Therefore, accounting for lithogenic interference of BSi measurements has been suggested to be location-specific (Ragueneau and Treguer, 1994).

Ragueneau and Treguer (1994) determined the interference of lithogenic material on BSi measurements at two sites near the Bay of Brest, France. They also conducted laboratory experiments on clays typical of these sites to determine the extent to which the NaOH digestion method may cause dissolution of the LSi, and therefore cause an overestimation of BSi concentrations. An analysis of the relationship between BSi and LSi concentrations at their sites found a significant linear regression between the biogenic and lithogenic material. They assumed the relationship was causative, and that increasing amounts of LSi would result in an increase in interference, and, thus, higher apparent BSi concentrations. Ragueneau and Treguer (1994) used the slope of the linear relationship to correct for the interference of LSi on BSi. This correction corresponded well with the amount of interference expected from the results of the clay dissolution experiments they conducted. Thus, it would appear that there are two possible ways of correcting for location-specific interference of LSi on BSi when using the NaOH digestion method: (a) determine a location-specific linear relationship between BSi and LSi and use the slope of the line as a correction factor, and/or (b) determine the clay composition at each site and

correct the BSi measurements based on the dissolution characteristics of those clays. In order to conduct method (b), data on clay composition at each site is necessary along with data on the quantitative dissolution of those clays subjected to NaOH treatment.

Results from previous studies published in the literature on sediment composition in the Bering and Chukchi shelves, and dissolution rates of clay minerals, lead me to hypothesize that there is potential for lithogenic interference in the estimation of seawater BSi concentrations on the Bering and Chukchi shelves. Based on Naidu et al. (1982), sediments in the Bering Sea are composed mostly of illite and smectite, with kaolinite and chlorite present only in minor amounts. Sediments in the Chukchi Sea have large illite and smectite percentage compositions, with kaolinite comprising about 4% of the clay (Viscosi-Shirley et al., 2003). According to Viscosi-Shirley (2003), the chlorite composition of clay in the Chukchi Sea is around 23%, while Naidu et al. (1982) found the chlorite concentration in that area to be minor. By combining the sediment composition data from the literature, it is possible to calculate a lower and upper bound for dissolution amounts for different types of clay minerals at specific locations on the Bering and Chukchi shelves (Table 2.1).

The dissolution characteristics for most of the clay minerals in the Bering and Chukchi Seas can also be found in the literature. Ragueneau and Treguer (1994) found that approximately 13% of kaolinite and 7% of illite dissolves using the NaOH digestion method. Krausse et al. (1983) determined that <0.2% of chlorite dissolves using this method however, their digestion time was considerably shorter than that used by Ragueneau and Treguer (1994). No measurements are available to indicate the percent dissolution of smectite using the NaOH digestion, however, Bauer and Berger (1998)

found that at elevated temperatures and alkaline pH levels, the dissolution of smectite is 1 to 2 orders of magnitude lower then kaolinite.

This chapter addresses the measurement of BSi in the Bering and Chukchi Sea, and accounts for the interference of LSi on those measurements. LSi concentrations will be measured, but the characterization of LSi samples will be inferred from previous studies published in the literature. Relatively few studies have attempted to determine this type of interference (e.g., Krausse et al., 1983, Ragueneau and Treguer, 1994), and the findings of the Rageuneau and Treguer (1994) have not been tested at other locations. These data will build upon the scarcity of BSi data in this area of the world oceans and provide direction on the possible methods for determining LSi interference on BSi measurements.

Table 2.1 Clay component percentage at five stations in the Bering and the Chukchi Seas, based on data from the literature. ND means that no data was available.

Station	Clay component percentage				Source
	Illite	Chlorite	Smectite	Kaolinite	
Central Bering	28 - 38	ND	30 - 40	ND	Naidu and Mowatt 1983
Anadyr Stream	38 - 48	minor	20 - 30	minor	Naidu et al. 1982
	38 - 48	ND	10 - 30	ND	Naidu and Mowatt 1983
Alaska Coastal Current	38 - 48	minor	20-30	minor	Naidu et al. 1982
	38 - 48	ND	10 - 30	ND	Naidu and Mowatt 1983
Chukchi 1	48	23	23	4	Viscosi-Shirley et al. 2003
	49 - 59	minor	12 - 19	minor	Naidu et al. 1982
	38 - 59	ND	20 -30	ND	Naidu and Mowatt 1983
Chukchi 2	48	23	23	4	Viscosi-Shirley et al. 2003
	49 - 59	minor	12 - 19	minor	Naidu et al. 1982
	38 - 48	ND	10 - 20	ND	Naidu and Mowatt 1983

2.2 Methods

2.2.1 Sampling

Sampling in the Bering and Chukchi Sea was conducted aboard the CCGS Sir Wilfrid Laurier from July 11th to July 21st 2006. Station locations were chosen to sample different water masses throughout the Bering and Chukchi Seas (Fig. 2.1 and Table 2.2). A minimum of five depths were sampled at shallow stations, and up to nine depths were sampled where water column depth permitted (to a maximum of 79 m at the Central Bering station). A rosette sampler was used to collect seawater at “irradiance” depths

within the euphotic zone and below the euphotic zone. In this study, “euphotic zone” was defined as the area between the surface (100%) and the depth of the 1% surface incidence irradiance. A Secchi disk was utilized to derive the 100, 50, 30, 10, 3 and 1% irradiance levels.

2.2.2 Station Descriptions

Sampling was conducted at three stations in the Bering Sea and two stations in the Chukchi Sea (Fig. 2.1 and Table 2.2). The southernmost station in the Bering Sea is located in the central domain of the Bering Sea, which is the area between the 50 and 100 m isobath and has an average salinity from surface to bottom of 31.6 (Coachman, 1986). The vertical structure of the Central Bering water mass during the spring and summer usually has two layers, with a surface layer ranging from 10 to 40 m (Coachman, 1986). The second station in the Bering Sea is located in the Anadyr Stream as characterized by its high salinity (>32) (Coachman et al., 1975). The northernmost station in the Bering Sea is located in the Bering Strait. This station had a lower salinity compared to the central domain (31.3, surface to bottom average (data shown in Chapter 3)) and is located within the Alaskan Coastal Current water mass that flows through the Bering Strait. The water column of the Alaskan Coastal Current typically has an homogeneous structure, and salinity tends to vary with the season according to freshwater runoff (Coachman, 1986). The two Chukchi Sea stations are located directly north of the Bering Strait and have bottom water salinities of >32. Due to their relatively high bottom salinities, they are thought to be located in a plume of Anadyr Stream water (bottom water salinities are used for classification of these two stations to avoid distinguishing between a freshwater lens over the Anadyr Stream water, or freshwater at the surface from another source such

as ice retreat meltwater). The most northern station is influenced by sea ice meltwater with a surface salinity of approximately 29.3.

At each station, samples were collected for the measurements of chl *a*, $Si(OH)_4$, BSi, and LSi concentrations. The data presented in this chapter is part of a larger suite of measurements. These same stations were sampled to collect measurements of particulate carbon and nitrogen, carbon and nitrate incorporation, BSi net incorporation, and the dissolved nutrients nitrate, phosphate and silicate. These data are presented in Chapter 3.

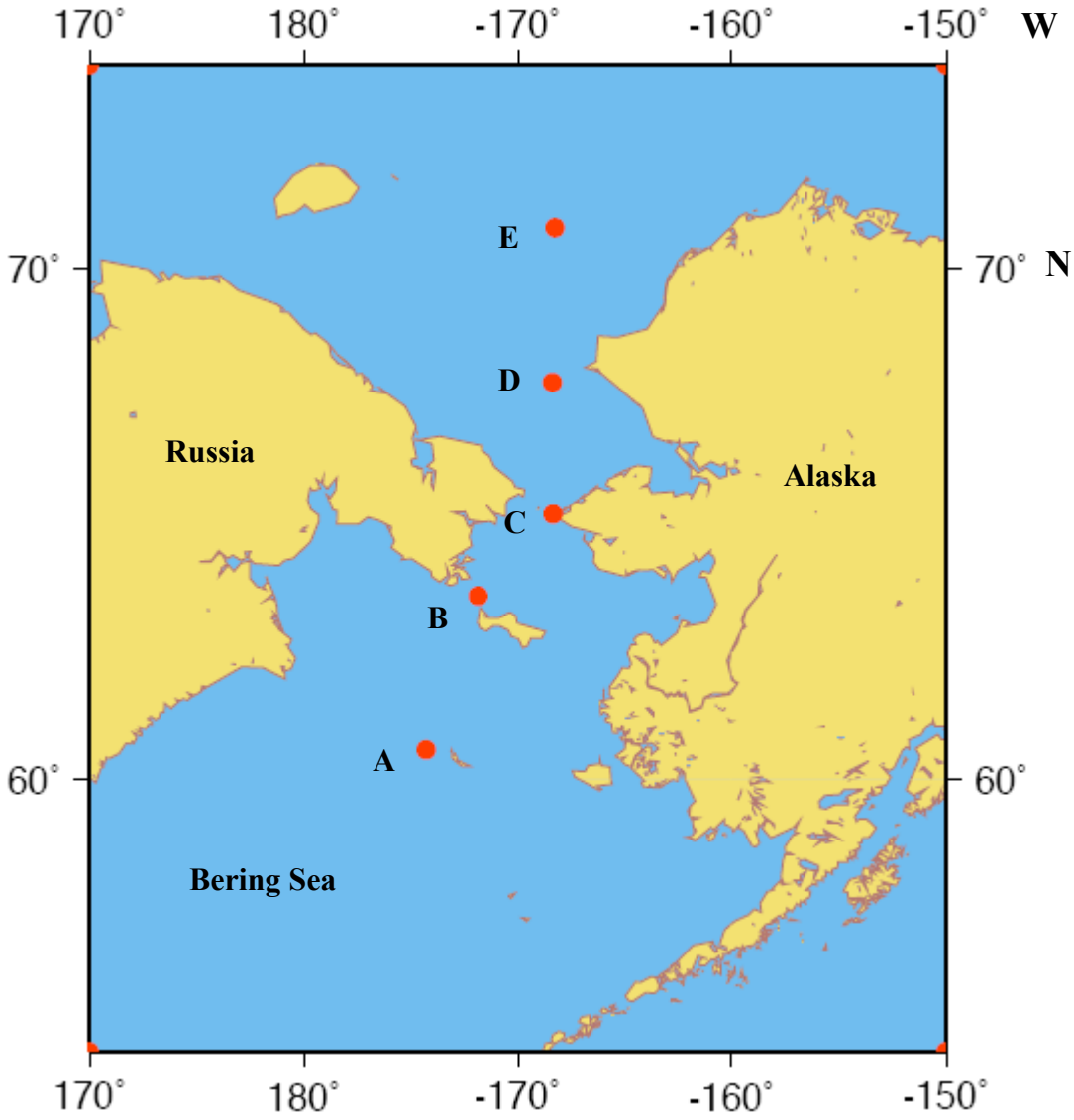

Figure 2.1. Location of sampling stations in the Bering and Chukchi Seas on board the CCGS Sir Wilfrid Laurier from July 11th to July 21st of 2006: Central Bering (A), Anadyr Stream (B), Alaska Coastal Current (C), Chukchi 1 (D) and Chukchi 2(E).

Table 2.2. Latitude, longitude and bottom depth for three stations in the Bering Sea and two stations in the Chukchi Sea sampled from July 11th to July 21st of 2006.

Station	Latitude (°N)	Longitude (°W)	Depth (m)
Central Bering	60° 41.503’	174° 15.570’	91
Anadyr Stream	64° 01.986’	171° 49.897’	53
Alaska Coastal Current	65° 39.710’	168° 20.263’	50
Chukchi 1	68° 5.235’	168° 21.675’	57
Chukchi 2	70° 37.970’	168° 14.393’	45

2.2.3 Chlorophyll *a* Concentrations

Chlorophyll a was collected on glass fiber filters of 0.7 μm porosity, and kept frozen at -20°C in the dark until analysis. Upon analysis, chl *a* was extracted in 90% aqueous acetone for 24 hrs at -20°C in the dark. Analysis was conducted according to Parsons et al. (1984) and samples were read on a Turner Designs 10 AU (Sunnydale California) fluorometer. Samples were corrected for the presence of phaeopigments by acidifying the sample with two drops of 1.0N HCl, measuring the remaining fluorescence and subtracting this from the total.

2.2.4 Silicic Acid Concentrations

Samples for the measurement of $Si(OH)_4$ were collected in 30 mL polypropylene acid washed bottles. Samples were frozen at -20°C until analysis and then analyzed using the Astoria 2 Nutrient Autoanalyzer (Astoria Pacific International, Oregon) according to the method outlined in Barwell-Clarke and Whitney (1996).

2.2.5 Apparent Biogenic Silica Concentrations

Apparent BSi (BSi_a) is defined as the BSi concentration without correction for LSi interference (Ragueneau and Treguer, 1994). For BSi_a concentrations, 2 L samples were collected and filtered under low vacuum pressure at 5 mg Hg using 0.65 μm polycarbonate filters. Filters were stored at -20°C until analysis. Samples were analyzed using the method outlined in Brzezinski and Nelson (1989) with the modification of a digestion time of 1 hr instead of 40 minutes. This method results in the digestion of less lithogenic material than similar methods using Na_2CO_3 and has a recovery of 97.8% (Krausse et al., 1983). In brief, filters were dried at 60°C for 48 hrs. Filter samples were then digested in 4 mL 0.2 M NaOH at 95°C for 1 hr, cooled in an ice slurry for 5 minutes after which 1 mL of 1 N HCl was added. Four of the 5 mL in the digestion tube were removed for $Si(OH)_4$ analysis. Samples were read on a Beckman DU 530 spectrophotometer at 810 nm.

2.2.6 Apparent Lithogenic Silica Concentrations

Apparent LSi (LSi_a) is defined as the LSi concentration without correction for the LSi that was previously dissolved and measured as BSi_a (Ragueneau and Treguer, 1994). LSi_a was analyzed following the method described in Brzezinski and Nelson (1989). After filters were digested for BSi, there remains 1 mL of sample along with the original filter in the digestion tube. The 1 mL volume was diluted with 12 mL of deionized water and the tubes were spun down in a centrifuge. The supernatant was removed and the process was repeated once more. This washing step reduces potential interference on LSi_a from any dissolved BSi remaining in the tube. LSi_a concentrations are also corrected

mathematically for this possibility prior to correcting for possible lithogenic dissolution during the previous NaOH digestion using the equation:

Equation 2.1 LSi = LSi μmol filter^{-1} – [(1/5)*(1/13)*(1/13)]*BSi μmol filter^{-1}

Following the removal of the supernatant, these same filters were dried at 60°C for 48 hrs. Filters were then digested in 0.2 mL of 2.5 M HF for 48 hours. Samples were then diluted to 10 mL using 9.8 mL boric acid and analyzed for $Si(OH)_4$ on a Beckman DU 530 spectrophotometer at 810 nm.

2.2.7 Statistical Analysis

All statistical analyses were conducted using Statistical Package for Social Sciences (SPSS**)** 15.0 for Windows. A significance level of $p<0.05$ was used for all tests. Correlation analysis and linear regression were performed to determine relationships between BSi and LSi.

2.2.8 Corrected Biogenic and Lithogenic Silica

Both methods (a) and (b) described in the introduction were utilized to correct for the interference of LSi on BSi concentrations, and estimates of BSi corrected (BSi_c) and LSi corrected (LSi_c) were derived. For the application of method (a), statistical analyses were performed to determine if there was a significant linear relationship between BSi_a and LSi_a. Ragueneau and Treguer (1994) found significant linear relationships between BSi_a and LSi_a for their two stations. They attributed these relationships to the slight dependence of BSi concentrations on LSi concentrations, i.e. as the concentration of LSi increased, so did BSi. Separate statistical tests for relationships between LSi and BSi

were conducted for each station to account for location differences in the interference of LSi on BSi (Ragueneau and Treguer, 1994).

Clay composition estimates used in correction method (b) are listed by station in Table 2.1. The upper and lower values for the range of clay compositions were both used to calculate a possible range of lithogenic Si interference using the following equation.

Equation 2.2

$$LSi_d = \{ [(I_p * I_c * LSi_a) + (C_p * C_c * LSi_a) + (S_p * S_c * LSi_a) + (K_p * K_c * LSi_a)]_u$$

$$+ [(I_p * I_c * LSi_a) + (C_p * C_c * LSi_a) + (S_p * S_c * LSi_a) + (K_p * K_c) * LSi_a]_l \} / 2$$

Where LSi_d represents the concentration of LSi dissolved by the NaOH digestion, LSi_a is the apparent concentration of LSi, and the capital letters I, C, S, and K represent illite, chlorite, smectite and kaolinite, respectively. The subscript p represents the proportion of the clay mineral dissolved during the NaOH digestion, the subscript c represents the proportion of the clay mineral of the total lithogenic silica present in the sediments, and the subscripts u and l represent the upper limit, and the lower limit, respectively of the range of the clay mineral present in the sediments.

2.3 Results

2.3.1 Chlorophyll *a* Concentrations

The three stations in the Bering Sea show that chl *a* increases with depth, with the highest concentrations at the bottom of the euphotic zone (Fig. 2.2). Chlorophyll *a* concentrations ranged from 0.2 to 1.9 μg L^{-1} for the euphotic zone.

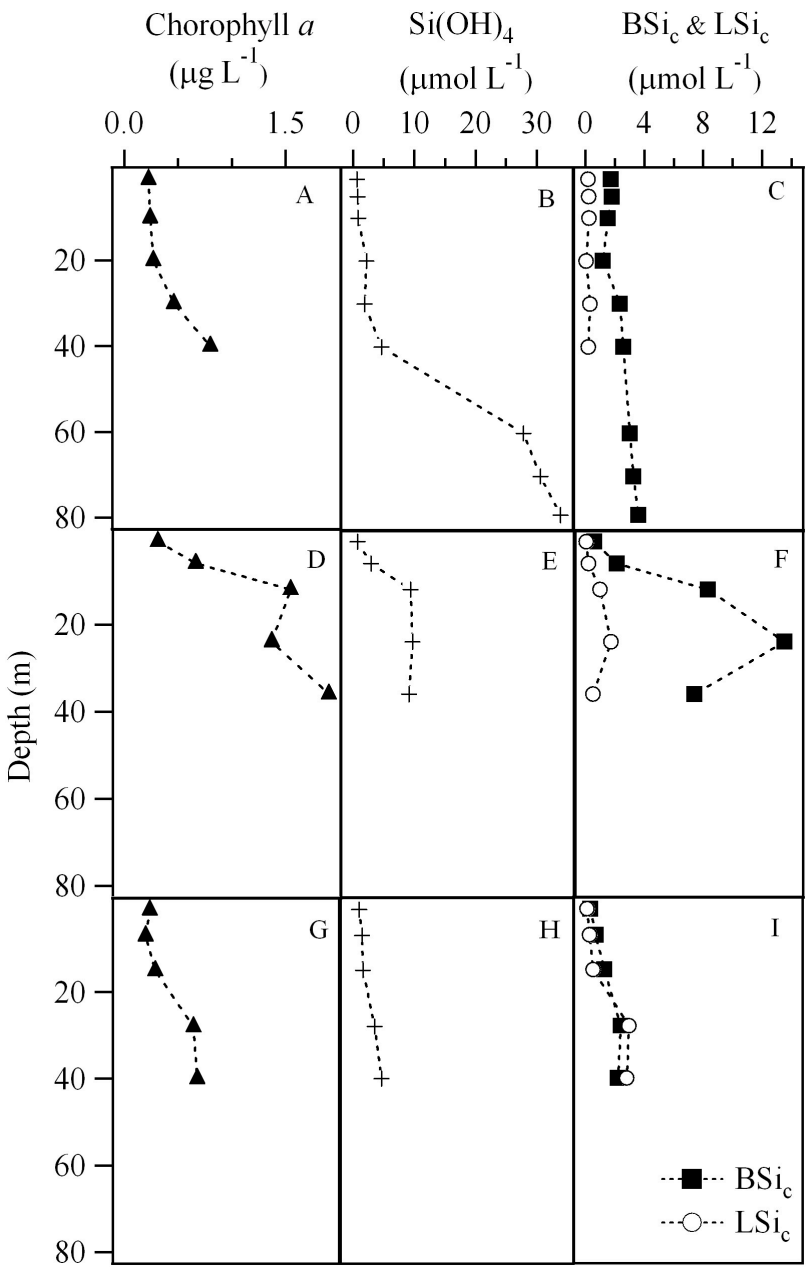

Figure 2.2. Vertical profiles of chlorophyll *a* (▲), Si(OH)$_4$ (+), BSi$_c$ (■) and LSi$_c$ (○) concentrations for the Central Bering (A-C), Anadyr Stream (D-F) and Alaska Coastal Current (G-I). LSi samples for the depths 60 m, 70 m and 79 m at the Central Bering station (C) were lost. Note that the chlorophyll *a* x-axis scale is different from the one in Figure 2.3.

Chukchi 1 exhibited a maximum chl *a* concentration at the 1% irradiance level (Fig. 2.3A), while the second station sampled exhibited a maximum at the 10% irradiance

level (Fig. 2.3D). Concentrations were higher in the Chukchi Sea compared to the Bering Sea, exhibiting ranges of 0.7 to 4.2 μg L^{-1} and 0.3 to 7.8 μg L^{-1} for the euphotic zone of stations Chukchi 1 and Chukchi 2, respectively.

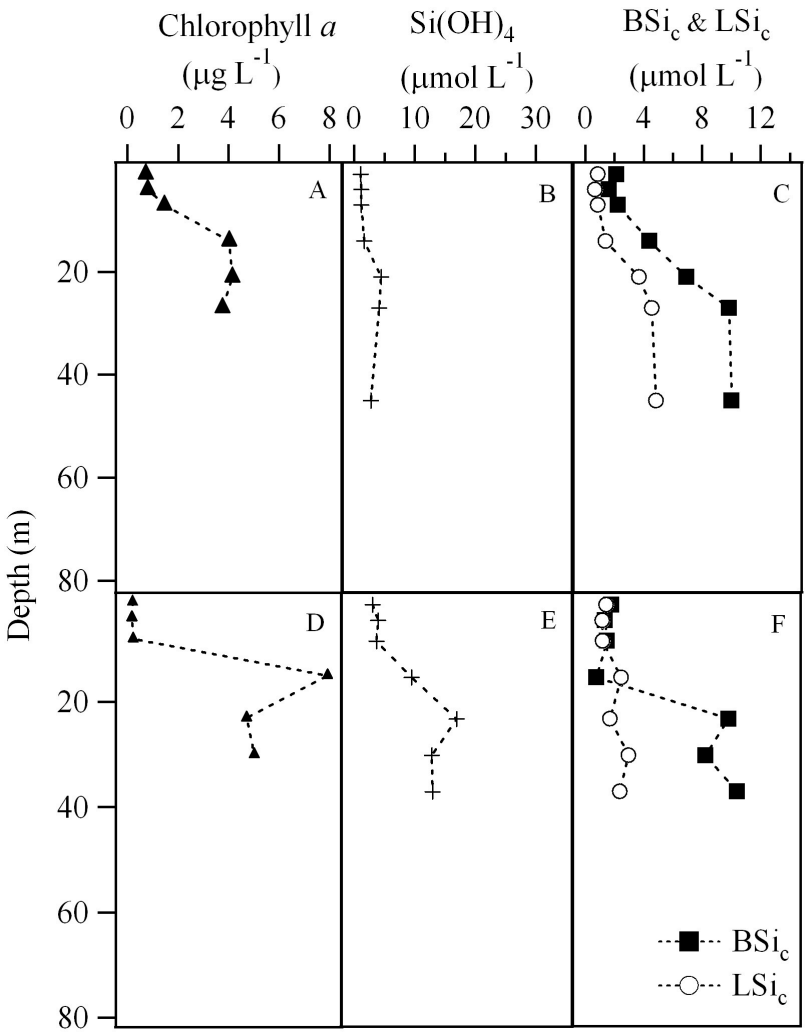

Figure 2.3. Vertical profiles of chlorophyll *a* (▲), $Si(OH)_4$ (+), BSi_c (■) and LSi_c (○) concentrations for Chukchi 1 (A-C) and Chukchi 2 (D-F).

2.3.2 Silicic Acid Concentrations

Silicic acid profiles at the Central Bering and Anadyr Stream stations exhibited low surface (1 m deep) concentrations (<1 μmol L^{-1}), with an identifiable nutricline, and higher concentrations at deeper depths (33.9 μmol L^{-1} for the Central Bering and 9.6

μmol L^{-1} for the Anadyr Stream) (Fig. 2.2B and E). The Alaska Coastal Current station had $Si(OH)_4$ concentrations ranging from 1.3 to 4.9 μmol L^{-1} (Fig. 2.2H). Both Chukchi Sea stations exhibited maximum $Si(OH)_4$ concentrations between 20 and 25 m depth (Fig. 2.3B and E). The maximum $Si(OH)_4$ concentration at the Chukchi 1 station was 4.4 μmol L^{-1}, and the maximum at the Chukchi 2 station was 17 μmol L^{-1}.

2.3.3 Correction Methods for Biogenic and Lithogenic Silica

An attempt was made to correct the BSi_a data using both method (a) and method (b). Method (a) was found to be unsuitable for the locations which were sampled in this study. It resulted in higher than previously reported correction factors and % dissolved LSi. The process through which method (a) was determined to be unsuitable is explained in this section.

Regression analyses show a significant linear relationship between BSi_a and LSi_a at the stations Anadyr Stream, Alaska Coastal Current and Chukchi 1 ($p<0.05$) with r squared values of 0.93, 0.93 and 0.98, respectively (Fig. 2.4). No significant relationship was found between BSi_a and LSi_a for stations Central Bering and Chukchi 2. Significant correlations were also found for stations Anadyr Stream, Alaska Coastal Current and Chukchi 1 (Table 2.3). Regression analyses were performed in order to most closely follow the correction method described by Ragueneau and Treguer (1995). However, a regression analysis assumes a causative relationship between BSi and LSi. As this assumption has not been validated for our study sites, a correlation analysis was also conducted. Correlation analysis lacks the causation assumption, and is therefore the more conservative statistical test. Slopes of the regression lines were 7.72, 0.67 and 2.03 for Anadyr Stream, Alaskan Coastal Current and Chukchi 1, respectively, and are

significantly higher than the 0.15 slope determined by Ragueneau and Treguer (1994) for their two sites. If method (a) was employed, the slopes of the linear regressions would be used as correction factors. This method resulted in corrected values for LSi that were drastically higher than LSi_a. In fact, according to method (a), 89, 40, and 67% of LSi originally contained on the filters collected for BSi, dissolved during the NaOH digestion process. This is contrary to previous studies conducted by Paasche (1980), Krausse et al., (1983) and Ragueneau and Treguer (1994). For Example, Paasche (1980) found that digesting a silt mix of approximately 30% illite and chlorite with NaOH resulted in dissolution of less than 0.5% of the initial lithogenic material. Krausse et al., (1983) found that less than 1.5% of silica in a variety of silicate minerals dissolved upon treatment with NaOH digestion. Ragueneau and Treguer (1994) found that 15% of LSi was digested with the NaOH method. Hence, lower correction factors than 7.72, 0.67 and 2.03 were expected. Based on the data from the studies mentioned above, correction factors ranging from 40 to 89% seem unrealistic compared to correction factors of <1.5 to 15%. In addition, digestion of 89% of LSi material (e.g. Anadyr Stream station) using the NaOH method would be an unacceptable error for a method of BSi measurement.

A closer look at the chemistry of the NaOH/HF method casts further doubt on the appropriateness of method (a) in this case. NaOH is corrosive to BSi (Martin-Jezequel et al., 2000) and as a base, it corrodes organic material, such as the organic matrix which coats diatom frustules. Once that coating is removed, diatom frustules dissolve readily in solutions undersaturated in $Si(OH)_4$ (Bidle and Azam, 1999). In contrast, HF is a strong acid, capable of dissolving glass (LSi). It seems unlikely that a high percentage of LSi

material, which regularly requires a strong acid to dissolve it, would readily dissolve in a relatively dilute base.

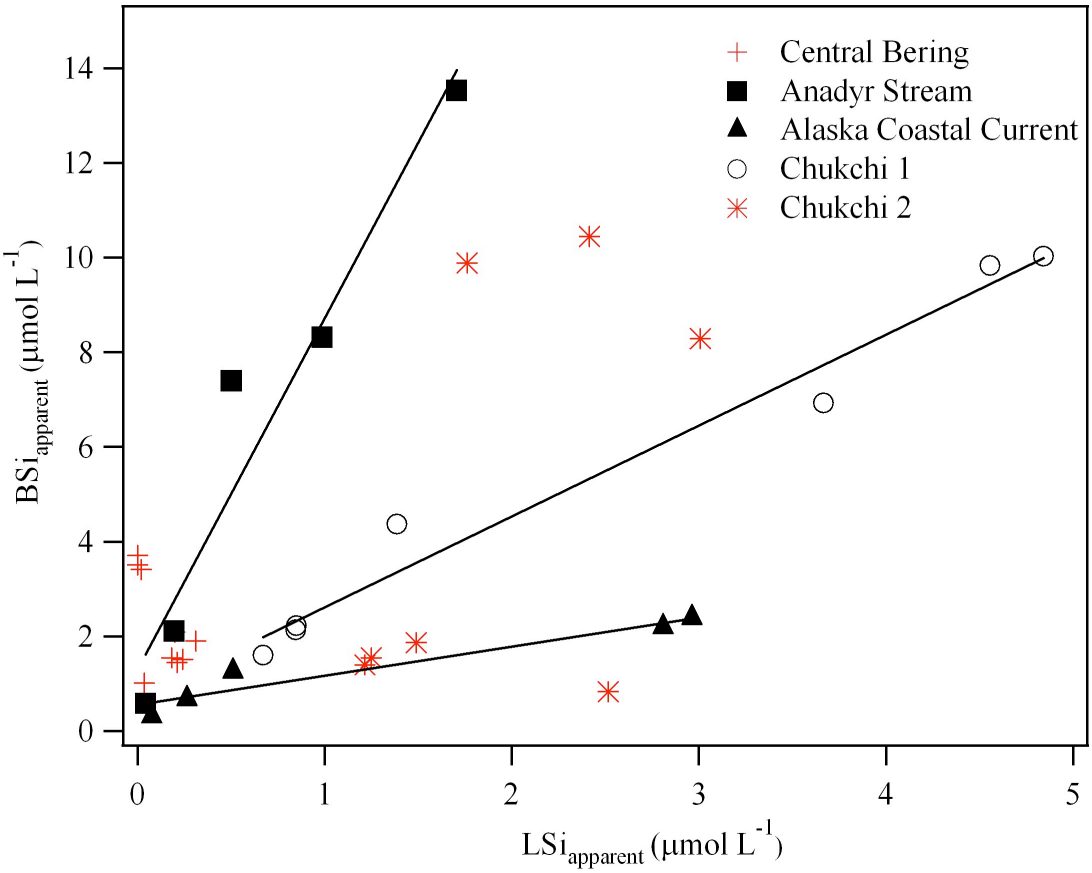

Figure 2.4. Linear relationships between apparent biogenic and lithogenic silica for stations at Anadyr Stream, Alaska Coastal Current and Chukchi 1. All three relationships were significant ($p<0.05$). No significant relationship was found for the Central Bering and Chukchi 2 stations, however data points are still displayed.

Table 2.3. P and r values for correlation analyses between apparent biogenic (BSi_a) and lithogenic silica (LSi_a) for each station. $p<0.05$ indicates a significant correlation.

Station	P value	R value
Central Bering	0.082	0.755
Anadyr Stream	0.008	0.964
Alaska Coastal Current	0.006	0.971
Chukchi 1	0.000	0.988
Chukchi 2	0.34	0.426

Correction factors for LSi and BSi concentrations were also calculated by applying method (b), using regional clay composition from previous data and the dissolution characteristics of those clay minerals (Table 2.1). For each clay component present in the Bering and Chukchi sediment samples, there is a range of possible concentrations (Table 2.1). Corrections were calculated using the upper and lower limit of each range. Upper and lower corrections differed less than 1%. Hence, the average of the two corrections was used to adjust biogenic and lithogenic silica concentrations by using Equation 2.2. The correction factor was added to the LSi_a and subtracted from the BSi_a concentration. Corrected BSi concentrations (BSi_c) ranged from less than 1% to just over 10% lower than BSi_a concentrations. According to method (b), approximately 2.8 to 3.8% of LSi originally on the filter dissolved during the digestion with NaOH. These percentages are slightly higher than those found by Paasche (1980), and Krausse et al., (1983) but lower than Ragueneau and Treguer (1994). Therefore method (b) agrees better with the literature than method (a).

Based on previous studies, clay compositions of sediments in our study area, and dissolution characteristics of these clays, method (a) must be rejected as a suitable method for determination of lithogenic interference on the measurement of BSi in this study. Reasons for the unsuitability of method (a) for our study despite its use in the literature will be addressed in the Discussion section of this chapter.

Table 2.4. Apparent biogenic and lithogenic silica concentrations and corrected biogenic and lithogenic silica for each depth at each station. The sum of corrected biogenic silica and lithogenic silica concentrations is displayed as total particulate silica (PSi). Corrected values were calculated using method (b), in which digestion of lithogenic silica is estimated using dissolution characteristics and sediment composition data from the literature. The percent that corrected silica makes up of apparent silica is also displayed.

Station	Depth (m)	BSi_a (μmol L^{-1})	BSi_c (μmol L^{-1})	BSi_c % of BSi_a	LSi_a (μmol L^{-1})	LSi_c (μmol L^{-1})	LSi_c % of LSi_a	Total PSi (μmol L^{-1}) (BSi_c+LSi_c)
Central Bering	1	1.55	1.55	100.0	0.18	0.18	100.0	1.73
	5	1.45	1.45	100.0	0.20	0.21	105.0	1.66
	10	1.52	1.52	100.0	0.23	0.24	104.3	1.76
	20	1.02	1.02	100.0	0.04	0.04	100.0	1.06
	30	1.91	1.90	99.5	0.30	0.31	103.3	2.21
	40	2.09	2.09	100.0	0.19	0.20	105.3	2.29
	60	3.41	N.D.	N.D.	N.D.	N.D.	N.D.	N.D.
	70	3.51	N.D.	N.D.	N.D.	N.D.	N.D.	N.D.
	79	3.71	N.D.	N.D.	N.D.	N.D.	N.D.	N.D.
Anadyr Stream	1	0.59	0.58	98.3	0.04	0.04	100.0	0.62
	6	2.12	2.11	99.5	0.19	0.20	105.3	2.31
	12	8.35	8.31	99.5	0.95	1.00	105.3	9.31
	24	13.58	13.52	99.6	1.65	1.71	103.6	15.23
	36	7.42	7.40	99.7	0.48	0.50	104.2	7.9
Alaska Coastal Current	1	0.31	0.31	100.0	0.07	0.08	114.3	0.39
	7	0.68	0.67	98.5	0.25	0.26	104.0	0.93
	15	1.28	1.26	98.2	0.49	0.51	104.1	1.77
	28	2.49	2.38	95.6	2.86	2.97	103.8	5.35
	40	2.30	2.20	95.7	2.71	2.82	104.1	5.02
Chukchi 1	1	2.17	2.13	98.2	0.81	0.85	104.9	2.98
	4	1.63	1.60	98.2	0.64	0.67	104.7	2.27
	7	2.26	2.22	98.2	0.82	0.85	103.7	3.07
	14	4.42	4.37	98.9	1.33	1.40	105.3	5.77
	21	7.07	6.92	97.9	3.53	3.68	104.2	10.6
	27	10.00	9.82	98.2	4.38	4.57	104.3	14.39
	45	10.21	10.01	98.0	4.66	4.86	104.3	14.87
Chukchi 2	1	1.93	1.87	96.7	1.43	1.49	104.2	3.36
	4	1.45	1.40	96.6	1.17	1.22	104.3	2.62
	8	1.60	1.55	96.9	1.20	1.25	104.2	2.8
	15	0.92	0.82	89.1	2.42	2.52	104.1	3.34
	23	9.95	9.88	99.3	1.69	1.76	104.1	11.64
	30	8.40	8.29	98.7	2.89	3.01	104.2	11.30
	37	10.54	10.44	99.1	2.32	2.42	104.3	12.86

2.3.4 Corrected Biogenic Silica and Lithogenic Silica Concentrations

Corrected BSi concentrations in the Central Bering and Alaska Coastal Current ranged from 0.3 to 3.6 μmol L^{-1} (Fig. 2.2C and I, and Table 2.4). In contrast, the BSi_c concentrations in the Anadyr Stream were the highest measured on the cruise, up to 13.5 μmol L^{-1} at 24 m (Fig. 2.2F and Table 2.4). Corrected BSi concentrations in the Chukchi Sea were also high, ranging from 0.8 to 10.4 μmol L^{-1} (Figs. 2.3C and F, and Table 2.4). The highest concentrations of BSi_c in the Chukchi Sea were at depths corresponding to the 3% light level and below. In fact the highest BSi_c concentration measured at the Chukchi 2 station was below the 1% light level (37 m) at 10.4 μmol L^{-1}. In conclusion, BSi_c concentrations in the Bering and Chukchi Seas ranged from 0.3 to 13.5 μmol L^{-1}, with the highest values observed at the Anadyr Stream station and the two Chukchi stations.

For all stations in the Bering and Chukchi Seas, LSi_c increased from the surface to depth in the water column. Concentrations were lower in the Bering Sea ranging from 0.02 to 2.9 μmol L^{-1} (Fig. 2.2, and Table 2.4). LSi_c concentrations in the Chukchi Sea ranged from 0.7 to 4.8 μmol L^{-1} (Fig. 2.3, and Table 2.4). Average LSi_c concentrations at all stations ranged from 22% to 77% of BSi_c concentrations throughout the water column.

Differences in chl *a*, $Si(OH)_4$, BSi_c and LSi_c concentrations among stations support the idea that stations are located in different water masses. The only two stations that exhibited similar trends in biogenic and lithogenic concentrations were the Chukchi Stations, which are located in the same water mass.

2.4 Discussion

The analysis showed that method (b) was the appropriate method for correcting lithogenic interference of BSi measurement for the locations sampled in this study. Accepting method (b) as the correction method for these data leaves two main issues unresolved. The first issue is: why is method (a) a suitable correction factor for the Ragueneau and Treguer (1994) study but not for this study? The second is: why is there a linear relationship between BSi_a and LSi_a? This section addresses these two questions.

The BSi to LSi relationship in our study is different from that found in Ragueneau and Treguer (1994). Several major differences between our study sites and the study sites of Ragueneau and Treguer (1994) shed some light on this discrepancy. These include the difference in the composition of particulate material and the difference in concentration of LSi material. The two stations of Ragueneau and Treguer (1994) had relatively high LSi concentrations (15-20 μmol L^{-1}) compared with mine (0.05-5.2 μmol L^{-1}). In this study, when LSi concentrations were higher than BSi concentrations, biogenic material still made a significant contribution to particulates: the minimum percentage of BSi relative to LSi was 38%. Chlorophyll *a* concentrations at the sites of Ragueneau and Treguer (1994) were <0.7 μg L^{-1}, while the average for all sites in our study was 1.1 μg L^{-1} with values reaching 7.8 μg L^{-1}. Thus, differences between our study sites and those of Ragueneau and Treguer (1994) could explain why method (a) was appropriate for their study location, but not for more productive locations such as the ones sampled in this study.

The question remains as to why there is such a strong correlation between BSi and LSi at three stations in our study. One possibility is that here, the BSi measurements are

interfering with the LSi measurements. Biogenic interference can be accounted for by calculating the amount of BSi left in the centrifuge tube after 2 rinses with 12 mL deionized water (see Methods). The resulting correction gave an LSi concentration which was less than one percent different from the original LSi concentration, and thus it would not be the cause of the strong linear correlation.

Results show that LSi, BSi and chl *a* all increase with depth. Chlorophyll *a* concentrations seem to either have a similar depth profile to LSi and BSi (e.g. Central Bering) or have a sub-surface maxima just above that of BSi. In fact, there is actually a significant linear relationship between chl *a* and LSi at the Central Bering station ($p<0.05$) (data not shown). This significant relationship is probably not causative; neither should the linear relationship between BSi and LSi be assumed to be so. The three stations, which have a strong linear relationship between BSi and LSi have bottom depths shallower than or equal to the 0.1% light level. It is possible that primary production is occurring at depths close to the bottom, where relatively higher concentrations of LSi may also be expected. It is also possible that phytoplankton aggregates are sinking through the water column, causing a high amount of chl *a* and BSi to be found at the same depths as high LSi concentrations. Unfortunately, BSi and LSi have not previously been measured in this area, and therefore there is no location-specific data with which to compare this data. Future studies will need to be conducted to confirm the appropriateness of using method (b).

My analysis has consequences for future studies involving BSi and LSi analysis. My results suggest that it is not sufficient to use the slope of a linear relationship between LSi and BSi as a correction factor for BSi, as has been done by previous studies (e.g.

Leblanc et al., 2003) since the 1994 analysis of Ragueneau and Treguer. Using the slope of a linear regression may lead to overestimating the LSi dissolution percentage in areas where LSi concentrations are relatively low, such as in this study. Sediment composition in the study area should be taken into consideration in addition to the BSi-LSi regression analyses. Chlorophyll *a* should also be measured as an indicator of phytoplankton biomass. Location-specific analyses should be conducted in all cases.

Chapter 3

Biological Cycling of Silicon, Nitrogen and Carbon in Surface Waters of the Northeastern Pacific Ocean and the Bering and Chukchi Seas during July 2006

3.1 Introduction

Arctic and sub-Arctic marine waters have been experiencing a major ecological shift over the past two decades, as the boundary between sub-Arctic and Arctic ecosystems is moving northwards (Grebmeier et al., 2006). Changes in primary production may be responsible for the observed changes at higher trophic levels in these ecosystems, such as lower benthic production (Grebmeier et al., 2006). However, inter-annual variations in primary production are large in the Bering and Chukchi Seas (Coachman, 1986), and therefore it is difficult to determine if changes in primary productivity are the result of a long-term trend, or merely year to year variations (Lee et al., 2007). Another obstacle for assessing the reasons for ecosystem fluctuations is the lack of recent and widespread data on primary production at these high latitudes. A better understanding of primary production in the sub-Arctic and Arctic is needed in order to understand changes in the marine food web in these areas.

Few studies have examined the abundance and activity of primary producers in the Bering and Chukchi Seas, or have focused on total and new primary production. Total primary production can be as high as 16 g C m^{-2} day^{-1} in the Anadyr Stream, but is generally in the order of 0.5 g C m^{-2} day^{-1} (Springer and McRoy, 1993). New production (based on the use of nitrate, NO_3^-) accounts for 2 g C m^{-2} day^{-1} in the nutrient rich Anadyr Stream water and an average of 0.4 g C m^{-2} day^{-1} in the lower nutrient waters of the

Alaska Coastal Current (Walsh et al., 1989). Only one study has addressed Si dynamics in the Bering Sea (Banahan and Goering, 1986) and they found that $Si(OH)_4$ uptake ranged from 1.8 to 50.9 mmol Si m^{-2} day^{-1} (0.33 to 9.41 g C m^{-2} day^{-1}). To the present, studies describing the cycling of Si have not been conducted in the Chukchi Sea. The most recent study examining total and new production in the Bering and Chukchi Seas reported lower primary production rates than in earlier studies, but was unable to conclude if differences were due to long-term trends or inter-annual variation (Lee et al., 2007). Primary production in the NE Pacific gyre is the subject of a review by Harrison et al. (1999). Total primary production ranges from 0.3-0.6 g C m^{-2} day^{-1} (Boyd and Harrison, 1999; Harrison et al., 1999), while new production is, on average, 0.046 g N m^{-2} day^{-1} (0.30 g C m^{-2} day^{-1}) in the NE Pacific (Varela and Harrison, 1999; Pena and Varela, 2007).

A quantification of new production and production by siliceous organisms and their contribution to total primary production is essential for understanding energy fluxes through the food web. Biogenic silica sinks more readily out of the euphotic zone than PC or PN (Dugdale et al., 1995). A high sinking rate of BSi out of the euphotic zone can lead a phytoplankton community to $Si(OH)_4$ limitation and thus affect community dynamics (Dugdale et al., 1995). Studies in the Chukchi Sea are required to determine whether BSi is mainly recycled or buried in sediments as it is unknown for this area.

The study of primary production in the NE Pacific Ocean and Bering and Chukchi Seas is especially important since climate change is expected to have a disproportionate impact at higher latitudes (IPCC, 2007). Some of the predicted changes that will directly affect phytoplankton communities include increased stratification of the upper water

column, decreased ocean mixing and a change in upwelling patterns (Carmack and Wassman, 2006). Increased stratification provides conditions amenable to the start of a phytoplankton bloom by allowing phytoplankton to remain in the sunlit upper ocean where production offsets the losses due to respiration. Stratification also contributes to the end of a bloom, once all the nutrients in the surface layer have been drawn down. A decrease in water column mixing will decrease the amount of nutrient input to the surface layers of the water column. Upwelling brings nutrients to the surface, resulting in high phytoplankton production (e.g. MacIsaac et al., 1985). A change in upwelling patterns will change the supply of nutrients to phytoplankton. Changes that affect primary production will in turn affect organisms higher up the food chain. Hence in order to understand changes in higher trophic levels of ecosystems, an understanding of primary production is necessary.

The objective of this study was to determine total and new primary production, and siliceous production through the NE Pacific Ocean and Bering and Chukchi Seas. Four water masses were sampled in the NE Pacific Ocean (the sub-Arctic Current, the Alaska Gyre, a frontal water mass within the Alaska Gyre, and the Alaska Stream), three water masses were sampled in the Bering Sea (the Central Bering, the Anadyr Stream and the Alaska Coastal Current) and two water masses in the Chukchi Sea. This study will contribute data on carbon, nitrogen and silicon cycling in the NE Pacific and Bering Sea and describe for the first time Si cycling in the Chukchi Sea.

3.2 Methods

3.2.1 Sampling

An oceanographic expedition was conducted aboard the CCGS Sir Wilfrid Laurier from July 1st to July 21st 2006 from Victoria, Canada to Barrow, Alaska. Along the cruise track, stations were chosen in order to sample as many different water masses throughout the NE Pacific and Bering and Chukchi Seas as possible (Table 3.1 and Fig. 3.1). Stations located in the sub-Arctic current, the Alaska Gyre and the Alaskan Stream were defined by latitude and longitude alone, as density was not expected to be different between stations. Based on the temperature profile, another station was also sampled in a frontal zone within the Alaska gyre. The front was identified by a temperature inversion in the upper 250 m of the water column observed with the use of the CTD (data not shown). Within the Bering Sea, the sampling stations were located in the central domain of the continental shelf (Central Bering), the Anadyr Stream water mass and the Alaska Coastal Current water mass. The central shelf of the Bering Sea was defined by bottom depth ($50 < z < 100$) and salinity (average from surface to bottom of 31.6) (Coachman, 1986), while the Alaskan Stream and the Alaskan Coastal Current water masses were defined by salinity alone (>32.5 and <31.5, respectively) (Coachman, 1986). Two stations were sampled in the Chukchi Sea and both stations were located in Anadyr Stream water based on their bottom salinities of >32. The most northern station in the Chukchi Sea was also influenced by sea ice melt water as exhibited by a salinity of <30 at the surface.

Table 3.1 Latitude, longitude and bottom depth for stations sampled in the NE Pacific Ocean and the Bering and Chukchi Seas from July 1st to July 21st, 2006.

Station	Latitude (N)	Longitude (W)	Bottom Depth (m)
Sub-Arctic Current	49° 54.916’	133° 18.401’	2004
Alaska Gyre	52° 51.917’	144° 21.075’	>1000
Front	53° 26.444’	150° 17.363’	>1000
Alaska Stream	53° 41.466’	161° 55.764’	>1000
Central Bering	60° 41.503’	174° 15.570’	91
Anadyr Stream	64° 01.986’	171° 49.897’	53
Alaska Coastal Current	65° 39.710’	168° 20.263’	50
Chukchi 1	68° 05.235’	168° 21.675’	57
Chukchi 2	70° 37.970’	168° 14.393’	45

At each station, CTD casts were performed with a Sea-Bird SBE 25 to measure conductivity, temperature and pressure. CTD data was collected and processed by the Canada/US/Japan Joint Western Arctic Climate Study program (see Acknowledgements). A rosette sampler was used to collect seawater at six “irradiance” depths within the euphotic zone and four depths below the euphotic zone where bottom depth permitted. In this study, “euphotic zone” was defined as the area between the surface (100%) and the depth of the 1% surface incident irradiance. A Secchi disk was utilized to derive the relative 100, 50, 30, 10, 3 and 1% irradiance levels. A Secchi disk with a 30 cm diameter was lowered over the side of the ship immediately prior to water sampling with the rosette. The following equation was used to calculate the depth at which the light levels to be sampled occurred:

$$\text{Equation 3.1 } I_z = I_o * e^{(-k_d * z)}$$

Where I_z is the percent irradiance level at depth z, I_o is the 100% irradiance level and k_d is the attenuation coefficient. An attenuation coefficient of 1.7 was used in the NE Pacific and an attenuation coefficient of 1.4 was used in the Bering and Chukchi Seas.

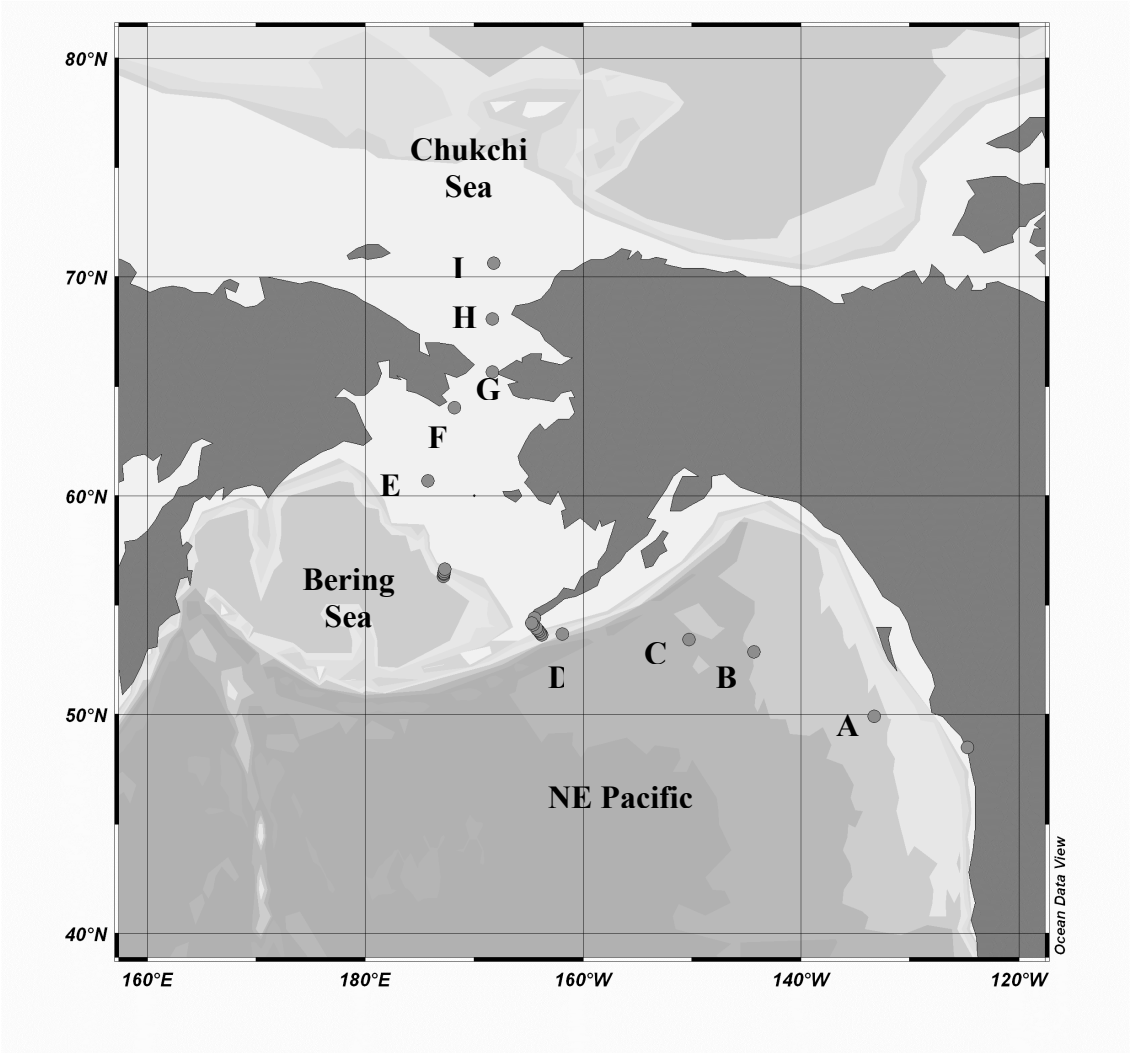

Figure 3.1 Sampling stations along a transect through the NE Pacific Ocean, Bering and Chukchi Seas from July 1st to July 21st, 2006 on board the CCGS Sir Wilfrid Laurier. Station A (sub-Arctic), B (Alaska Gyre), C (Front), D (Alaska Stream), E (Central Bering), F (Anadyr Stream), G (Alaska Coastal Current), H (Chukchi 1) and I (Chukchi 2).

3.2.2 Mixed Layer Depth Calculations

Mixed layer depths were determined according to the method outlined in Levitus (1982). The mixed layer depth was determined as the depth at which σ_τ differs by 0.125 compared to the surface value of σ_τ.

3.2.3 Chlorophyll *a* Analysis

Samples for the measurement of chl *a* (0.5 L) were collected at 6 "irradiance" depths in the euphotic zone (see section 3.2.1), and subsequently filtered on board ship onto glass fiber filters of 0.7 μm porosity. Filters were kept in the dark and frozen at -20°C until analysis ashore. Chlorophyll *a* was extracted with 90% aqueous acetone for 24 hrs at -20°C and analyzed on a 10-AU Turner Designs (Sunnydale, California) fluorometer. Samples were corrected for the occurrence of phaeopigments by degrading chl *a* with 1.0 N HCl, and subtracting the remaining phaeopigment concentration from the total (Parsons et al., 1984).

3.2.3 Dissolved Nutrient Analysis

Samples were collected in 30 mL acid-washed bottles at each depth sampled with the rosette (both within and below the euphotic zone) for the measurement of NO_3^-, PO_4^{-3} and $Si(OH)_4$. Samples were frozen at -20°C until analysis ashore. All samples were analyzed using the Astoria 2 Autoanalyzer (Astoria Pacific International, Oregon) according to the methods outlined in Barwell-Clarke and Whitney (1996). Detection limits were 0.03, 0.12 and 0.05 μmol L^{-1} for NO_3^-, PO_4^{3-} and $Si(OH)_4$, respectively.

3.2.4 Calculation of Carbon and Nitrate Incorporation Rates

Water samples to estimate C and NO_3^- incorporation rates were collected in 1.23 L polycarbonate bottles from 6 "irradiance" depths in the euphotic zone (see section 3.2.1). Samples were spiked using the double isotope method outlined in Dauchez et al. (1995). A 153 μmol L^{-1} addition of 99% ^{13}C enriched H_2CO_3 and a 0.1 μmol L^{-1} addition of 99% ^{15}N enriched Na_2NO_3 were made to the samples. Dissolved inorganic carbon (DIC) concentrations in the surface waters of this area of the ocean during this time of year are approximately 2460 μmol L^{-1} according to Wong et al. (2002). Therefore the addition of $H_2{}^{13}CO3$ was less than 10% of the total DIC present in the samples and was not expected to disturb nutrient dynamics in the samples. The percent of the total NO_3^- that the $Na_2{}^{15}NO_3^-$ addition contributed to the samples was typically below 1% in the NE Pacific. In the surface waters of the Bering and Chukchi Seas, where NO_3^- concentrations were drawn down below the detection limit of 0.05 μM, it was not possible to determine the % addition of NO_3^-. Where NO_3^- concentrations were detectable in the Bering and Chukchi seas, percent additions were usually below 10% but reached as high as 161% at the 7m depth in the Alaskan Coastal Current water and 200% at the 14m depth at the Chukchi 1 station.

Samples enriched with ^{13}C and $^{15}NO_3^-$ were incubated for 24 hrs in on-deck incubators and kept at ambient surface seawater temperature by pumping surface sea water through the incubators. Water temperature within the incubators remained at no more than 2-3°C above that of ambient surface water temperatures. This temperature increase was deemed to be acceptable by Lee et al. (2007) who conducted similar incubation experiments in the Bering and Chukchi Seas. Samples were screened with

neutral density screening in order to simulate irradiance levels of 100, 50, 30, 10, 3 and 1% of surface irradiance.

After 24 hrs, the samples were filtered onto 0.7 μm pore-size pre-combusted glass fiber filters and stored at -20°C until analysis. Upon analysis, samples were dried at 60°C for 48 hrs and prepared for isotopic and elemental analysis by mass spectrometry at the Stable Isotope Facility at the University of California, Davis. Both the ^{13}C and ^{15}N enrichment signals and the PC and PN concentrations from the incubated samples were determined. Carbon and NO_3^- incorporation rates were calculated according to equations (2) and (3) in Dugdale and Wilkerson (1986):

Equation 3.2

$$V_c = 1 / T * \ln (^{15}N_{enr} - (F)) / (^{15}N_{enr} - {}^{15}N_s) \quad (2)$$

where V_c is the specific uptake rate of NO_3^- (per unit time) assuming the uptake rate does not change over the course of the experiment, T is the time duration of the experiment, N_{enr} is the atom% ^{15}N in the initially labeled fraction, F is equal to $^{15}N_s - {}^{15}N_{xs}$, N_s is the atom% ^{15}N in the sample and N_{xs} is the atom % ^{15}N excess in the sample. The incorporation rate specific to PN was then calculated:

Equation 3.3

$$\rho_c = V_c \times PN_c \quad (3)$$

where ρ_c is the absolute NO_3^- incorporation rate in units of concentration per unit time and PN_c is the PN concentration at time t. For the calculation of C incorporation rates, N can be replaced with C, and PN can be replaced with PC. Carbon incorporation is used to estimate total primary production. Nitrate incorporation is used to determine new

production (Dugdale and Goering, 1967) by calculating the amount of carbon production that NO_3^- uptake contributes.

3.2.5 Particulate Carbon and Nitrogen Analysis

Particulate C and N concentrations were measured from material accumulated on the same filters used for the determination of C and NO_3^- incorporation rates (see above). Particulate C and PN were analyzed with an elemental analyzer at the Stable Isotope Facility at the University of California, Davis. Both were measured after the C and N incubation period of 24 hr. In order to obtain initial (ambient) values, the incorporation of C and NO_3^- by phytoplankton over a 24 hr period (see section 3.2.4 for calculations) was subtracted from the PC and PN concentrations obtained at the end of the incubation.

3.2.6 Total Particulate Silica Analysis

Total particulate silica (PSi) is the sum of BSi and LSi concentrations in a given water sample. Seawater samples for the measurement of BSi concentrations (2-L) were collected from each depth (within and below the euphotic zone) and filtered onto a 0.65 μm polycarbonate filter. Filters were stored at -20°C until analysis. Biogenic silica was measured using the method outlined in Brzezinski and Nelson (1989). Samples were read on a Beckman DU 350 spectrophotometer at 810 nm. Biogenic silica samples from the Bering and Chukchi Seas were corrected for lithogenic interference according to the method outlined in Chapter 2. In the NE Pacific, LSi concentrations were below 0.05 μmol L^{-1}; based on previous studies (Krausse et al., 1983; Paasche, 1980) and the results described in Chapter 2, concentrations of LSi <0.05μmol L^{-1} would not have significantly

affected BSi concentrations. Therefore, NE Pacific samples were not corrected for LSi interference.

Lithogenic silica concentrations were measured using the same filter from which BSi was analyzed. The analysis of LSi followed the method described in Brzezinski and Nelson (1989). Lithogenic silica concentrations from the Bering and Chukchi Seas were corrected for dissolution of BSi during the NaOH digestion according to the method outlined in Chapter 2. The amount of LSi, which would have dissolved during treatment of the samples fro BSi, was added to the measured LSi concentration values.

3.2.7 Calculation of Biogenic Silica Net Incorporation

Biogenic silica net incorporation represents the net incorporation of Si into silica (SiO_2) frustules (BSi) by all siliceous organisms. In order to determine BSi net incorporation, 2 L of seawater from 6 depths within the euphotic zone and 4 depths below the euphotic zone were collected and incubated for 48 hrs. Samples from the euphotic zone were incubated on deck using the same method as outlined for C and NO_3^- uptake (Section 3.2.4). Samples taken from below the euphotic zone were stored in the dark in refrigeration units set at temperatures matching *in situ* water temperatures. After 48 hrs, incubated samples were filtered onto 0.65 μm polycarbonate filters and filters were stored at -20°C until analysis. Daily BSi net incorporation rates were calculated with the following equation:

Equation 3.4

$$\text{BSi net incorporation} = (BSi_{inc} - BSi_o)/ t * (\text{units = concentration per unit time})$$

where BSi_{inc} is the BSi concentration in incubated samples, BSi_o is the BSi concentration at t = 0 (initial or ambient), and t is the incubation time. Positive rates of BSi net incorporation indicate that more BSi is being incorporated by siliceous organisms than is being dissolved. Negative BSi net incorporation rates indicate net dissolution.

3.2.8 Calculation of Particulate Elemental Ratios

Particulate elemental ratios of C, N and Si were calculated by dividing one ambient particulate value by another, e.g. PC / PN (mol:mol).

3.2.9 Calculation of Depth-Integrated Values

Carbon and NO_3^- uptake rates and PC and PN concentrations were integrated through the euphotic zone using a trapezoidal method (Massana and Pedrosalio, 1994). Depth-integrated BSi concentrations and BSi net incorporation were calculated for both the euphotic zone and for the entire depth of the water column sampled. C and N data was normalized to euphotic zone depth; these 'normalized' values are useful when comparing stations with euphotic zones of different depths. BSi concentrations and BSi net incorporation rates were normalized by the depth of the euphotic zone to compare with C and N data, and also by the depth of the entire water column sampled to compare with other BSi samples.

3.2.10 Statistical Analysis

All statistical analyses were conducted using Statistical Package for Social Sciences (SPSS) 15.0 for Windows. A significance level of $p<0.05$ was used for all tests. A discriminant function analysis was run in order to determine if the regions into which the stations were classified are appropriate. This statistical test requires that stations are

assigned into groups (or 'regions' in this case). A set of weightings are produced for the groups that allows the groups to be distinguished from each other. The test then 'un-assigns' one station at a time and uses the weightings to determine what group the station belongs too (Dytham, 2003). The discriminant function analysis reports whether each station was correctly 're-assigned' to the proper group.

Once the appropriateness of the regions into which the stations were classified was determined, depth-integrated and euphotic zone normalized variables were averaged by region. ANOVA's were run to determine if there were differences between regions in the average depth-integrated variables. If the variances of the variables were not homogeneous (a requirement for running an ANOVA), the non-parametric version of ANOVA, a Kruskal-Wallis test, was run. If a significant result was found using the Kruskal-Wallis test, then Mann-Whitney tests were run to determine which of the three regions differed from each other.

3.3 Results

3.3.1 Temperature, Salinity and Density

Mixed layer depth (Fig. 3.2) ranged from 3 m to 30 m along the transect and showed no trend between regions. Mixed layer seawater temperatures in the NE Pacific were typically between 8 and 12°C and decreased to 4°C below the thermocline (Fig. 3.2A, B, C and D). Surface seawater temperatures above the thermocline in the Bering Sea were as high as 7°C (Fig. 3.2E, F and G), while in the Chukchi Sea they were as low as -0.5°C (Fig. 3.2I). Temperatures below the thermoclines in the Bering and Chukchi Seas ranged from 2 to -2°C (Fig. 3.2E, F, G, H and I). Salinity at the Central Bering

station ranged from 31.3 to 31.9. Anadyr Stream deep water displayed salinities above 32.5. Salinity in the Alaskan Coastal Current ranged from 30.8 to 31.6. Salinity at Chukchi 1 was between 32.1 and 32.3 and Chukchi 2 it ranged from 29.2 to 32.8.

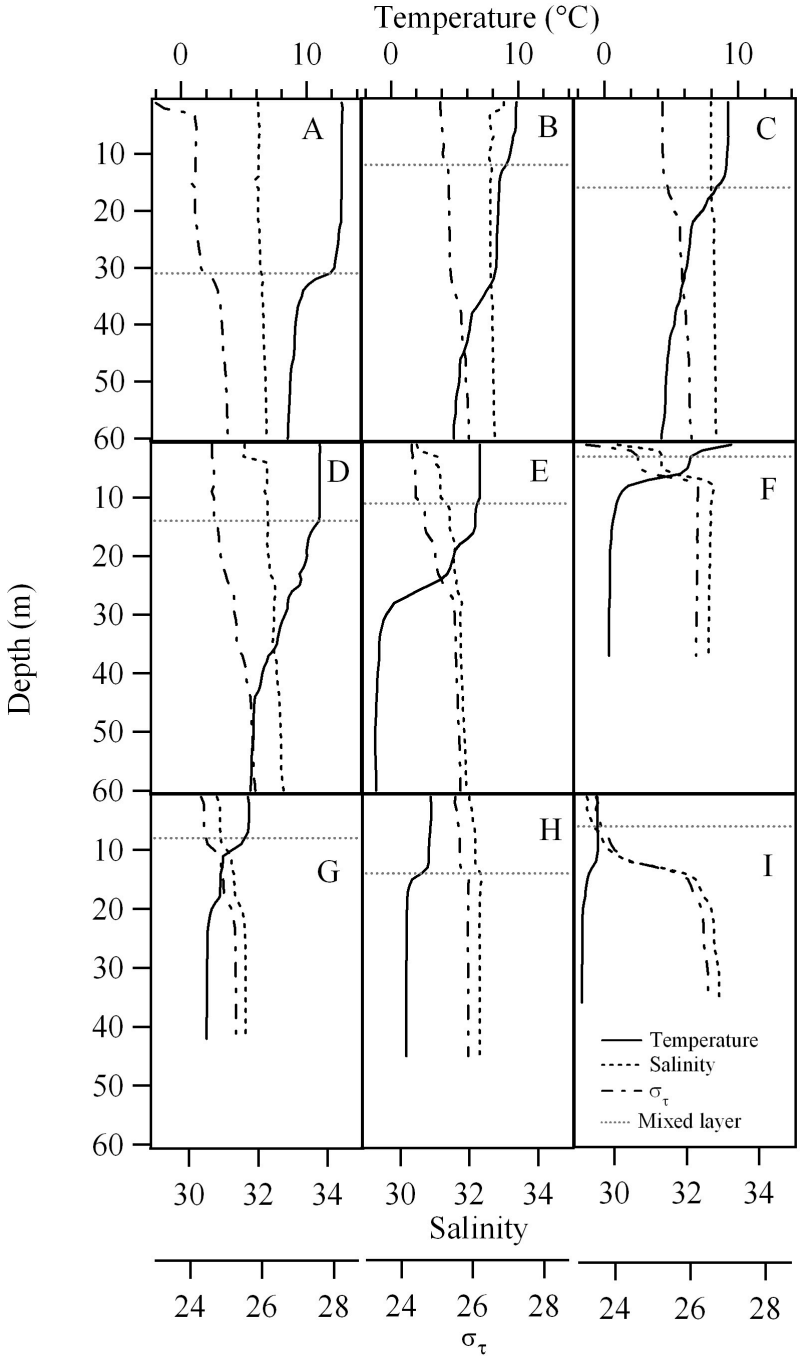

Figure 3.2. Temperature, salinity, sigma-theta (σ_τ), and mixed layer depth for stations in the NE Pacific Ocean, Bering and Chukchi Seas during the July 2006 cruise. A: Sub-Arctic Current, B: Alaska Gyre, C: Front, D: Alaska Stream, E: Central Bering, F: Anadyr Stream, G: Alaska Coastal Current; H: Chukchi 1, I: Chukchi 2. CTD data was collected and processed by the Canada/US/Japan Joint Western Arctic Climate Study program (see Acknowledgements).

3.3.2 Chlorophyll *a* Concentrations

Chlorophyll *a* concentrations differed between the three regions. In the NE Pacific chl *a* never exceeded 0.5 μg L^{-1} except at the Alaska Stream station, where concentrations reached 1.1 μg L^{-1} (Fig. 3.3A). Chlorophyll *a* from the Bering Sea and the Chukchi Sea was presented in Chapter 2 in order to explain trends in BSi data. The same chl *a*, BSi and LSi data will be presented in this chapter in order to compare to NE Pacific data. Chlorophyll *a* was relatively low (<1 μg L^{-1}) at the Central Bering station and the Alaska Coastal Current station (Fig. 3.3B). Maximum chl *a* concentrations for this region were seen at the Anadyr Stream site where they reached 1.9 μg L^{-1} (Fig. 3.3B). The Chukchi Sea had the highest chl *a* concentrations at depth of the three regions in this study (Fig. 3.3C). Maximum chl *a* concentrations in the Chukchi Sea were 4.2 and 7.8 μg L^{-1} at 21 m and 15 m (3% I_o) at stations Chukchi 1 and Chukchi 2, respectively. Depth-integrated values for chl *a* showed similar trends (Table 3.2) to those seen in the vertical profiles (Fig. 3.3). Normalized depth-integrated values were highest in the Chukchi Sea (2.86 and 3.81 mg m^{-3}), and relatively low in both the Bering Sea (0.36 to 1.28 mg m^{-3}) and the NE Pacific Ocean (0.20 to 0.76 mg m^{-3}).

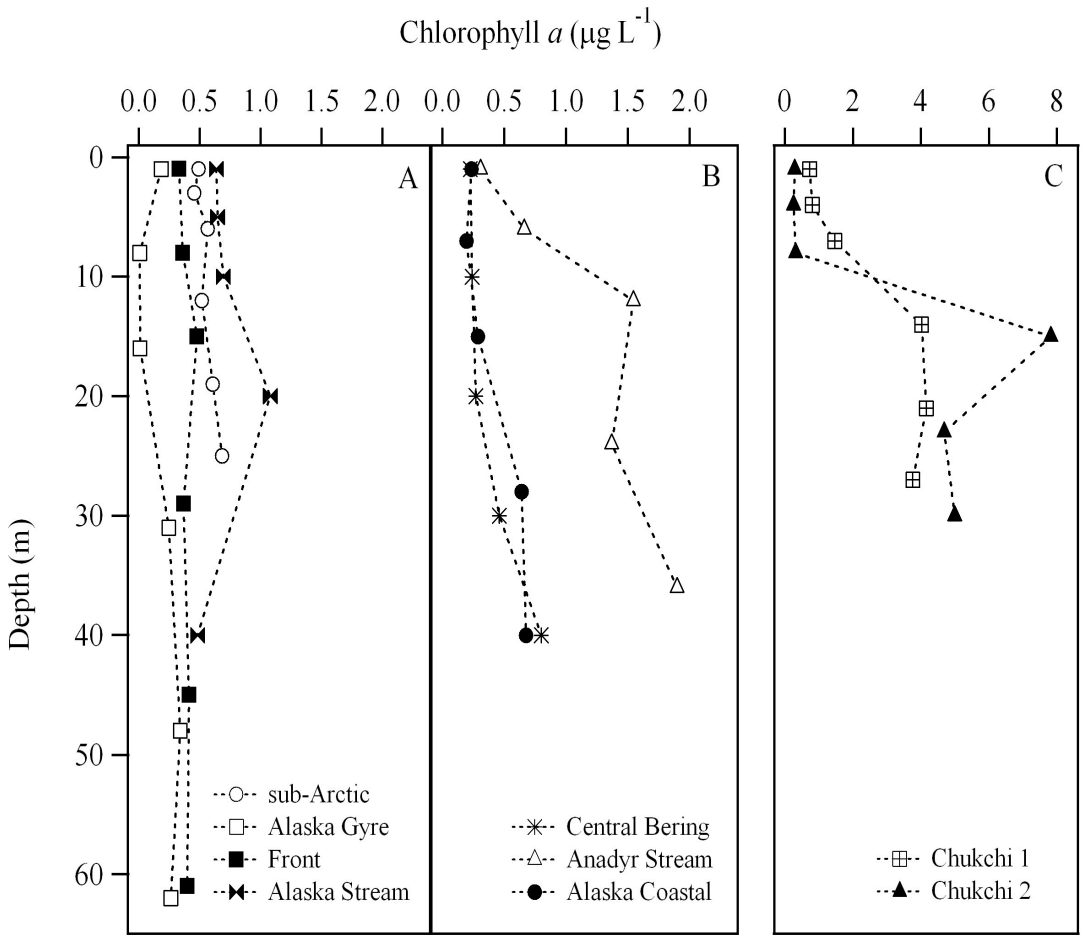

Figure 3.3. Vertical profiles of chlorophyll *a* concentrations (µg L^{-1}) for the NE Pacific (A), the Bering Sea (B) and the Chukchi Sea (C). Note the different x-axis in panels A and B compared to panel C. Chlorophyll *a* was measured at 6 depths within the euphotic zone corresponding to the 100, 50, 30, 10, 1% light levels.

Table 3.2 Depth-integrated chl *a*, PC, PN and BSi concentrations, and rates of C, N and Si incorporation. The first column for each parameter represents areal integrations (per m^{-2}) and the second column shows the depth-integration normalized by the depth of the euphotic zone.

	Chlorophyll *a*		Particulate Carbon		Particulate Nitrogen		Biogenic Silica		Carbon incorporation		Nitrate incorporation		BSi net incorporation	
Station	mg m^{-2}	mg m^{-3}	mmol m^{-2}	mmol m^{-3}	mmol m^{-2}	mmol m^{-3}	mmol m^{-2}	mmol m^{-3}	mmol m^{-2} day^{-1}	mmol m^{-3} day^{-1}	mmol m^{-2} day^{-1}	mmol m^{-3} day^{-1}	mmol m^{-2} day^{-1}	mmol m^{-3} day^{-1}
Sub-Arctic	13.5	0.54	192	7.7	36.5	1.5	6.3	0.25	16.8	0.67	1.05	0.042	0	0
Alaska Gyre	11.8	0.20	276	4.5	46.3	0.75	18.9	0.3	20.6	0.33	1.14	0.018	7.5	0.30
Front	24.0	0.39	290	4.8	53.4	0.9	36.6	0.6	32.9	0.54	2.23	0.037	5.9	0.10
Alaska Stream	30.4	0.76	278	7.0	60.0	1.5	11.9	0.3	41.0	1.0	1.48	0.037	3.3	0.08
Central Bering	14.6	0.36	322	8.0	50.9	1.3	60.6	1.5	10.4	0.26	2.88	0.072	5.0	0.12
Anadyr Stream	46.2	1.28	405	11.3	65.3	1.8	294	8.2	50.9	1.4	4.26	0.12	-125	-3.5
Alaskan Coastal Current	17.2	0.43	309	7.7	51.4	1.3	61.9	1.5	16.5	0.41	0.40	0.010	-12.8	-0.32
Chukchi 1	77.2	2.86	723	26.8	131	4.8	124	4.6	68.4	2.5	1.54	0.057	24.4	0.86
Chukchi 2	114	3.81	596	19.9	89.7	3.0	191	5.2	94.5	3.2	6.42	0.21	0.86	0.03

3.3.3 Particulate Carbon and Nitrogen

Particulate C and N concentrations followed the same trends between regions (Fig. 3.4 and 3.5) as seen with the chl *a* data. Within the NE Pacific, PC and PN concentrations were lowest at the Alaska Gyre and Front stations, ranging from 3.2 to 6.6 μmol L^{-1} and from 0.5 to 1.3 μmol L^{-1}, respectively. Particulate C concentrations were slightly higher at the sub-Arctic and Alaskan Stream stations, ranging from 4.8 to 10.7 μmol L^{-1}, while PN concentrations ranged from 0.68 to 2.2 μmol L^{-1} at the same stations. Concentrations of PC and PN were slightly higher at the three Bering Sea stations than in the NE Pacific. PC concentrations ranged from 6.4 to 13.2 μmol L^{-1} and PN concentrations ranged from 0.9 to 2.1 μmol L^{-1}. The highest concentrations of PC and PN were observed at the two stations in the Chukchi Sea. Particulate C reached 43 μmol L^{-1} and 31 μmol L^{-1} at stations Chukchi 1 and Chukchi 2 respectively, while PN reached 8.7 μmol L^{-1} and 5.6 μmol L^{-1}, respectively.

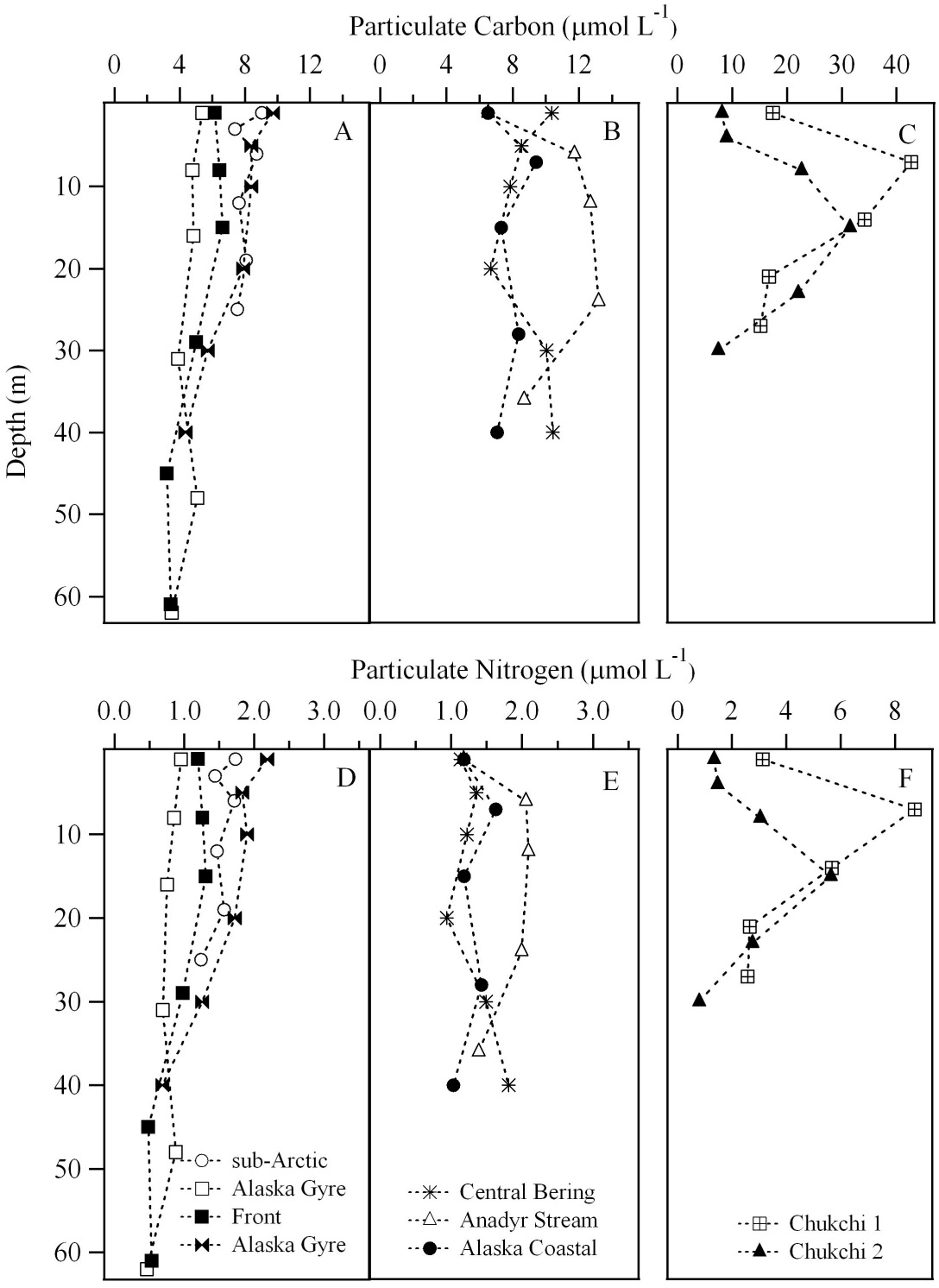

Figure 3.4. Vertical profiles of particulate carbon and particulate nitrogen concentrations (μmol L^{-1}) for stations in the NE Pacific Ocean (A and D), the Bering Sea (B and E) and the Chukchi Sea (C and F). Note the different x-axes between panels.

3.3.4 Biogenic Silica Concentrations

Biogenic silica concentrations varied between regions, but also between the water masses identified within each region. Biogenic silica was relatively low in the NE Pacific region with concentrations always below 1.0 μmol L^{-1} (Fig. 3.5A). An exception was the Front station where BSi was as high as 1.6 μmol L^{-1}. BSi was relatively high in the Bering Sea compared to values in the NE Pacific ocean (Fig. 3.5B). Concentrations at the Central Bering station and the Alaskan Coastal Current station ranged from 1.0 to 3.7 μmol L^{-1}, and 0.3 to 2.4 μmol L^{-1}, respectively. The Anadyr Stream station had BSi concentrations that were much higher than the other two stations in the Bering Sea. The highest concentration in the Anadyr Stream station was 13.5 μmol L^{-1} at a depth of 24 m (10% I_o). The two Chukchi stations showed similar depth profiles, with the highest BSi concentrations measured at the deeper depths (Fig. 3.5C). Concentrations at the Chukchi 1 station ranged from 1.6 to 10.0 μmol L^{-1}, while concentrations at Chukchi 2 ranged from 0.8 to 10.4 μmol L^{-1}.

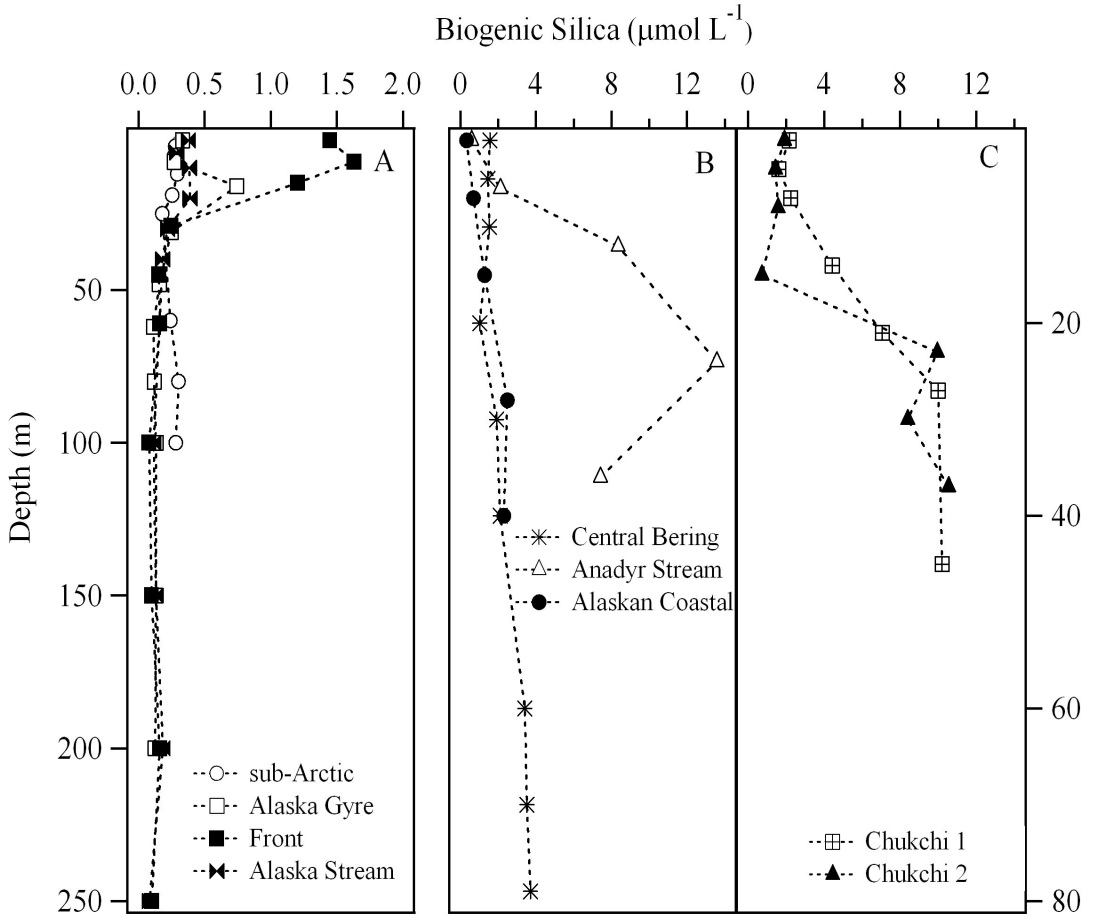

Figure 3.5. Vertical profiles of biogenic silica concentrations (μmol L^{-1}) for stations in the NE Pacific Ocean (A), the Bering Sea (B) and the Chukchi Sea (C). Vertical axis for A (left) ranges from 0 (surface) to 250 m depth. Vertical axes for B and C (right) range from 0 (surface) to 80 m depth. X-axis for A extends to 2 μmol L^{-1} only.

3.3.5 Lithogenic Silica

Lithogenic silica concentrations were lowest in the NE Pacific Ocean, never exceeding 0.06 μmol L^{-1} (Fig. 3.6A). Lithogenic silica concentrations in the Bering Sea were higher then those in the NE Pacific, but usually were below 1 μmol L^{-1} (Fig. 3.6B). The Chukchi Sea had the highest concentrations, reaching 4.84 μmol L^{-1} at Chukchi 1 (Fig. 3.6C).

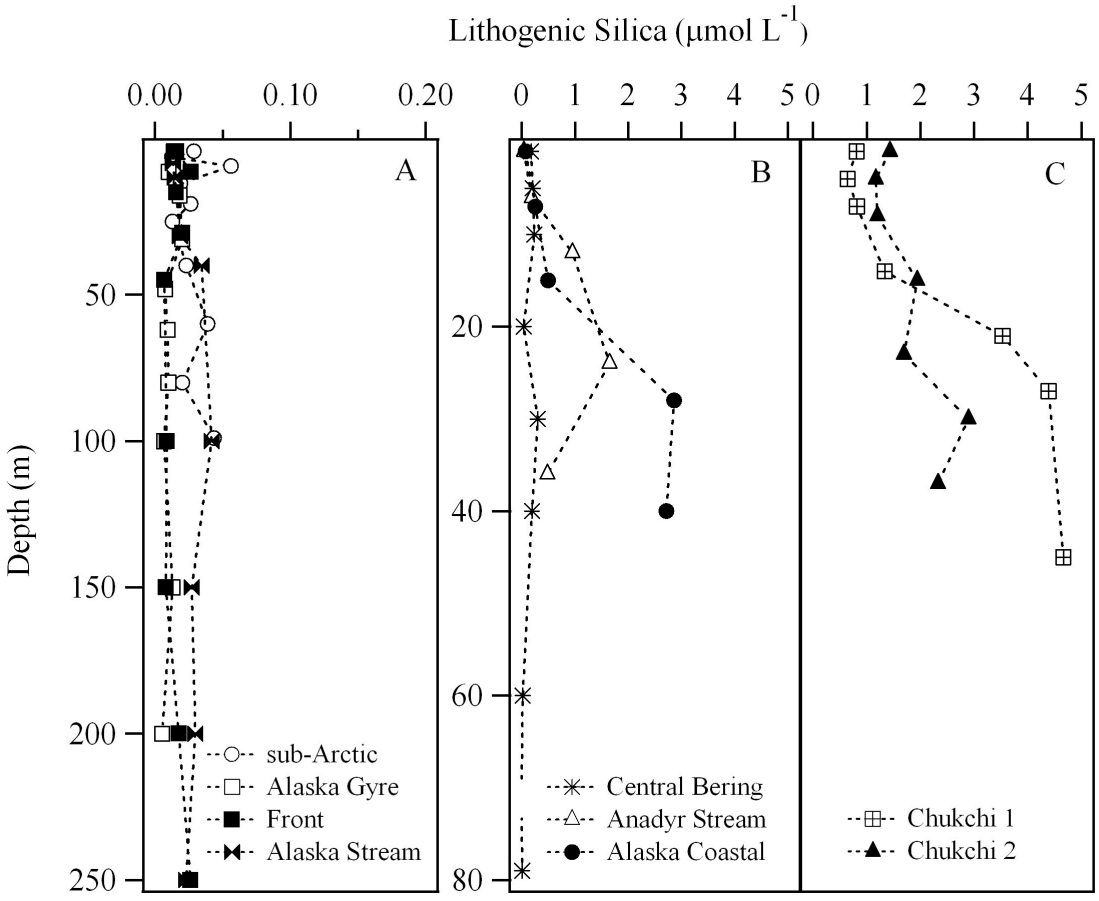

Figure 3.6. Vertical profiles of lithogenic Si concentrations (μmol L^{-1}) for the NE Pacific Ocean (A), the Bering Sea (B) and the Chukchi Sea (C). Vertical axis for panel A (left) ranges from 0 (surface) to 250 m depth. Vertical axes for panels B and C range from 0 (surface) to 80 m depth. Note the different x-axis between panels A and B and panel C.

3.3.6 Dissolved Nitrate, Silicic acid and Phosphate

Nitrate and $Si(OH)_4$ concentrations showed a wide range (from 0 to 50 and 100 μmol L^{-1}, respectively) throughout the entire area of study, while PO_4^{3-} ranged from 0.06 to 4.3 μmol L^{-1} (Fig. 3.7, 3.8 and 3.9). At the Central Bering station in the Bering Sea concentrations at depth reached 10.5 μmol L^{-1} (NO_3^-) and 34 μmol L^{-1} ($Si(OH)_4$)(Fig. 3.8A). Nitrate was below the detection limit at the surface depth at all stations in the Bering and Chukchi Seas (Fig. 3.8 and 3.9). Nitrate concentrations were particularly low

in the Alaskan Coastal Current where they were below the detection limit at every depth except for the 50% light level (0.06 μmol L^{-1}) (Fig. 3.8B). Phosphate and $Si(OH)_4$ were always above their respective detection limits but were generally lower in the Bering and Chukchi Seas than in the NE Pacific. Excluding the increase in PO_4^{3-} and $Si(OH)_4$ concentrations below 15 m at the Central Bering station, concentrations in the Bering and Chukchi Sea reached 2.7 and 17.0 μmol L^{-1}, respectively.

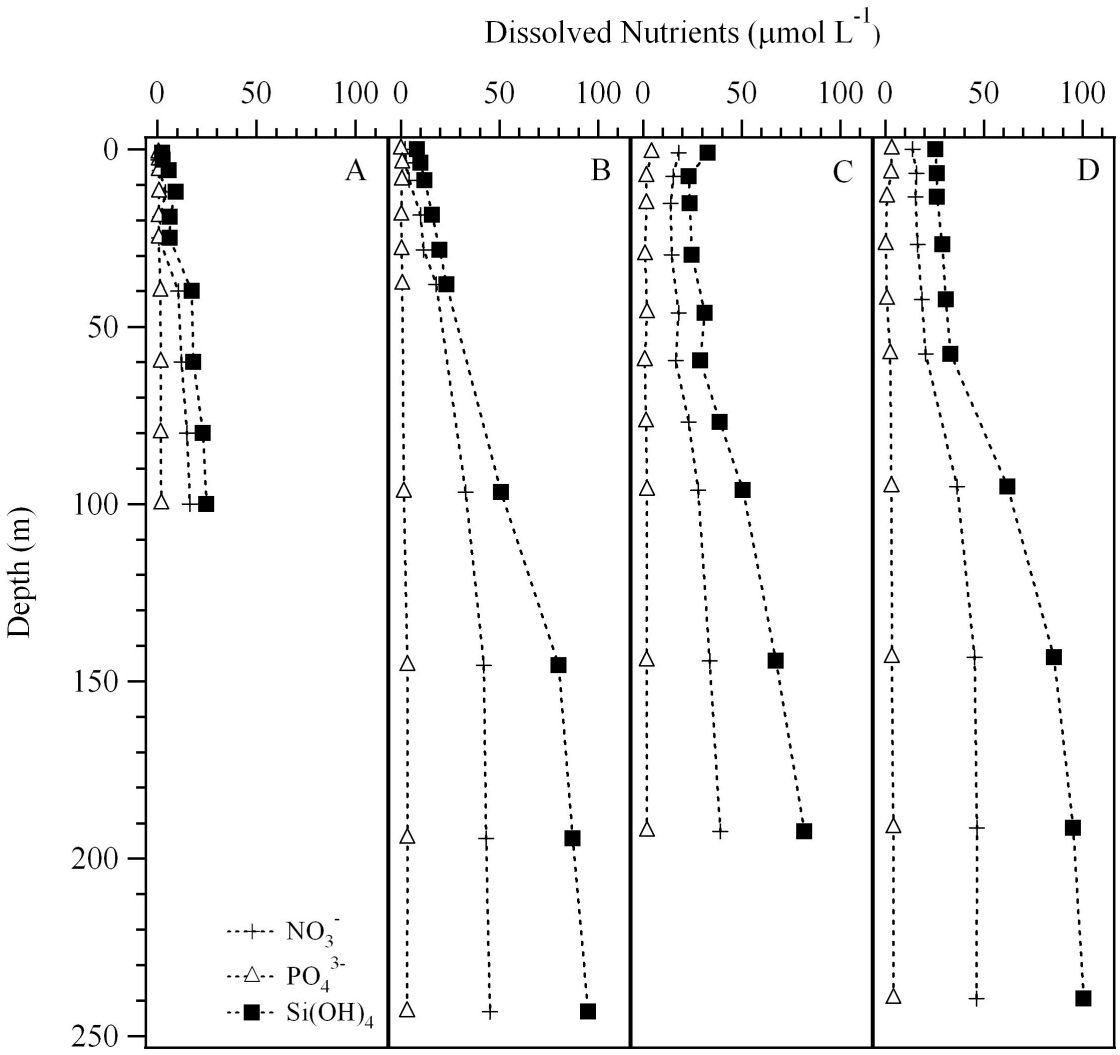

Figure 3.7. Vertical profiles of nitrate, phosphate and silicic acid concentrations (μmol L^{-1}) for the NE Pacific stations sub-Arctic Current (A), Alaska Gyre (B), Front (C) and Alaska Stream (D).

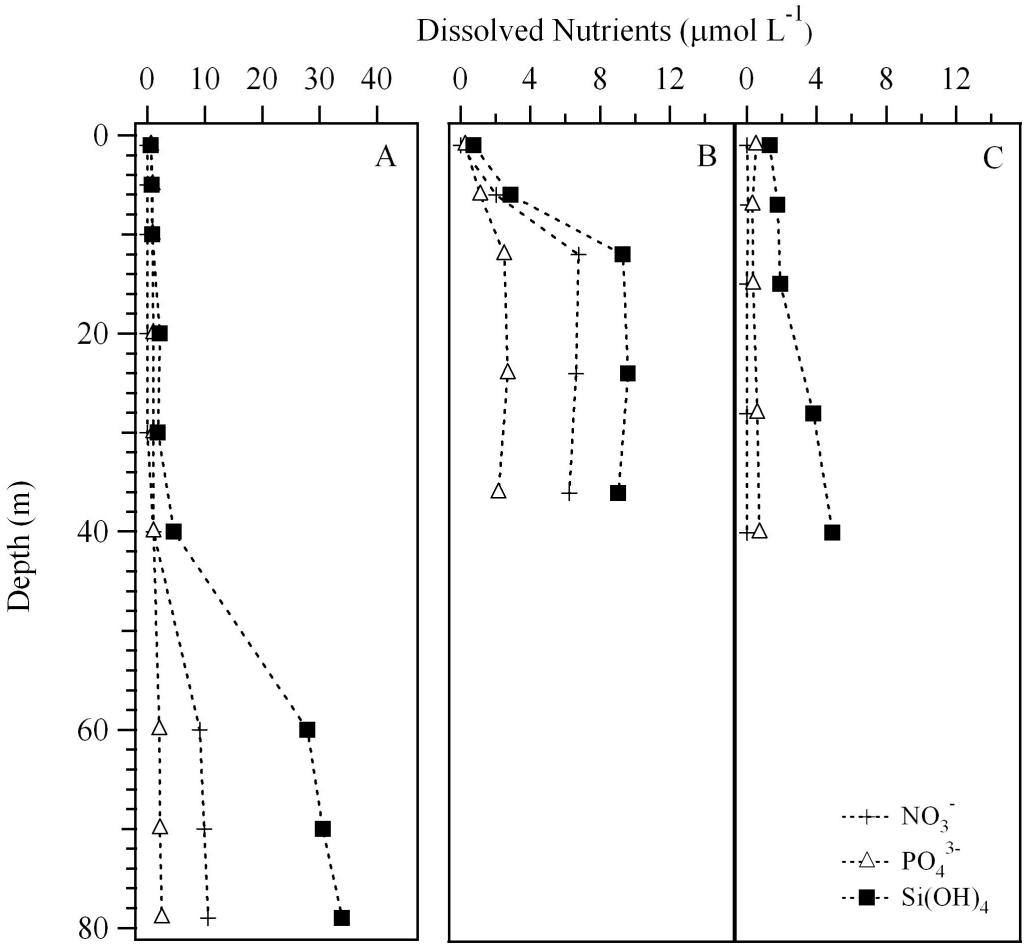

Figure 3.8. Vertical profiles of nitrate, phosphate and silicic acid concentrations (μmol L^{-1}) for Bering Sea stations Central Bering (A), Anadyr Stream (B), and Alaska Coastal Current (C). Note the different x-axis between panel A and panels B and C.

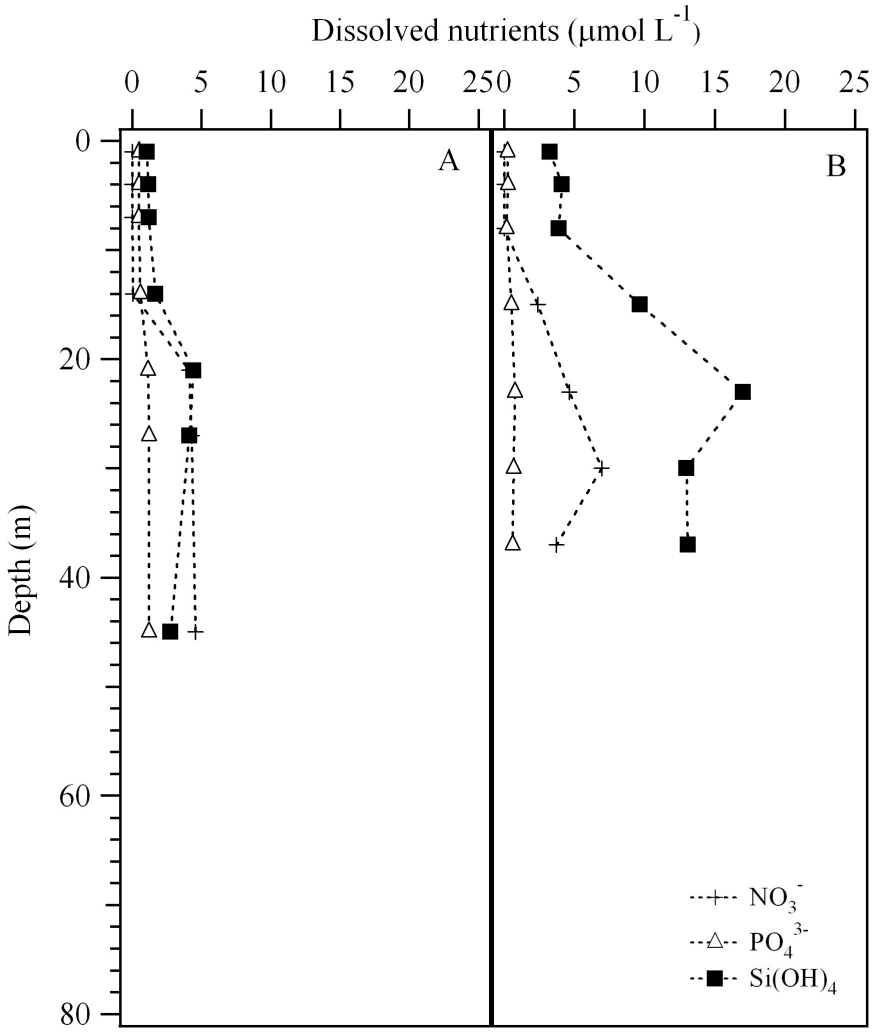

Figure 3.9. Vertical profiles for nitrate, phosphate and silicic acid concentrations (μmol L^{-1}) for Chukchi stations 1 (A) and 2(B). Note the difference in x-axis between Figures 3.8, 3.9 and 3.10.

3.3.7 Carbon and Nitrate Incorporation Rates

Carbon incorporation rates were lower in the NE Pacific Ocean (Fig. 3.10A, B, C and D) and the Bering Sea (Fig. 3.10E, F and G) compared to the Chukchi Sea (Fig. 3.10H and I). Carbon incorporation in the NE Pacific Ocean ranged from 0.02 to 2.0 μmol L^{-1} day^{-1}, while C incorporation rates in the Bering Sea ranged from 0.05 to 2.9 μmol L^{-1} day^{-1} through the euphotic zone. The Chukchi 1 and 2 stations exhibited

maximum rates at the 30% and 10% surface irradiance levels, respectively. The maximum C incorporation rate at Chukchi 1 was 6.1 μmol L^{-1} day^{-1} while the maximum at Chukchi 2 was 10.9 μmol L^{-1} day^{-1}. Depth-integrated normalized rates of C incorporation in the NE Pacific ranged from 0.33 to 1.0 mmol m^{-3} day^{-1} (Table 3.2). Carbon incorporation in the Bering Sea was highest at the Anadyr Stream station (1.4 mmol m^{-3} day^{-1}). The Chukchi Sea showed the highest rates of C incorporation at 2.5 and 3.2 mmol m^{-3} day^{-1} at station Chukchi 1 and Chukchi 2, respectively.

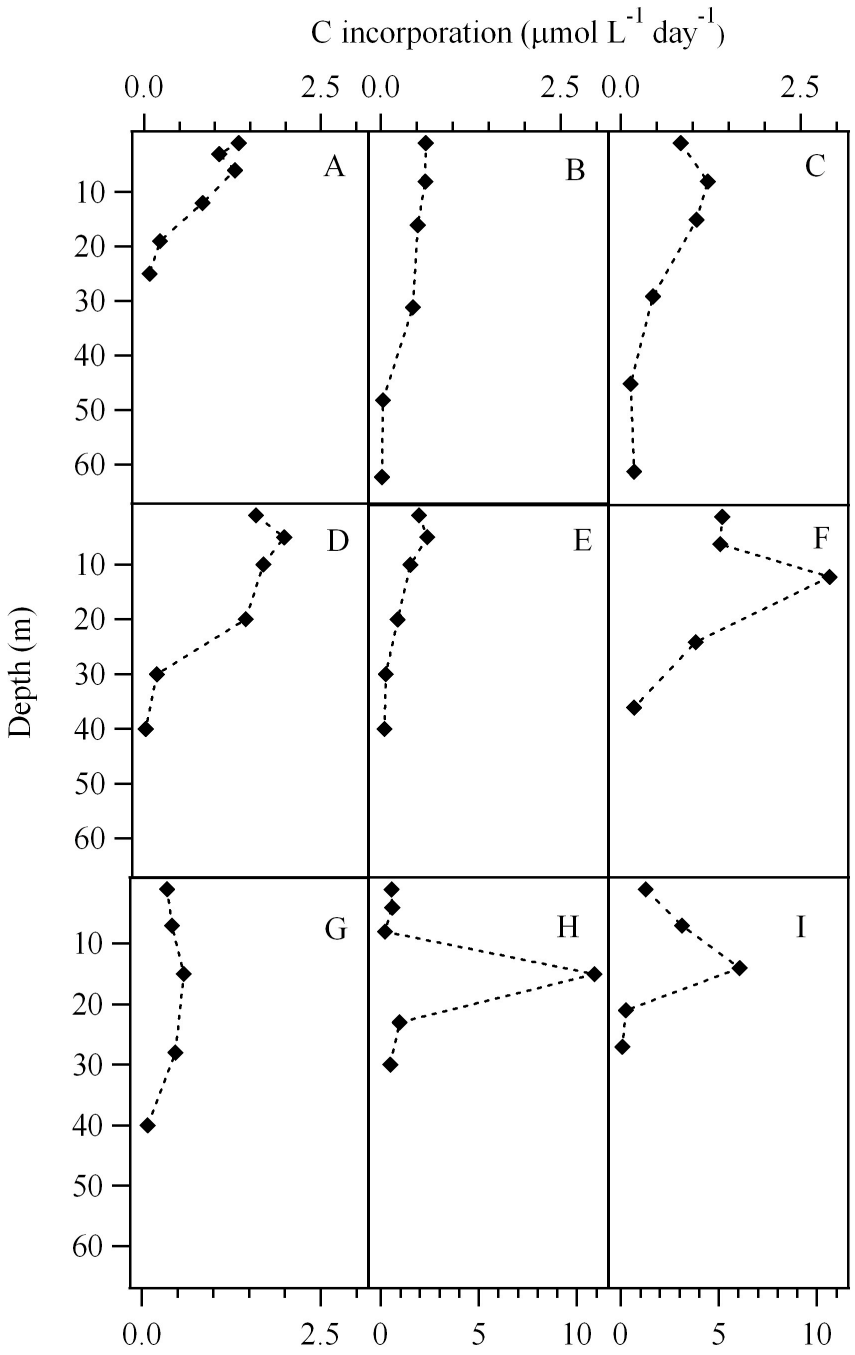

Figure 3.10. Vertical profiles of C incorporation rates (μmol L^{-1} day^{-1}) for all stations: sub-Arctic current (A), Alaska Gyre (B), Front (C), Alaska Stream (D), Central Bering (E), Anadyr Stream (F), Alaska Coastal Current (G), Chukchi 1 (H) and Chukchi 2 (I). Note the different x-axis scale for (H) and (I).

Nitrate incorporation rates were not uniform within each region, but instead were specific to the water mass within which they were measured. In the NE Pacific Ocean,

NO_3^- incorporation rates were lowest in the sub-Arctic Current (Fig. 3.11A) and the Alaska Gyre (Fig. 3.11B), ranging from 3.0 to 83 nmol L^{-1} day^{-1} and 0 to 57 nmol L^{-1} day^{-1} throughout the euphotic zone, respectively. In the Front (Fig. 3.11C) and Alaska Stream (Fig. 3.11D) water masses, the NO_3^- incorporation rates reached 137 and 92 nmol L^{-1} day^{-1}, respectively. In the Bering Sea, rates reached 290 nmol L^{-1} day^{-1} at the Anadyr Stream station (Fig. 3.11F); this contrasted with the Alaskan Coastal Current station (Fig. 3.12G) where incorporation rates ranged from 0.5 to 28 nmol L^{-1} day^{-1}. Nitrate incorporation rates were highest for the entire transect at Chukchi 1 and 2 (Fig. 3.11H and I); at Chukchi 2, rates ranged from 263 to 484 nmol L^{-1} day^{-1} at the three bottom depths.

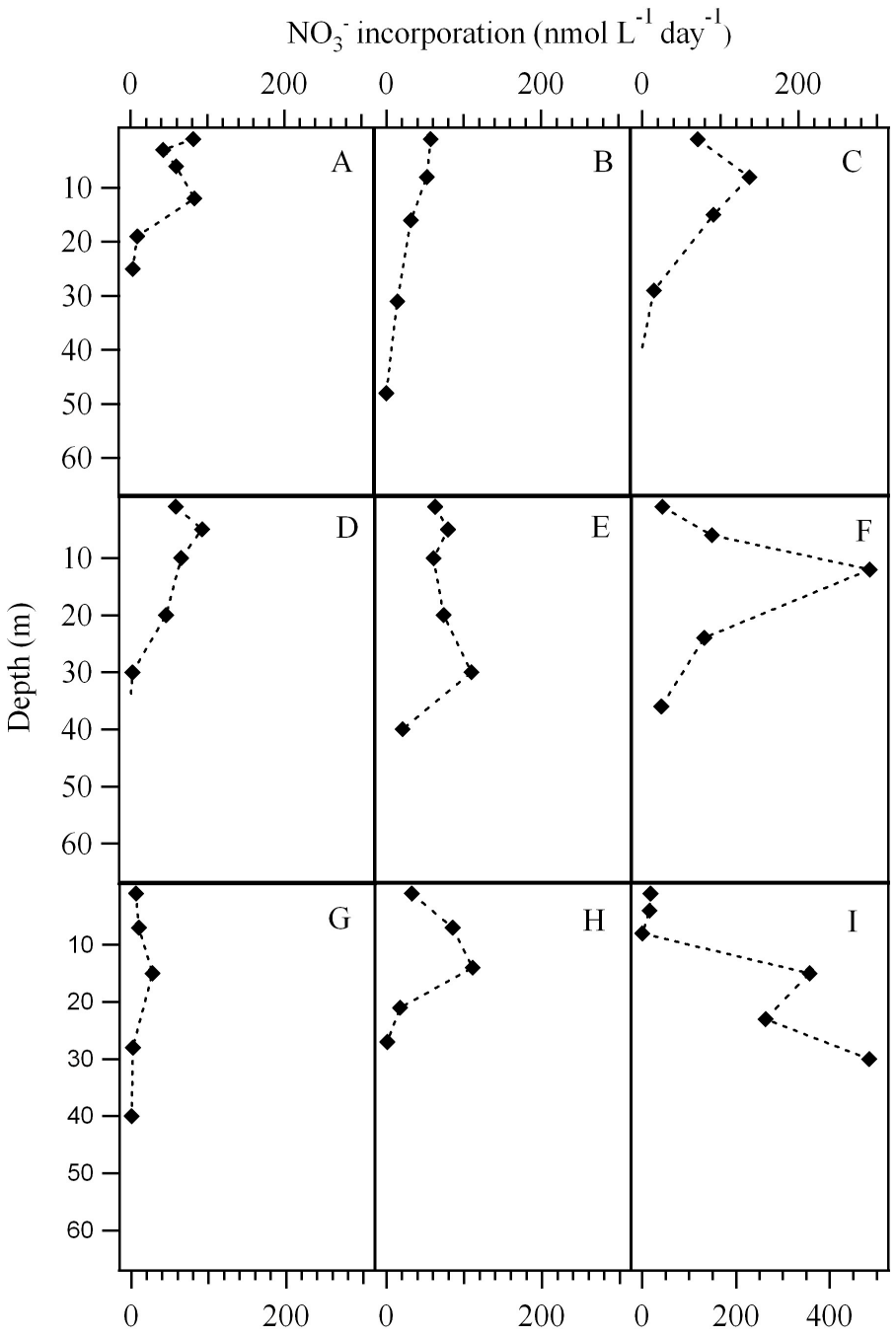

Figure 3.11. Vertical profiles of nitrate incorporation rates (nmol L^{-1} day^{-1}) for all stations: sub-Arctic current (A), Alaska Gyre (B), Front (C), Alaska Stream (D), Central Bering (E), Anadyr Stream (F), Alaska Coastal Current (G), Chukchi 1 (H) and Chukchi 2 (I). Note the different x-axis scale on (I).

3.3.8 Biogenic Silica Net Incorporation Rates

Biogenic silica net incorporation rates were low in the NE Pacific Ocean (Fig 3.12A, B, C and D), ranging from -1 to 0.76 μmol L^{-1} day^{-1}. Net incorporation occurred throughout the euphotic zone, while net dissolution was measured below the euphotic zone at each station. In the Bering Sea, the Central Bering station showed a similar depth profile as stations in the NE Pacific, with net incorporation in the euphotic zone and net dissolution below the euphotic zone (Fig. 3.12E). At the Anadyr Stream station there was high BSi net dissolution rates throughout the entire water column ranging from -0.25 to -6.0 μmol L^{-1} day^{-1} (Fig. 3.12F). The Alaska Coastal Current station exhibited net dissolution at each depth except the surface depth; net dissolution rates reached -0.65 μmol L^{-1} day^{-1} (Fig. 3.12G). Both stations in the Chukchi Sea had relatively high rates of BSi net incorporation in the upper the water column, with net dissolution measured at the deeper depths (Fig. 3.12H and I). Biogenic silica net production rates in the Chukchi Sea ranged from -6.1 to 6.3 μmol L^{-1} day^{-1}. Depth-integrated euphotic zone normalized BSi net incorporation was low but positive in the NE Pacific Ocean (Table 3.2). The highest net incorporation rate was at the Chukchi 1 station at 0.86 mmol m^{-3} day^{-1}.

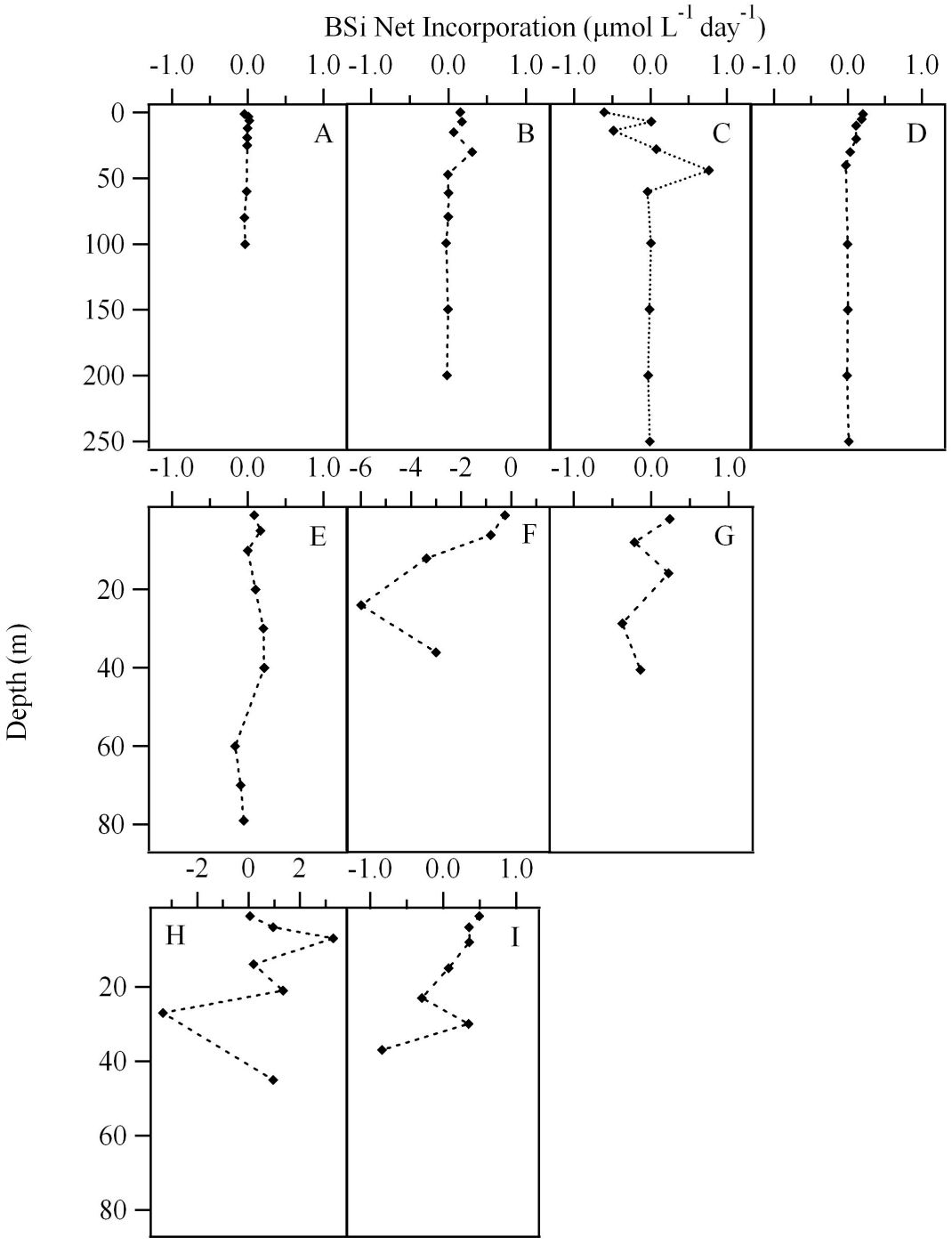

Figure 3.12. Vertical profiles of biogenic silica net incorporation rates (µmol L^{-1} day^{-1}) for all stations: sub-Arctic current (A), Alaska Gyre (B), Front (C), Alaska Stream (D), Central Bering (E), Anadyr Stream (F), Alaska Coastal Current (G), Chukchi 1 (H) and Chukchi 2 (I). Note the different x-axis of F and H.

Table 3.3 Depth-integrated particulate elemental ratios and incorporation ratios for all stations sampled. The subscript 'inc' denotes incorporation rates. Note that BSi_{inc} represents net incorporation. Negative incorporation ratios are included for completeness, but do not necessarily have biological relevance.

Station	C:N	C_{inc}:N_{inc}	BSi:C	BSi_{inc}:C_{inc}	BSi:N	BSi_{inc}:N_{inc}
Sub-Arctic Current	5.1	15.8	0.07	0	0.38	0
Alaska Gyre	5.9	17.8	0.07	0.91	0.41	16.2
Front	5.6	14.7	0.10	0.19	0.56	2.72
Alaska Stream	3.0	26.9	0.03	0.08	0.13	2.15
Central Shelf	4.1	3.6	0.12	0.46	0.76	1.7
Anadyr Stream	6.0	11.9	0.68	-2.5	4.3	-29.7
Alaska Coastal Current	5.9	4.1	0.20	-0.78	1.2	-3.2
Chukchi 1	5.5	43.6	0.15	0.34	0.92	15.0
Chukchi 2	6.8	15.0	0.29	0.01	2.4	0.14

3.3.9 Depth Integrated Particulate Carbon, Nitrogen and Biogenic Silicon Concentrations and Incorporation Rates

Integrated particulate concentrations normalized to euphotic zone depth are shown in Fig. 3.13. Integrated concentrations of PC were lowest in the NE Pacific (4.5-7.7 mmol m^{-3}), higher in the Bering Sea (8.0-11.3 mmol m^{-3}) and highest in the Chukchi Sea (26.8 and 9.9 mmol m^{-3}). In the NE Pacific, PN was higher than integrated BSi, while in the Bering and Chukchi Seas, integrated PN was approximately the same concentration or lower than BSi values. Integrated PN values ranged from 0.7 to 1.5 mmol m^{-3} in the NE Pacific Ocean, 1.3 to 1.8 mmol m^{-3} in the Bering Sea, and 4.8 and 3.0 mmol m^{-3} in the

Chukchi Sea. Integrated BSi ranged from 0.25 to 0.6 mmol m^{-3} in the NE Pacific Ocean. In the Bering Sea, at stations Central Bering and Alaskan Coastal Current, the integrated values for BSi were 1.5 mmol m^{-3} day^{-1}, while for the Anadyr Stream station, BSi was much higher, with a value of 8.0 mmol m^{-3} day^{-1}. At 6.7 and 5.2 mmol m^{-3} day^{-1}, the integrated BSi values in the Chukchi Sea were higher than values throughout the rest of the transect except for the Anadyr Stream station (Table 3.2).

3.3.10 Particulate Elemental Stoichiometry

Integrated particulate ratios of C:N, BSi:C and BSi:N through the euphotic zone are presented in Table 3.3. C:N ratios were below the Redfield ratio of 6.6 everywhere except for the Chukchi 2 station, where the average PC:PN ratio was 6.8. BSi:PC ratios were above the Brzezinski (1985) ratio of 0.11 in the Bering and the Chukchi Sea, but not the NE Pacific Ocean. Integrated BSi:PC ratios were especially high at the Anadyr Stream station (0.68) and at the Chukchi 2 station (0.29). The BSi:PN ratios were lower than the Brzezinski (1985) ratio (0.9) in the NE Pacific, but above the Brzezinski ratio at all stations in the Bering and Chukchi Seas, except for the Bering Shelf station.

Integrated ratios of incorporation rates (and net incorporation for BSi) are shown in Table 3.3. Ratios involving BSi net incorporation should be treated as a rough estimate since net incorporation of Si is being compared to absolute incorporation of C or N. Incorporation ratios exhibit a large range and are often well above the Redfield/Brzezinski ratio. No trends are apparent between regions and incorporation rates appear to be water mass specific.

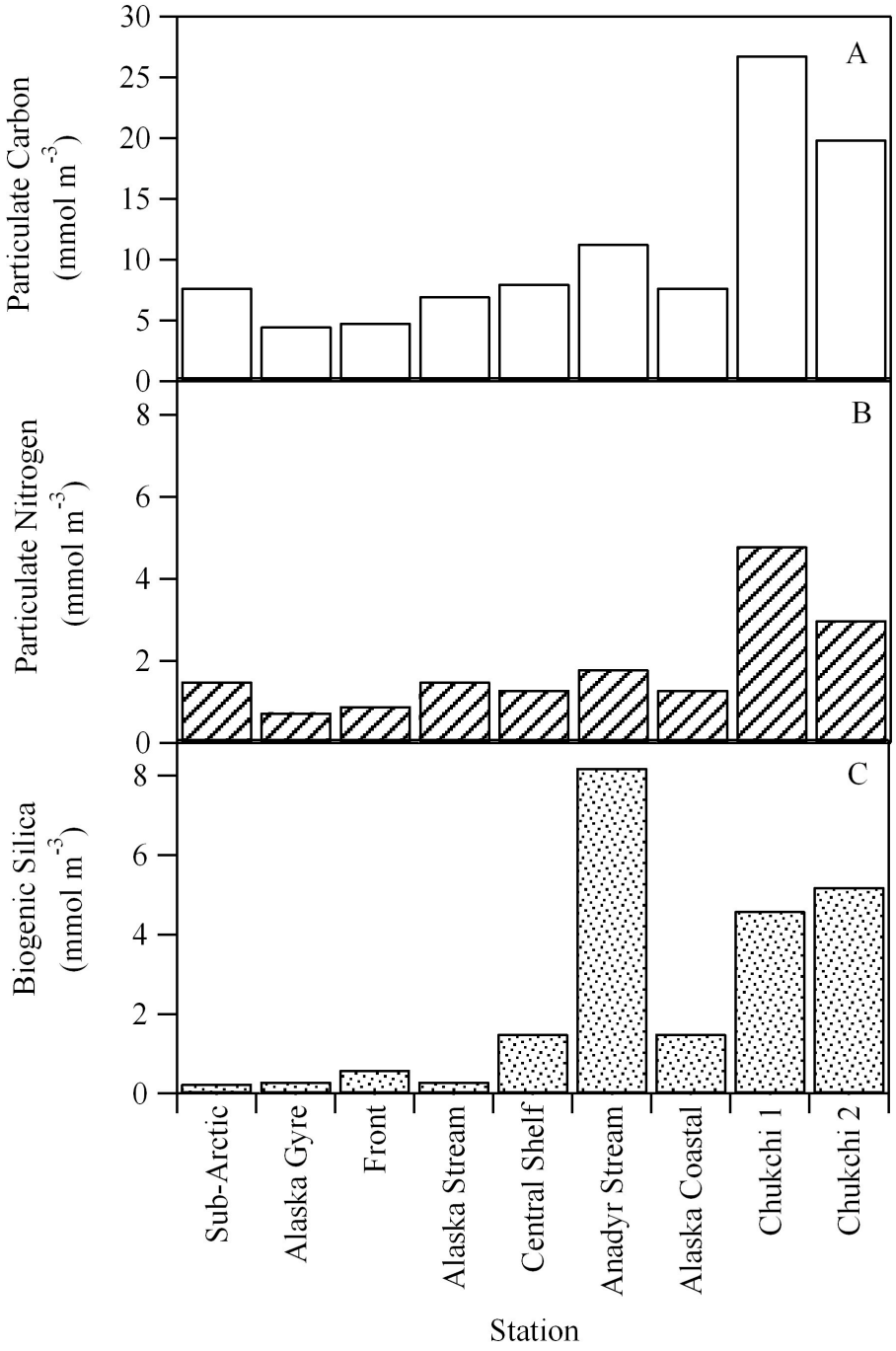

Figure 3.13. Depth-integrated particulate carbon (A), nitrogen (B) and biogenic silica (C) concentrations normalized by depth of the euphotic zone (mmol m^{-3}) for each station along the transect in the NE Pacific Ocean, Bering and Chukchi Sea. Note the different y-axis of A.

Trends of integrated rates of C incorporation and net incorporation of BSi (Fig. 3.14) were different from particulate trends (Fig. 3.13). Depth-integrated rates for C

incorporation were relatively low in the NE Pacific Ocean, higher at the Anadyr station in the Bering Sea and highest in the Chukchi Sea. At the two other stations in the Bering Sea, the Central Bering and the Alaskan Coastal Current station, however, incorporation rates were lower than the in NE Pacific Ocean. There was evidence of BSi dissolution at the Anadyr Stream Station and the Alaskan Coastal Current station in the Bering Sea. BSi net incorporation was highest at the Chukchi 1 station (0.9 mmol m^{-3} day^{-1}) (Table 3.2). Integrated NO_3^- incorporation rates remained low throughout the entire transect (0.02-0.2 mmol m^{-3} day^{-1}), with only two measurements above 0.1 mmol m^{-3} day^{-1}, at stations Anadyr Stream and Chukchi 2 (Fig. 3.14) (Table 3.2).

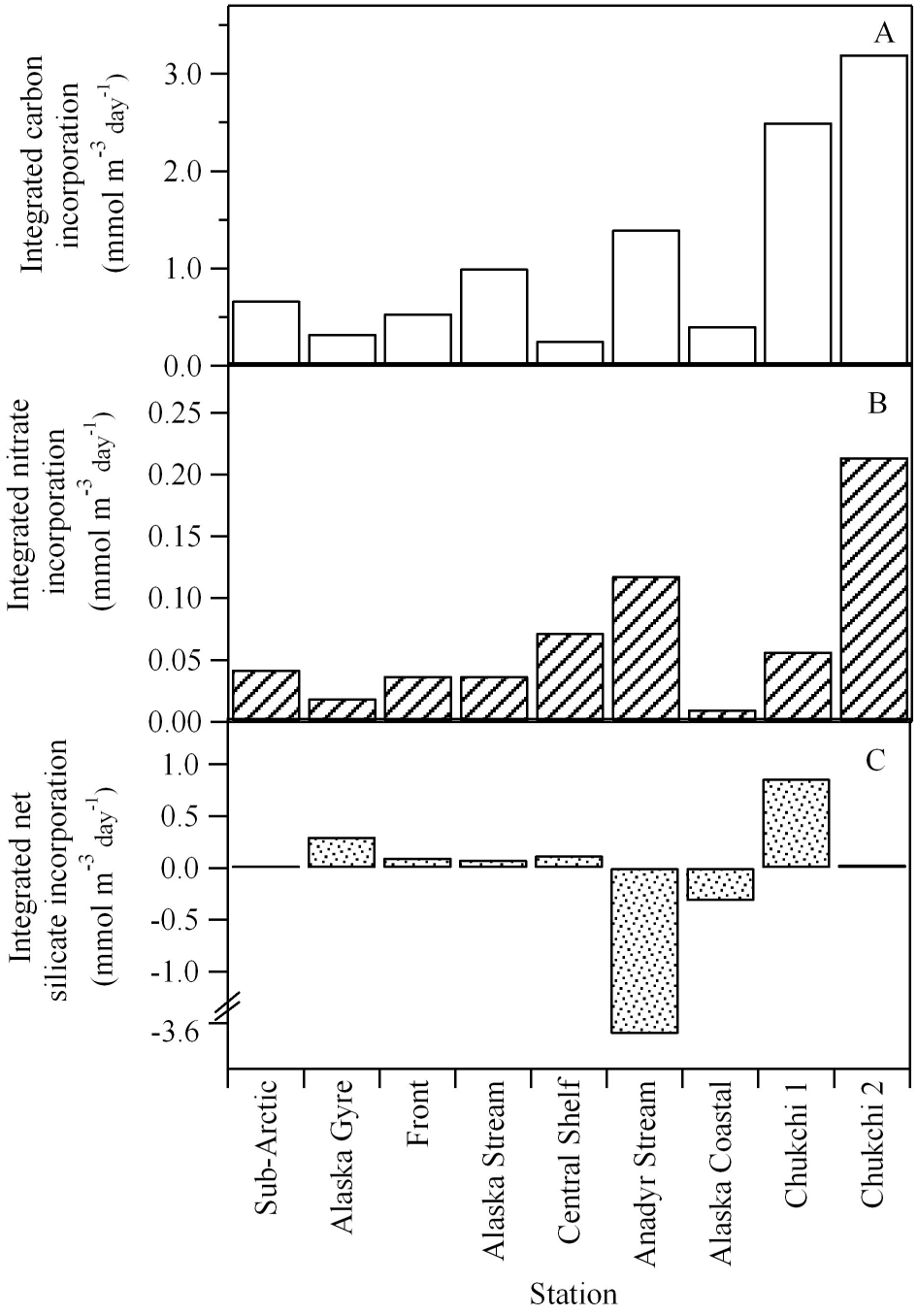

Figure 3.14. Depth-integrated C (A), NO_3^- (B) and BSi (C) incorporation rates normalized by the depth of the euphotic zone (mmol m^{-3} day^{-1}) for all stations from the NE Pacific Ocean the Bering and Chukchi Sea.

Cumulative BSi net incorporation rates are shown in Fig. 3.15. By using cumulative rates, it is possible to determine at what depth in the water column net

incorporation is equal to net dissolution (i.e. BSi net = 0 mmol m^{-2} day^{-1}). In the NE Pacific, BSi net incorporation rates remained positive down to the maximum depth sampled at each station except for the sub-Arctic current station (Fig. 3.15, A-D). This means that more BSi was incorporated in the water column than was dissolved. At the Anadyr Stream station and the Alaska Coastal Current station, net dissolution was occurring through the entire water column (Fig. 3.15F and G). At the Central Bering station and the Chukchi 2 station, cumulative net incorporation had reached zero at the deepest depth sampled, while at the Chukchi Sea 1 station, cumulative net incorporation remained positive throughout the water column (Fig. 3.15H and I). Positive cumulative net incorporation rates indicate accumulation of BSi in surface waters and the potential for BSi export. This way of presenting the data helps to determine whether BSi was being recycled or exported out of the euphotic zone.

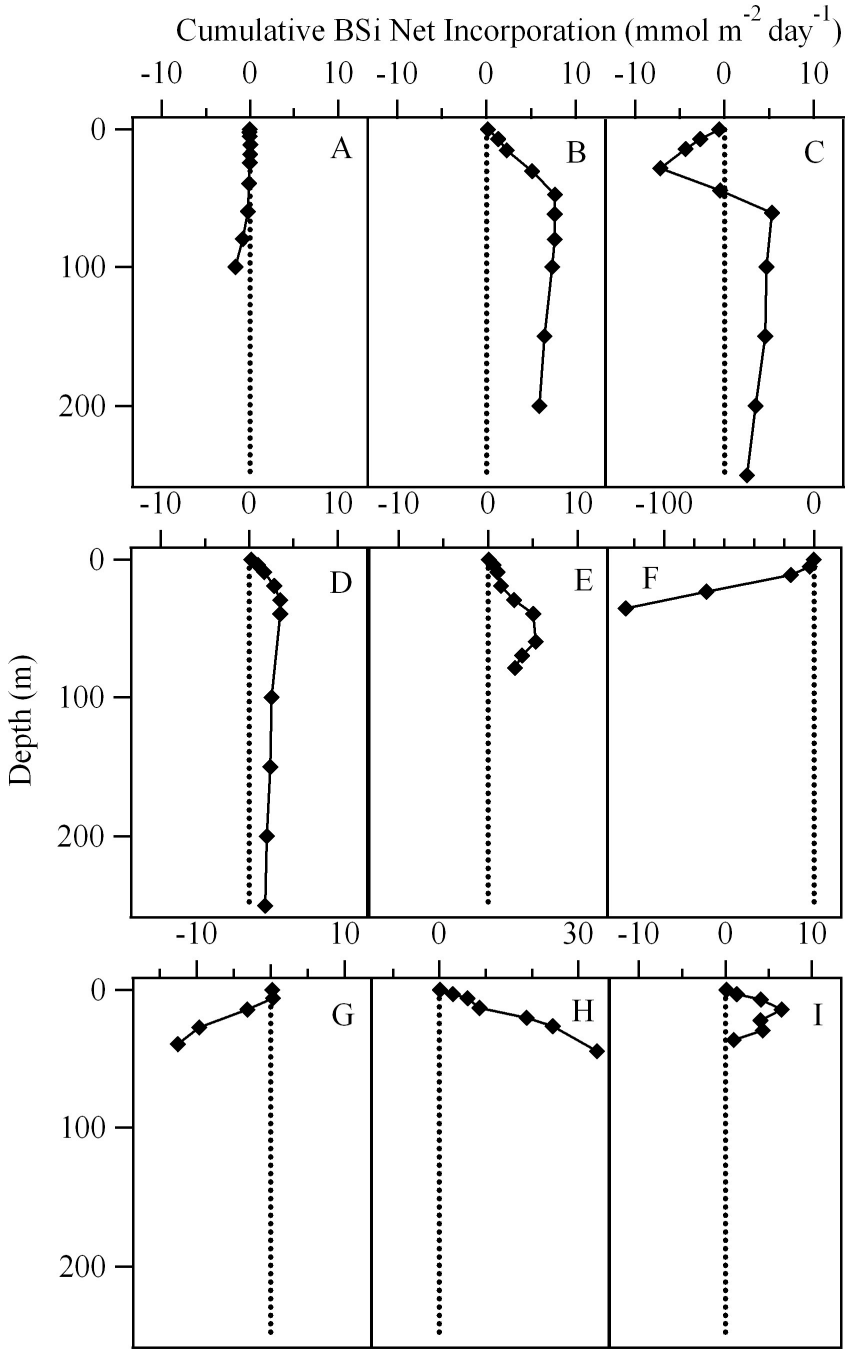

Figure 3.15. Cumulative integrated biogenic silica net incorporation rates throughout the water column for sub-Arctic(A), Alaska Gyre (B), Front (C), Alaska Stream (D), Bering Shelf (E), Anadyr Stream (F), Alaskan Coastal Current (G), Chukchi 1 (H) and Chukchi 2(I). A vertical line has been drawn at 0 mmol m^{-2} day^{-1}. Data to the right of the line indicates that incorporation is greater than dissolution, and data to the left indicates incorporation is less than dissolution. The depth at which the data crosses the line is where net incorporation is equal to dissolution. Note the different x-axes.

3.3.11 Total and New Primary Production and Siliceous Plankton Production

The amount of total and new production and production by siliceous plankton are shown in Table 3.4 in carbon units. The conversion from NO_3^- and BSi incorporation to C was done using known nutrient ratios (Redfield, 1958; Brzezinski, 1985). The amount of BSi net production was higher than that represented by total production, i.e. the amount of BSi net incorporation multiplied by the Brzezinski (1985) ratio was higher than the total production estimate. Exceptions to this are the two stations at which BSi net production was actually negative (Anadyr Stream and Chukchi 2) and may represent C remineralization. Converting BSi data to C units is problematic due to the fact that Si and C are not necessarily coupled in the cell cycle. Therefore BSi data converted to C units may not be biologically relevant.

The amount of new production as a percent of total production is shown in Fig. 3.16. In the NE Pacific Ocean, new production made up between 17 and 38% of total production. New production made up approximately 50% of total production at stations Anadyr Stream and Chukchi 2. At stations Alaskan Coastal Current and Chukchi 1 new production was relatively low, at approximately 15%. The new production at station Central Bering actually made up more then 100% of total production and reasons for this anomaly will be put forth in the discussion section.

Table 3.4. Depth-integrated total, new and biogenic silica productivity (in g C m^{-2} day^{-1} and g C m^{-3} day^{-1}) for each station sampled along the transect through NE Pacific and Bering and Chukchi Sea.

Station	Total Productivity		New Productivity		Production by Siliceous organisms	
	g C m^{-2} day^{-1}	g C m^{-3} day^{-1}	g C m^{-2} day^{-1}	g C m^{-3} day^{-1}	g C m^{-2} day^{-1}	g C m^{-3} day^{-1}
Sub-Arctic	0.202	0.008	0.067	0.003	0	0
Alaska Gyre	0.247	0.004	0.084	0.001	0.594	0.024
Front	0.395	0.006	0.15	0.002	0.467	0.008
Alaska Stream	0.492	0.012	0.086	0.002	0.261	0.006
Central Bering	0.125	0.003	0.214	0.005	0.396	0.01
Anadyr Stream	0.611	0.017	0.307	0.008	-9.9	-0.277
Alaska Coastal	0.198	0.005	0.029	0.007	-1.014	-0.025
Chukchi 1	0.821	0.03	0.108	0.004	1.932	0.068
Chukchi 2	1.134	0.038	0.547	0.018	0.068	0.002

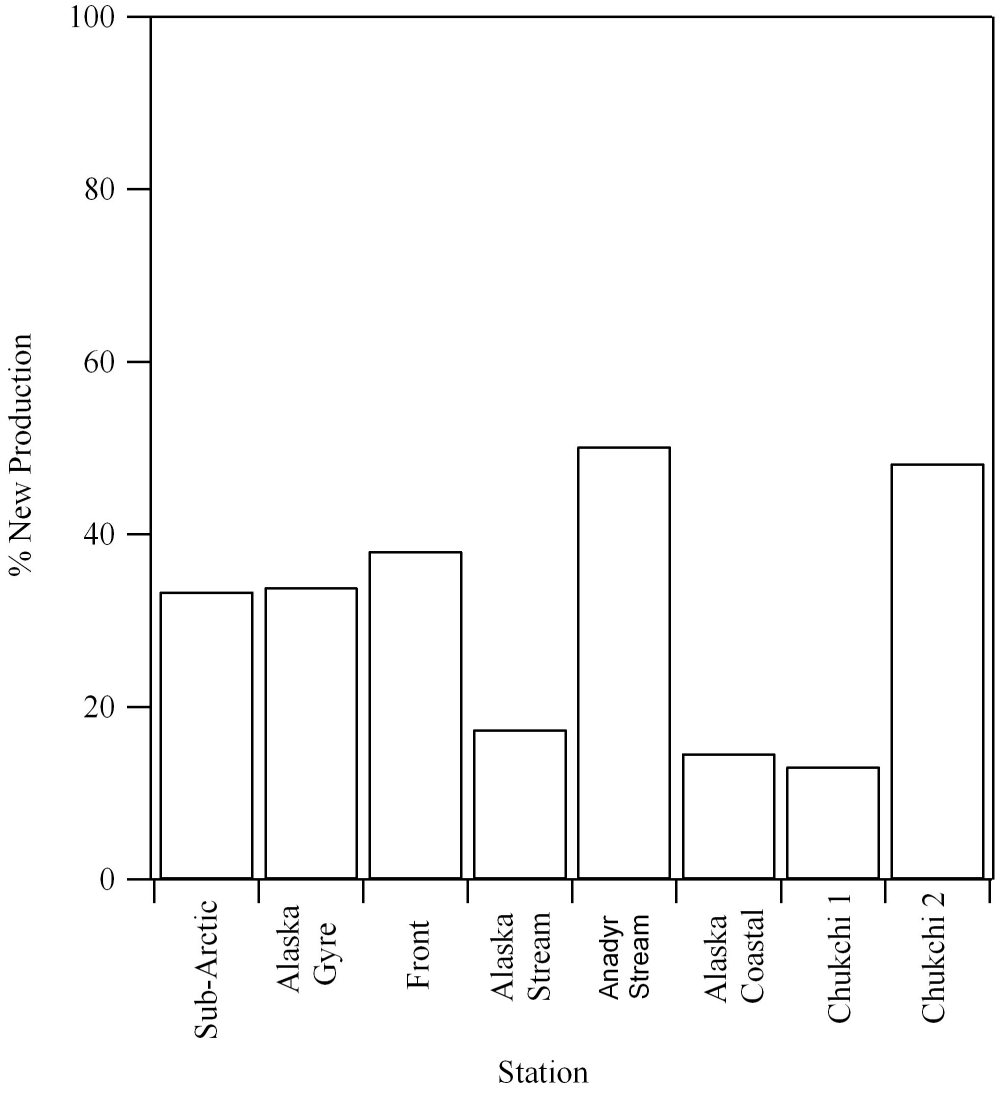

Figure 3.16. Percent new production at each station along the transect, excluding the Central Bering station. Central Bering had a new production % higher than 100 and will be discussed in the text.

3.3.12 Statistical Analysis

The discriminant function analysis which was run to determine if the stations were categorized appropriately into the three regions showed that 100% of originally grouped cases were classified correctly (Wilk's Lambda $p<0.05$). This means that the regions of NE Pacific, Bering Sea and Chukchi Sea were an appropriate way to group the stations. The average depth-integrated value for each variable for the three regions is

shown in Table 3.5. Note that there are only two stations in the Chukchi Sea region and the average of two data points is not statistically relevant.

Levene's test for homogeneity of variance showed that only chl *a* and C incorporation had homogeneous variances. ANOVA's were run on these two parameters. Both the NE Pacific Ocean and the Bering Sea were significantly different from the Chukchi Sea regarding chl *a*, however, the NE Pacific and the Bering Sea were not significantly different from each other ($p<0.05$). The same results were found for C incorporation. Particulate C, PN, BSi, N incorporation, Si net incorporation and LSi were tested using the Kruskal-Wallis test to determine if there were differences between regions. Significant differences were found for PC, BSi, N incorporation and LSi ($p<0.05$). The Mann-Whitney test returned the same results for each of these variables: PC, BSi, N incorporation and LSi were significantly different between the NE Pacific and the Bering Sea, and between the NE Pacific and the Chukchi Sea, but not between the Bering Sea and the Chukchi Sea ($p>0.05$).

Table 3.5 Depth-integrated parameters (normalized to euphotic zone depth) averaged by region ± 1 S.D. Samples sizes for the NE Pacific, Bering and Chukchi are four, three and two, respectively. Note that there is no standard deviation listed for the Chukchi region as there were only two data points in this region.

	NE Pacific	Bering Sea	Chukchi Sea
Chlorophyll *a* (mg m^{-3})	0.47±0.24 •	0.69±0.51 •	3.33
Particulate Carbon (mmol m^{-3})	5.96±1.59	9.01±1.96 *	57.78 *
Particulate Nitrogen (mmol m^{-3})	1.15±0.39 *	1.46±0.31 *	9.34 *
Biogenic Silica (mmol m^{-3})	0.36±0.16	3.75±3.84 *	27.24 *
Lithogenic Silica (mmol m^{-3})	0.03±0.06	0.88±0.67 *	2.56 *
Carbon Incorporation (mmol m^{-3} day^{-1})	0.64±0.29 •	0.69±0.63 •	2.84
Nitrogen Incorporation (mmol m^{-3} day^{-1})	0.0003± 0.0001	0.003± 0.006 *	0.028 *
Biogenic Silica Net Incorporation (mmol m^{-3} day^{-1})	0.08±0.05 *	-1.23±1.97 *	0.70 *

• - no significant difference between region averages (ANOVA, LSD $p<0.05$)
* - no significant difference between region averages (Kruskal Wallis, Mann Whitney $p<0.05$)

3.4 Discussion

3.4.1 Comparison Between Regions and Water Masses

Clear differences exist between the three regions of the NE Pacific Ocean, the Bering Sea and Chukchi Sea. The hydrography of these three regions is complex and is the subject of several reviews (e.g. Coachman, et al., 1975; Coachman, 1986). However for this study, a simplified view of major circulation patterns was chosen as the basis for classifying the regions. Each depth profile sampled a different water mass, with different

physical and chemical characteristics affecting the biological properties of the water mass.

Statistical analysis showed that characterizing this set of stations into the three regions of the NE Pacific, the Bering Sea and the Chukchi Sea was appropriate. The NE Pacific was significantly different from the Chukchi Sea with regards to most parameters. Differences between the Bering Sea and the Chukchi were less frequently significant, however. The ANOVA and Kruskal-Wallis tests must be treated with caution in this situation, however, due to the small sample size for the Chukchi region. One possible reason for the similarity between the Bering and Chukchi Shelf regions is that they are considered to be iron replete (Aguilar et al., 2007), as opposed to the NE Pacific Ocean (Martin and Fitzwater, 1988). Another possibility could be the influence of the Anadyr Stream, which originates in the Bering Sea, but flows into the Chukchi Sea (Springer and McRoy, 1993). It would be interesting for future studies to further characterize the Anadyr Stream, specifically the extent of its influence over the Chukchi Sea, and its range of interannual variability.

Although I have shown statistically that the water masses sampled fall into three regions with regards to certain biological variables, some differences between water masses still exist and warrant further explanation. The Anadyr Stream station in the Bering Sea showed unique Si dynamics. As nutrient rich water is upwelled in the Gulf of Anadyr and flows along the Siberian shelf and through the Anadyr Strait, conditions are ideal for the formation of a diatom bloom. Indeed, Springer and McRoy (1993) showed that Anadyr water is dominated by chain forming diatoms; this coincides with my observation that BSi concentrations were elevated in Anadyr water and subsequently the

Chukchi Sea, compared with the other Bering Sea locations. High BSi concentrations coupled with high BSi net dissolution indicate large amounts of remineralization. New production was also high (>50%) in the Anadyr Stream compared with the other two Bering Sea stations, probably as a result of the upwelled Anadyr water being high in NO_3. In contrast to the Anadyr Stream water, the Alaskan Coastal Current water is low in nutrients through the entire depth of the water column. As this water mass travels along the western coast of Alaska, nutrients are consumed by phytoplankton and only replenished during summer storm events (Whitledge et al., 1986). As a result, total, new and BSi production are low in the Alaskan Coastal Current. As both the Anadyr and the Alaskan Coastal Current waters flow through the Bering Strait, stations sampled in the Chukchi Sea would be expected to be different based on whether they are situated in the Alaska Coastal Current water or the Anadyr Stream water.

In the case of this study, the two Chukchi stations are thought to be situated in the Anadyr Stream water due to their salinity and high nutrient concentrations at depth. Total production at the Chukchi stations was the highest for the entire transect. The two Chukchi stations still showed differences among total, new and BSi net production, however. Station Chukchi 2 had higher new and BSi net production, but lower total production than Chukchi 1. Differences may be due to the fact that surface waters of the Chukchi 2 station were also influenced by its proximity to the ice edge. Chukchi Sea areas outside the influence of Anadyr Stream were not sampled. However, the C, N, and Si cycling in those waters would be important to measure to understand the biogeochemistry of the shelf as a whole.

3.4.2 Biogenic Silica Net Incorporation

To the best of my knowledge, this study is the first to measure BSi net production in the Chukchi Sea. Silica production studies conducted in other marine environments, such as Monterey Bay off the coast of California (Shipe and Brzezinski, 2003), the Eastern equatorial Pacific (Dugdale and Wilkerson, 1998), the Southern Ocean (Nelson et al., 1995) and the South Eastern Bering Sea (Banahan and Goering, 1986), have used either stable or radioisotope tracer techniques (^{30}Si and ^{32}Si, respectively) or the relative drawdown of $Si(OH)_4$ to determine uptake and production. The technique used in my study for determining BSi net production (i.e. BSi difference between ambient and incubated samples) is relatively new and has not been published in the literature yet. However, as discussed below, estimates of BSi net production from this technique agree with previously published data for these regions.

Banahan and Goering (1986) conducted the only previous BSi production study in the Bering Sea. They estimated the uptake of $Si(OH)_4$ in the South Eastern Bering Sea using the stable isotope ^{30}Si as a tracer during 24 hr incubations. Their estimates of $Si(OH)_4$ uptake on the Bering Sea central shelf range from 7.0 to 50.9 mmol m^{-2} day^{-1} down to the 0.01% irradiance level, while our estimate falls just below theirs, at 5.0 mmol m^{-2} day^{-1}; this suggests our method of estimating BSi net incorporation in the Bering Sea is approximately in the same range.

Our estimates of BSi net incorporation in the NE Pacific also agree with previous findings. Wong and Matear (1999) estimated $Si(OH)_4$ uptake in the NE Pacific by measuring changes in $Si(OH)_4$ surface water concentrations. They estimated an average $\Delta Si(OH)_4$ value of 5.1 mmol m^{-2} day^{-1} for the 1970-1980 period. Our average BSi net

incorporation value for the NE Pacific was 4.2±3.3 mmol m^{-2} day^{-1}. Our range of BSi net incorporation overlaps with the drawdown found by Wong and Matear (1999) and suggests, that similar to the Bering Sea, our estimates of BSi net incorporation in the NE Pacific ocean agree with previously published results.

When the estimates of BSi net incorporation are converted to C units and compared to C incorporation (Table 3.4), BSi net production appears to be relatively high, except for at the Chukchi 2 station. This implies that the phytoplankton community is incorporating a larger amount of BSi compared to C than what would be expected based on the Redfield-Brzezinski ratio of 106:16:16:1 C:Si:N:P; this is supported by the incorporation ratios (Table 3.3). Brzezinski et al. (2003) found that net Si uptake was greatly enriched compared to gross uptake in the Southern Ocean. Their average net uptake ratio for Si:C was 0.52±12, which is around the median mark for my net Si:C ratios (excluding negative values). Net Si:N incorporation ratios are also high compared to what would be expected based on the Redfield/Brzezinski ratios. In the NE Pacific Ocean, this could be due to iron limitation, as Hutchins and Bruland (1998) found iron limitation led to increased incorporation of Si compared to NO_3^-.

The high particulate and net incorporation ratios involving Si, could also be an indication of preferential export of Si (the silicate pump). Preferential export of BSi compared to C has been found in other areas of the ocean (eg. Monterey Bay, Shipe and Brzezinski, 2003), and has been shown for the NE Pacific Ocean through the use and analysis of sediment traps (Wong and Matear, 1999; Whitney et al., 2005). Further evidence for the silicate pump in the NE Pacific area is that $Si(OH)_4$ can be drawn down below the concentration of NO_3^-, to less then 1 μmol L^{-1}, suggesting that primary

production can occasionally be limited by $Si(OH)_4$ in the NE Pacific Ocean (Wong and Matear, 1999),

Evidence for the silicate pump in the NE Pacific Ocean can be seen in Fig. 3.16. Cumulative integrated rates were positive at three of the four NE Pacific Stations as deep as 250 m, indicating that there is opportunity for export. In contrast to the NE Pacific, all the stations in the Bering and Chukchi Seas except for station Chukchi 1, show negative values for the cumulative integrated BSi net incorporation rate. This indicates that there is a large amount of recycling of BSi in the water column of the Bering and Chukchi Seas. Although a silicate pump may not be functioning in the Bering and Chukchi Seas, there exist other explanations for the relatively high net BSi incorporation rates compared to C uptake.

BSi:PC ratios were higher in the Bering and Chukchi Sea than in the NE Pacific Ocean, always exceeding the Brzezinski (1985) ratio of 0.11. Higher BSi:PC ratios could be due to a higher proportion of siliceous organisms in the phytoplankton community. As well, the Brzezinski ratio of 0.11 is an average and individual diatom species have exhibited a BSi:PC ratio as high as 0.42 in culture (Brzezinski, 1985). High BSi:PC ratios could also be an indication of low phytoplankton growth rates, as diatoms are known to incorporate higher amounts of BSi at low growth rates (Martin-Jezequel et al., 2000). Low growth rates are expected as temperature is a limiting factor for the rate of diatom growth, and temperatures in the Bering and Chukchi Seas were colder than in the NE Pacific Ocean. Although estimates of BSi net production using the method applied in this study appear to be within the ranges found by other studies, this method should be validated before future studies commence.

3.4.3 Total and New Production

New production estimates can provide insights into the functioning of different ecosystems and whether they are fuelled by new or regenerated nutrients. In the NE Pacific, new production contributed between 17 and 38% of total production. These results imply that phytoplankton in this system are fed mainly by recycled sources of nitrogen.

One anomaly in the new production data occurred at the Central Bering station, where new production accounted for 146% of total production. Uptake of nitrate was not higher than uptake of carbon, but when multiplied by the Redfield ratio of 6.6, the relative contribution of new to total production was more than 100%. This could be explained by luxury uptake of NO_3^- by the phytoplankton community (Elrifi and Turpin, 1985). In that case, the phytoplankton take up more NO_3^- than necessary based on the C uptake rates, and store the excess NO_3^- in their cells for times when NO_3^- is scarce.

Incorporation rates of C:N were higher than the Redfield ratio at all stations except for the Central Bering and the Alaska Coastal Current. Higher C:N incorporation ratios in the NE Pacific could be explained by an inhibition of nitrate uptake due to iron limitation. However, a suitable explanation for the high C incorporation ratios at the Anadyr Stream, and both Chukchi stations has yet to be found.

3.4.4 Comparison to Previous Studies

Results from this study for the NE Pacific Ocean generally agree with previous work. Chlorophyll *a* concentrations in the sub-Arctic Current, the Alaska Gyre and the

Front station ranged from 0.19 to 0.54 mg m^{-3} which is what is expected for this HNLC area (usually less than 0.5 mg m^{-3} (Boyd and Harrison, 1999; Harrison et al., 1999)), while concentrations at the Alaska Stream station were slightly higher (0.78 mg m^{-3}). Total primary production estimates from our study in the NE Pacific fall within or just below estimates from previous studies. Total primary production in the sub-Arctic Current and the Alaska Gyre was 247 and 202 mg C m^{-2} day^{-1}, respectively; below the 300-600 mg C m^{-2} day^{-1} range reported by (Boyd and Harrison, 1999; Harrison et al. (1999). However, total primary production at the Front and the Alaska Stream stations did fall within the range reported by Harrison et al. (1999). My new production estimates in the NE Pacific Ocean of 17-38% agree with those reported by Varela and Harrison (1999) and Pena and Varela (2007) (32±15%). Depth-integrated uptake rates of NO_3^- for the NE Pacific fall within the low end of the range reported by Pena and Varela (2007) from the C-JGOFS study. The range they reported was between 1.04 to 6.32 mmol m^{-2} day^{-1}, while our range was from 1.06 to 2.24 mmol m^{-2} day^{-1}. Station locations between studies were not exactly the same however the areas of the Alaska gyre and sub-Arctic current were sampled in both studies.

My data from the Bering and Chukchi Seas often fell below those reported by previous studies. Biological seasonal variability is high in the Bering and Chukchi Seas, and can be as high as inter-annual variability (Coachman, 1986). Due to climatic and hydrographic forcing, it is most appropriate to compare our study to those conducted during the same time of the year. Depth-integrated chl *a* concentrations in the Chukchi Sea were 77 and 114 mg m^{-2}, which fall below those of Lee et al. (2007) who measured 200 to 500 mg m^{-2}. Our chl *a* values are also below those found by Walsh et al. (1989) in

the Bering Strait of 4-10 mg m^{-3}. Walsh et al. (1989) also found that concentrations in Anadyr bottom water can be higher than 2.5 mg m^{-3}, while concentrations in our study did not reach 2 mg m^{-3}.

The total primary production values of 0.8 and 1.1 g C m^{-2} day^{-1} in the Chukchi Sea fall within the range reported by Lee et al. (2007) (0.1 to 1.5 g C m^{-2} day^{-1}). However, Springer and McRoy (1993) found that C production in the Gulf of Anadyr and the Chukchi Sea ranged from 2.8 to 7.2 g C m^{-2} day^{-1}. South of the Bering Strait, Hansell et al. (1993) found C incorporation was 3.1 g C m^{-2} day^{-1} in the Anadyr Stream, while north of the Bering Strait in the same water mass C incorporation was 2.4 g C m^{-2} day^{-1}. Our estimates for C incorporation in the Bering and Chukchi Seas range from 0.13 to 1.1 g C m^{-2} day^{-1}. Our estimates of total primary production in the Anadyr Stream water were closer to the estimate of 3.8 g C m^{-2} day^{-1} of Springer and McRoy (1993).

Walsh et al. (1989) determined new production measurements of 120 mg NO_3^- m^{-2} day^{-1} in the Anadyr water, 90-280 mg NO_3^- m^{-2} day^{-1} in the Bering Shelf water, and 20 mg NO_3^- m^{-2} day^{-1} in Alaskan Coastal Current water. Converting data from Table 3.3 to mg NO_3^-, our study found 60 mg NO_3^- m^{-2} day^{-1} in the Anadyr water, 40 mg NO_3^- m^{-2} day^{-1} in the Bering Shelf water and 6 mg NO_3^- m^{-2} day^{-1} in the Alaskan Coastal water. Our estimates are lower by at least one half their estimates. The range of values Walsh et al. (1989) found for NO_3^- uptake in 1985 was 0.07 g m^{-2} day^{-1} on the Bering Shelf to >0.25 g m^{-2} day^{-1} in the Anadyr Stream. However, incorporation rates could be <0.01 g in the Alaska Coastal Current. In 1987 estimates in the Bering Sea ranged from 0.02 to 0.28 g NO_3^- m^{-2} day^{-1}.

Based on previous studies, it has been difficult to determine whether primary production is declining or whether apparent trends are in part due to inter-annual variations. In general, but not without exception, our study found lower levels of chl *a*, and C and NO_3^- incorporation rates than earlier studies. Since our sampling was conducted only once at each station throughout the season, we have no temporal range over which to compare our data. However, our values do not even fit within data sets which were collected multiple times throughout the season (e.g. Walsh et al., 1989). Schell (2000) suggested that there has been a decrease in primary production in the Bering Sea over the past few decades of 30-40% based on isotope records from baleen whales. However, Whitledge et al. (1986) determined that NO_3^- concentrations in the Middle Shelf of the Bering Sea did not change from the 1970's to the 1990's. It has been postulated that if the amount of NO_3^- supply to the Bering Sea shelf remains unchanged, then the potential new production available in the system may remain unchanged as well (Hunt et al., 2002). Continued studies may shed more light on the state of primary production in these regions.

The diversity of the geography and the complexity of current flow through the Bering Sea meant that only a limited number of the total possible water masses were sampled. As a result, our study is lacking data from some key areas in the Bering Sea. For example, depth profiles of the Bering Sea Green Belt (the area of upwelling along the slope dividing the Bering Sea shelf from the Bering Sea basin) (Springer et al., 1996) would have added a great deal of information to this study. Sampling the middle and inner shelves of the Bering Sea would have also benefited our study, especially since BSi data for these two sections has been previously collected by Banahan and Goering

(1986). Hopefully data acquisition of BSi and LSi for this area of the world ocean will continue in the future, as it is a dynamic and unique Si cycling system, and the true breadth of the temporal and spatial variation in the Si cycle has not yet been captured in this area.

Important changes that may occur in the Arctic as a result of climate change include changes in water stratification, upwelling and mixing (Carmack and Wassman, 2006). A change in upwelling along the Bering Sea slope would have major implications for the Bering Sea shelf. In contrast, an increase in stratification and a decrease in vertical mixing may not have a large effect. Water column depths are shallow along the Alaskan Coast, and in the Northern Bering Sea and the Southern Chukchi Sea, with the euphotic zone extending all the way to the bottom. At the northern Bering and southern Chukchi stations, maximum particulate concentrations and incorporation were measured at depths below the mixed layer. Increased stratification and a decrease in vertical mixing may not affect the magnitude of primary production in these very shallow areas, as phytoplankton can produce at all depths in the water column.

3.5 Conclusions

3.5.1 Comparison between regions and water masses

Although important differences exist between the individual water masses sampled, the appropriate categorization of stations into the three regions of NE Pacific Ocean, Bering Sea and Chukchi Sea was confirmed by statistical analysis. Significant differences existed between these regions for chl *a*, PC, BSi, C incorporation, N incorporation and LSi. Particulate C was the variable which maximized differences and

explained 89.7% of the variance between regions. Future studies may benefit from using this categorization in order to predict variable ranges.

3.5.2 Biogenic Silica Net Incorporation

The method applied in this study to determine BSi net incorporation produced data that agreed well with previous results obtained using other methods. However, this method would benefit from validation using stable isotopes of Si. Results from the measurement of BSi net incorporation indicate that in the NE Pacific Ocean, there is an export of siliceous material out of the upper water column. In the Bering and Chukchi Seas, siliceous material is recycled more effectively within the water column before reaching the ocean floor.

3.5.3 Total and New Production

Total and new production were highest in water masses that were influenced by the upwelled nutrient-rich water of the Anadyr Stream. Total and new production in the Bering and Chukchi Seas outside of the Anadyr influence were generally low. When determining total and new production in the Bering and Chukchi Seas, it is important to identify the water mass in order to properly interpret results.

3.5.4 Comparison to Previous Studies

Chlorophyll *a* concentrations, total and new production and production by siliceous organisms measured during this study are consistently lower than estimates obtained in the 1980's and 1990's, however they agree relatively well with results from the most recent study by Lee et al. (2007). Whether a long term decline in primary production is occurring or whether apparent lower production is due to interannual

variability can only be determined from a regular sampling program in the Bering and Chukchi Seas.

Chapter 4

Effect of Temperature and Irradiance on the Growth and Nutrient Stoichiometry of Two Polar Diatom Species: *Thalassiosira antarctica* and *Porosira glacialis*

4.1 Introduction

Temperature and irradiance vary on temporal and spatial scales in the marine environment, and both have been found to affect diatom physiology (eg. Mortain-Bertrand, 1989; Suzuki and Takahashi, 1995), including diatom growth rates (e.g. Fiala and Oriol, 1990). Laboratory studies have been conducted on the effects of irradiance (e.g. Leu et al., 2006) and temperature (e.g. Villareal and Fryxell, 1983; Furnas, 1978; Durbin, 1977) on polar diatom species. However, the combined effect of these two factors on the cellular stoichiometry of polar species has not been addressed to date. The interest in polar species arises from high rates of temperature increase in polar environments relative to other areas due to global climate change (IPCC, 2007). Reduced ice coverage in the Arctic (Stroeve et al., 2005) will also increase the amount of irradiance available to phytoplankton. Determining the combined effect of irradiance and temperature variations on the nutrient stoichiometry of polar diatoms will help predict the potential impact of environmental changes on biological nutrient cycling at high latitudes.

Diatoms account for up to 40% of global marine primary production, and are responsible for the cycling of $Si(OH)_4$ in the marine environment (Nelson et al., 1995). As prominent members of the marine phytoplankton community, diatoms are responsible

for a large amount of cycling of other macronutrients such as carbon and nitrogen as well. Nutrient cycles can be affected when environmental variables influence the cellular nutrient concentrations of phytoplankton. The cellular C content in temperate diatoms can be affected by irradiance (Thompson, 1999) and temperature (Furnas, 1978). Cellular N has been found to decrease with decreasing temperature in Arctic diatoms (Durbin, 1977), while it is unaffected by irradiance in temperate diatoms (Furnas, 1978). Irradiance has an effect on the growth rate of polar diatoms (Mortain-Bertrand, 1989), however it is less clear how it affects the Si quota of diatom cells. Understanding nutrient cycling by phytoplankton in any environment requires knowledge of how cellular nutrient content changes with environmental variables.

The utilization of Si by diatom cells is not coupled to that of C and N in the cell cycle (Claquin et al., 2002). Therefore environmental variables may affect cellular Si differently than cellular C and N. For example, Si incorporation is not linked directly to photosynthesis, but uses energy produced through aerobic respiration instead (Brzezinski, 1992). Instead, Si is tightly coupled to the cell cycle, and therefore to growth rate (Brzezinski, 1992). The concentration of BSi normalized to surface area is inversely correlated with growth rates (Flynn and Martin-Jezequel, 2000), as slower growth rates allow more time for a maximum deposition of Si into cell walls (Martin-Jezequel et al., 2000). Therefore, those environmental factors that affect growth rate may also indirectly affect the cellular Si content.

Polar phytoplankton species have optimized their physiology to low temperatures and irradiances (Kirste and Wiencke, 1995). The biological basis behind changes in the nutrient content in diatom cells results from adaptations to changes in environmental

conditions; then cellular functions and components change as the cell acclimates to the new conditions (Klausmeier et al., 2004). Both irradiance and temperature can affect the cellular allocation of carbon between structural components, storage compounds and macromolecules (Shuter, 1979). In general, polar phytoplankton have a larger proportion of lipids (31-59%) and a lower proportion of proteins (20-24%) than do temperate phytoplankton (Smith et al., 1989). According to Sakshaug and Slagsted (1991), the maximum photosynthetic rate (normalized to chl *a*) is lower for polar phytoplankton than for other phytoplankton. It is possible to theoretically calculate a lower and upper limit for nutrient ratios in a diatom cell. Potential optimum N:P ratios have been calculated by Klausmeier et al. (2004). Optimum nutrient ratios involving Si have yet to be determined.

This study examines the nutrient incorporation and stoichiometry of two polar diatom species: *Thalassiosira antarctica* and *Porosira glacialis* exposed to four different combinations of irradiances and temperatures. These two species can dominate spring phytoplankton blooms in polar waters (von Quillfeldt, 2000) and thus are important components of Arctic and Antarctic ecosystems. Both species have been found in the Arctic in near-shore shelf environments (Zielinski and Gersonde, 1997), as well as the open ocean (Maddison et al., 2005; Bak et al., 2007) and are used as paleoindicators (Maddison et al., 2006; Stickley et al., 2005). Determining how the cellular components of these two species change with environmental variables will help us understand nutrient cycling in polar and sub-polar environments.

The objective of this study was to determine the effect of four different irradiance and temperature regimes on the growth rate, C, N and Si content and incorporation of two polar diatom species. Irradiance and temperature are two environmental variables which

can exhibit a large range in the Arctic environment where these two diatom species are found. Understanding the influence of these two variables over the nutrient cycling of polar diatoms is important, especially as conditions in the Arctic shift with global climate change.

4.2 Methods

4.2.1 Experimental Design

Experiments were conducted with unialgal cultures of two polar diatoms. Diatom cultures were obtained from the Provasoli-Guillard National Center for Culture of Marine Phytoplankton (CCMP), at the Bigelow Laboratory for Ocean Sciences, Maine, USA. The two species used in this study are: *Thalassiosira antarctica* (CCMP strain #982) and *Porosira glacialis* (CCMP strain #671). The two species were maintained in a low temperature Percival culture chamber in f/2 media (Guillard and Ryther, 1962; Guillard, 1975) with added selenium (Harrison et al., 1980). Cool white light was provided on a 14:10 light:dark cycle. Maintenance temperature and irradiance were 6 °C and 110 μmol quanta m^{-2} s^{-1}, respectively. Diatoms were maintained at exponential growth phase by using semi-continuous batch cultures. Relative growth rate was monitored by *in-vivo* fluorescence with a Turner Designs 10-AU fluorometer at the same time every day.

Experiments were conducted in triplicate by culturing the two diatom species in unialgal semi-continuous batch cultures in 2.5 L polycarbonate flasks under four combinations of irradiance and temperature. Cultures were acclimated to the experimental conditions for 10 generations prior to the commencement of experiments. The four irradiance/temperature treatments were:

- High irradiance/high temperature (110 μmol quanta m^{-2} s^{-1}/ 10°C) (HI / HT)
- High irradiance/low temperature (110 μmol quanta m^{-2} s^{-1}/ 6°C) (HI / LT)
- Low irradiance/high temperature (40 μmol quanta m^{-2} s^{-1}/ 10°C) (LI / HT)
- Low irradiance/ low temperature (40 μmol quanta m^{-2} s^{-1}/ 6°C) (LI / LT)

Irradiance of <70 μmol quanta m^{-2} s^{-1} is considered "low" (Gosselin et al., 1990); two irradiance levels corresponding to 'low' and relatively 'high' irradiance within the range of both species were chosen. Temperatures of 6 and 10°C were chosen because temperatures in the polar environment of the Bering Sea can reach up to 10°C in the summer time (Coachman, 1986). Experimental cultures were sampled every 48 hrs at the same time of the day (midday) for five days. Sampling was conducted for the measurement of chl *a*, cellular carbon (C), cellular nitrogen (N), cellular silicon (Si), cell numbers and cell volumes. Growth rate was estimated with *in vivo* fluorescence and cell numbers (Anderson, 2005).

4.2.2 Specific Growth Rates

Specific growth rates (μ day^{-1}) were calculated using the equation:

Equation 4.1

$$\mu = \ln (N/N_o)/t$$

where N represents cells L^{-1} at the end of the experimental period, N_o represents cells L^{-1} at the beginning of the experimental period and t represents the length of the experimental period in days.

4.2.3 Sample Collection and Analysis

4.2.3.1 Cell counts and cell volumes

Samples for cell counts were collected and preserved using Lugol's solution. Cell counts for both species were conducted using an inverted Olympus IX71 microscope. Cell counts for *T. antarctica* were conducted with a Sedewick-Rafter cell counter. The Sedgewick-Rafter counter was divided into 4 quadrants and a minimum of 10 fields of view per quadrant were counted. *P. glacialis* cells were counted with a 0.1 mm depth hemacytometer due to their smaller size. For *P. glacialis,* a minimum of 8 fields of view were counted.

Samples for the calculation of cell volumes were collected and preserved using glutaraldehyde. Cells were photographed using InVitro version 3.1.0 and measured using Image Processing and Analysis in Java (Image J) software for calculations of cellular volume. Both species have morphologies similar to that of a cylinder (Sun and Lui, 2003) and their volume and surface area were calculated accordingly.

4.2.3.2 Chlorophyll *a* Content

Chlorophyll *a* was collected on glass fiber filters of 0.7 μm porosity, and kept frozen at -20 °C in the dark until analysis. Upon analysis, chl *a* was extracted in 90% acetone for 24 hrs in the dark. Analysis was conducted according to Parsons et al. (1984) and read on a Turner Designs 10 AU (Sunnydale California) fluorometer. Samples were corrected for the occurrence of phaeopigments by degrading chl *a* with 1.0N HCl, and subtracting the remaining phaeopigment concentration from the total (Parsons et al., 1984).

Carbon and Nitrogen Content

Samples for particulate C and N were collected in triplicate on 25 mm combusted glass fiber filters of 0.7 μm porosity and dried at 60 °C for 48 hrs. They were measured at the Stable Isotope Facility at UC Davis with an elemental analyzer.

Silicon Content

Silicon content (or biogenic silica) was collected in triplicate on 25 mm 0.6 μm polycarbonate filters and dried for 48 hrs at 60°C. Biogenic silica was analyzed according to the method outlined in Brzezinski and Nelson, (1989). Blanks for BSi determination averaged 12 nmol L^{-1}. The majority of BSi in a diatom cell forms the frustule (Martin-Jezequel, et al., 2000), therefore Si content was normalized to surface area, in addition to cell number and cell volume.

Calculation of Nutrient Cellular Content

Calculations were conducted to determine the concentration of chl *a*, C, N and Si per cell as well as per cell volume. Ratios between the three nutrients as well as the C:chl *a* ratio were calculated to compare between species and among treatments.

Nutrient Incorporation rates

The incorporation of C, N and Si into the cells was determined by calculating the rate at which C, N and Si increased per unit of cell volume and per unit time. The following equation was used:

Equation 4.2

$$\text{C incorporation } (\mu\text{mol } \mu\text{m}^{-3} \text{ day}^{-1}) = (C-C_o) / [(N-N_o)*\text{average volume}] *t$$

where C represents the concentration of C at the end of the experimental period, C_o represents the concentration of C at the first sampling, N represents the final cell number

and N_o represents the original cell number, and t represents the experimental time period in days. N and Si can be interchanged for C.

4.2.4 Statistical Analysis

All statistical analyses were conducted using Statistical Package for Social Sciences (SPSS**)** 15.0 for Windows. A significance level of $p<0.05$ was used for all tests. Differences in cellular parameters between species, and among treatments were determined using Students t-tests and analysis of variance (ANOVA). Levene's test was used to determine the homogeneity of variances prior to each t-test and ANOVA, as is required to satisfy the assumption of homogeneous variances between treatments. Student's t-test was used to determine species differences between identical treatments. One-way ANOVA's were conducted to determine significant differences for the same species between treatments. The post hoc Least Significant Difference (LSD) test was used after significant differences were found in one-way ANOVA's to identify which treatments were significantly different. Where variances were not homogeneous, the Mann Whitney test was used in place of the Student's t-test and the Kruskal Wallis test was used in place of the one-way ANOVA.

4.3 Results

4.3.1 Specific Growth Rates

Average growth rates (μ,, day^{-1}) and standard deviations for both species under each treatment are displayed in Table 4.1. Growth rates were calculated using both cell numbers and *in vivo* fluorescence (Anderson, 2005), and were not significantly different except in two cases. Where growth rates differed, the rate calculated using cell number

was used, as it is a direct measurement. Specific growth rate expressed as doublings per day can also be found in Table 4.1.

4.3.1.1 Comparison between species

Significant differences in growth rates between *T. antarctica* and *P. glacialis* were found for two of the four treatments: the HI/HT and HI/LT treatments (Student's t-test, $p>0.05$) (Table 4.1). Irradiance and temperature affected the two species differently. Higher irradiance coincided with higher μ at both temperatures for *T. antarctica*, while high irradiance coincided with higher μ only at the high temperature in *P. glacialis*. The μ of *P. glacialis* increased with increased temperature, while μ of *T. antarctica* decreased with increased temperature.

4.3.1.2 Comparison between treatments

Significant differences in μ occurred between treatments for each species (Table 4.1). The μ at the HI/HT treatment for *T. antarctica* was significantly different from the HI/LT treatment. For *P. glacialis*, significant differences were found between μ at the high irradiance treatments but not the low irradiance treatments (one-way ANOVA, $p<0.05$).

Table 4.1. Specific growth rates (μ, , day^{-1}) for *T. antarctica* and *P. glacialis* calculated from cell number and *in vivo* fluorescence under four combinations of irradiance and temperature. Doublings per day are calculated as ln2/μ (cell number). Values are the average of triplicate cultures ± 1 S.D.

	T. antarctica		*P. glacialis*	
Treatment	μ (Cell #)	Doublings Per day	μ (Cell #)	Doublings Per day
HI/HT	0.24 ± 0.035^{ab}	2.9±0.66	0.38 ± 0.08	1.8±0.04
HI/LT	0.31 ± 0.001^{c}	2.2±0.004	0.13 ± 0.015	5.3±0.69
LI/HT*	0.21 ± 0.048^{a}	3.3±0.61	0.28 ± 0.037^{d}	2.5±0.32
LI/LT*	0.27 ± 0.026^{bc}	2.4±0.25	0.27 ± 0.014^{d}	2.6±0.14

The * symbol denotes no significant difference between species for the same treatment. Letters denote which specific growth rates are not significantly different within each species i.e. specific growth rates that have the same letter are not significantly different.

4.3.2 Cell Size and Cell Volume

Cell diameters and cell volumes were significantly different between species (Student's t-test, $p<0.05$). *T. antarctica* cells exhibited significantly larger diameters and volumes than *P. glacialis* cells under all treatments; the size difference between these two species was noted prior to the commencement of acclimation for these experiments and was not due to a specific change in irradiance or temperature. In addition to the difference in size between these two diatom species, I observed that *P. glacialis* cells formed chains in culture, while *T. antarctica* cells did not. Average cell volumes and diameters for the triplicate cultures ± 1 standard deviation are displayed in Table 4.2. Within each species, there was no significant difference in cell diameter or volume between treatments (one way ANOVA, $p>0.05$ (*T. antarctica*); Kruskal Wallis $p>0.05$ (*P. glacialis*)).

Table 4.2. Cell diameter and volume for *T. antarctica* and *P. glacialis* under each irradiance/temperature treatment. Values represent the average of triplicate cultures ± SD.

Treatment	*T. antarctica*		*P. glacialis*	
	Diameter (μm)	Volume (μm^3)	Diameter (μm)	Volume (μm^3)
HI/HT	14.9±0.29	2770±240	3±0.1	90±10
HI/LT	14.7±0.25	2660±180	3±0.2	110±20
LI/HT	14.4±0.6	2590±240	3±0.2	100±20
LI/LT	14.5±0.31	2650±140	3±0.2	110±10

4.3.3 Chlorophyll *a*

Chlorophyll *a* content will be presented per cell, and per unit volume (Fig. 4.1A), in order to facilitate comparison between species, but also per surface area (Fig. 4.1B) as chl *a* is linearly proportional to cell surface area (e.g. Durbin, 1977).

4.3.3.1 Comparison between species

Chlorophyll *a* content ranged from 5.0 to 8.0 pg $cell^{-1}$ for *T. antarctica* and from 0.097 to 0.17 pg $cell^{-1}$ for *P. glacialis* (data not shown). Normalized to cell volume, chl *a* concentrations ranged from 1.8 ± 0.30 to 3.1 ± 0.64 fg μm^{-3} for *T. antarctica* and from 0.89 ± 0.23 to 1.8 ± 0.73 fg μm^{-3} for *P. glacialis* (Fig. 4.1A). Chlorophyll *a* content of *P. glacialis* normalized by volume was always significantly lower than *T. antarctica* (Student's t-test, $p<0.05$), except for the LI/HT treatment, where no significant difference was found between species. Chlorophyll *a* normalized to cell surface area ranged from 4.6 to 7.7 fg μm^{-2} for *T. antarctica* and from 0.69 to 1.3 fg μm^{-2} for *P. glacialis* (Fig.

4.1B). Normalized to cell surface area, chl *a* was always significantly higher in *T. antarctica* compared to *P. glacialis*.

4.3.3.2 Comparison between treatments

Significant differences in chl *a* content existed between treatments for both species when normalized to cell volume (Fig. 4.1A), but only for *T. antarctica* when normalized to cell surface area (Fig. 4.1B). Chlorophyll *a* content per cell volume at the LI/HT treatment was significantly higher than the three other treatments for *P. glacialis* (ANOVA, LSD, $p<0.05$). The chl *a* content per cell volume of *T. antarctica* for the LI/HT treatment was significantly higher than both high irradiance treatments, while the chl *a* content per cell volume for the LI/LT treatment of *T. antarctica* was significantly higher than only the HI/HT treatment (ANOVA, LSD, $p<0.05$).

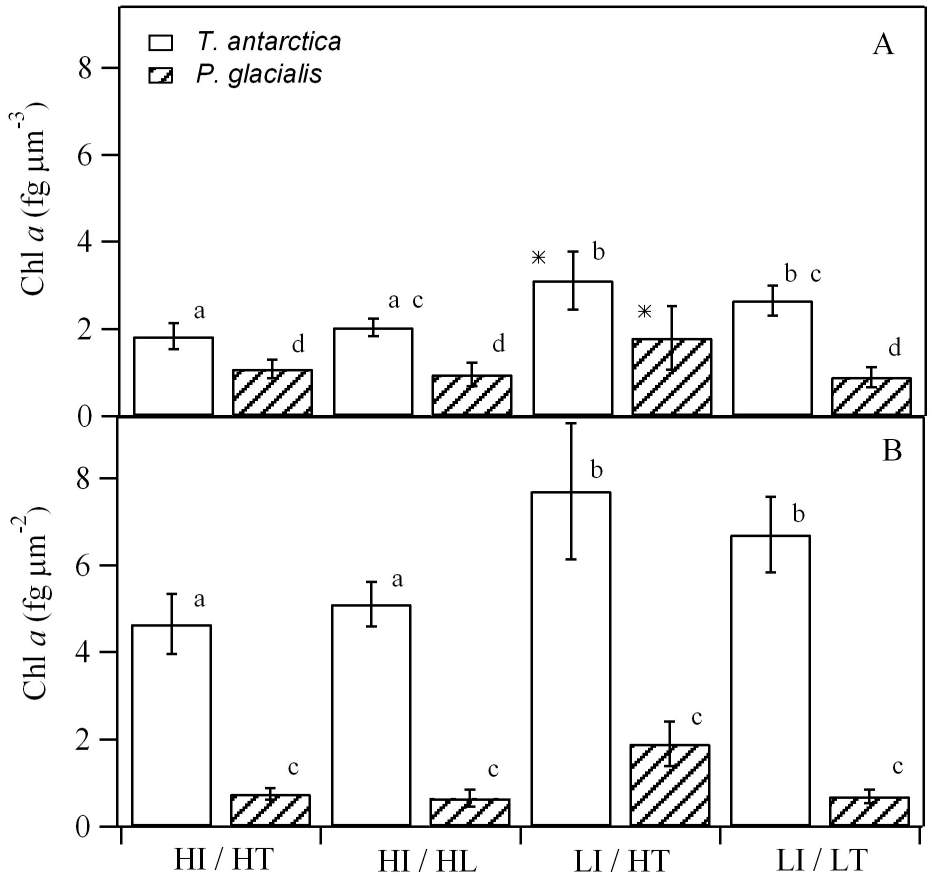

Figure 4.1 Chlorophyll *a* content expressed per unit volume (A) and surface area (B) for *T. antarctica* and *P. glacialis* under each irradiance/temperature treatment. Bars represent the mean of triplicate cultures and the error bars represent ± 1 S.D. from the mean. The * symbol indicates no significant difference between species for the same treatment (Student's t-test, $p<0.05$). Letters indicate no significant difference between treatments within each species (one-way ANOVA, $p<0.05$).

4.3.4 Cellular Carbon Content

4.3.4.1 Comparison between species

Carbon content ranged from 32 to 45 pmol cell^{-1} for *T. antarctica* and from 0.077 to 1.8 pmol cell^{-1} for *P. glacialis* (data not shown). Carbon content normalized by cell volume ranged from 12 to 18 fmol µm^{-3} in *T. antarctica* and from 7.2 to 18 fmol µm^{-3} in *P. glacialis* (Fig. 4.2A). Carbon content of *T. antarctica* was significantly higher than *P.*

glacialis at the low temperature, but not significantly different at the high temperature (Student's t-test, $p<0.05$).

4.3.4.2 Comparison between treatments

Significant differences in C content occurred between treatments for both species (Fig. 4.2A). The LI/HT C content of *T. antarctica* was significantly higher than the three other treatments (ANOVA, LSD, $p<0.05$). High temperature treatments resulted in significantly higher C content compared with low temperature treatments for *P. glacialis* (ANOVA, LSD, $p<0.05$).

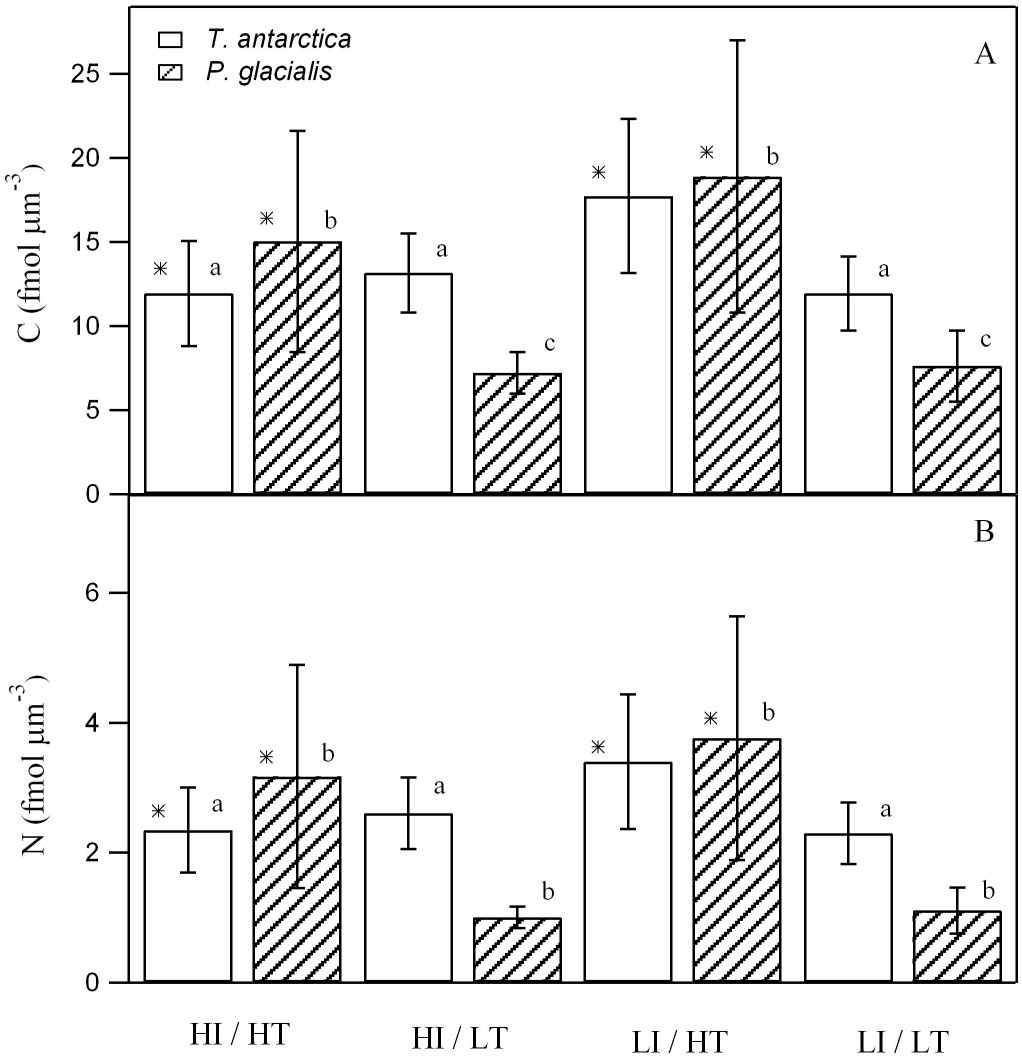

Figure 4.2. Carbon (A) and nitrogen (B) content normalized to cell volume for *T. antarctica* and *P. glacialis* under each irradiance/temperature treatment. Bars represent the average for triplicate cultures and the error bars represent ± 1 S.D. from the mean. The * symbol indicates no significant difference between species for the same treatment (Student's t-test, $p<0.05$). Letters indicate no significant difference between treatments within each species (one-way ANOVA, $p<0.05$). Note the different y-axis range between the upper and lower panel.

4.3.5 Cellular Nitrogen Content

4.3.5.1 Comparison between species

Cellular N content ranged from 6.1 to 8.7 pmol cell^{-1} for *T. antarctica* and from 0.11 to 0.35 pmol cell^{-1} for *P. glacialis* (data not shown). Normalized to cell volume, N content ranged from 2.3 to 3.4 fmol μm^{-3} for *T. antarctica* and from 1.0 to 3.8 fmol μm^{-3} for *P. glacialis* (Fig. 4.2B). Significant differences in N content existed between species for the LT treatments.

4.3.5.2 Comparison between treatments

The LI/HT N content of *T. antarctica* was significantly higher than in the three other treatments for this species (ANOVA, LSD, $p<0.05$) (Fig. 4.2B). Nitrogen content within *P. glacialis* was higher as a result of the high temperature treatments compared to the low temperature treatments, however, the differences were not significant (Kruskal-Wallis, $p<0.05$).

4.3.6 Cellular Silicon Content

Silicon content was normalized to cell, to cell volume, and to cell surface area. Normalizing Si to cell surface area is useful, as Si is incorporated into the cell frustule. However, Si should also be normalized to cell volume, as significant amounts of Si may be stored intracellularly (Martin-Jezequel et al., 2000).

4.3.6.1 Comparison between species

Cellular Si content ranged from 3.2 to 11.0 pmol cell^{-1} for *T. antarctica* and from 0.10 to 0.45 pmol cell^{-1} for *P. glacialis* (data not shown). Silicon content normalized to volume ranged from 1.2 to 4.3 fmol μm^{-3} for *T. antarctica* and from 0.90 to 4.8 fmol

μm^{-3} for *P. glacialis* (Fig. 4.3A). Silicon content normalized to surface area ranged from 3.0 to 11 fmol μm^{-2} in *T. antarctica* and from 0.68 to 3.4 fmol μm^{-2} in *P. glacialis* (Fig. 4.3B). The LI/LT combination was the only treatment for which there was no significant difference in Si content between species normalized to cell volume.

4.3.6.2 Comparison between treatments

The same trends were found for both *T. antarctica* and *P. glacialis* when normalized to cell volume (Fig. 4.3A). The HT treatments produced significantly higher Si content than the low temperature treatments. Silicon content normalized to surface area exhibited the same trend as Si normalized to cell volume (Fig. 4.3B).

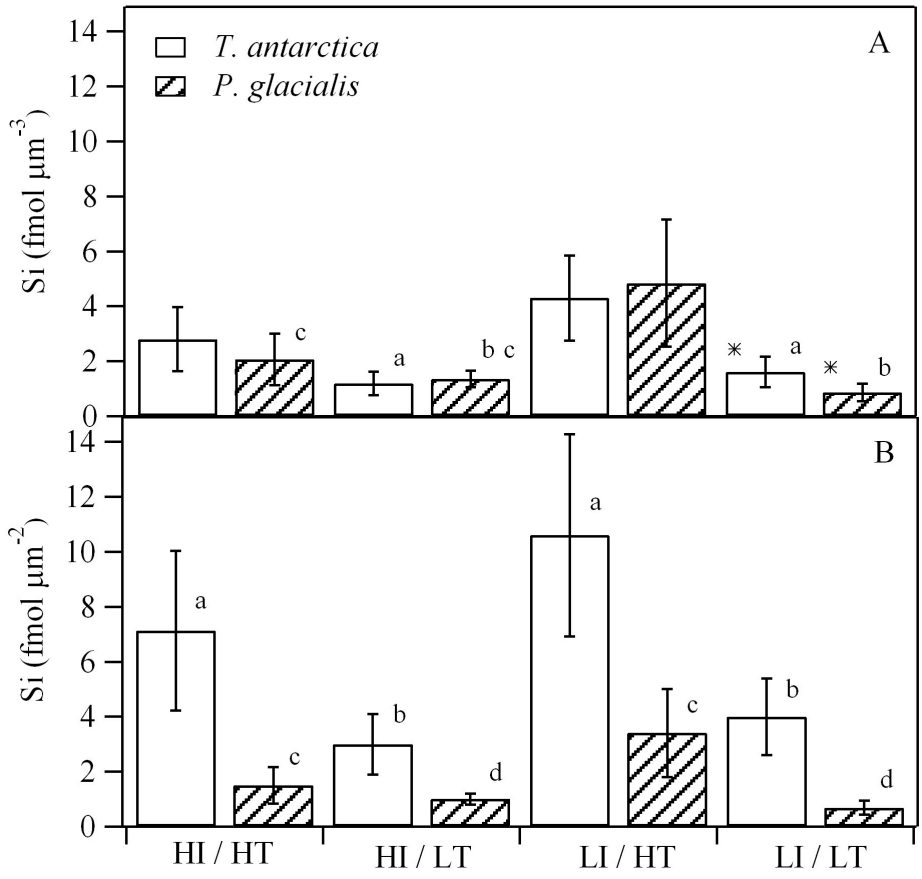

Figure 4.3. Silicon content expressed per cell volume (A) and surface area (B) for *T. antarctica* and *P. glacialis* under each irradiance/temperature treatment. Error bars represent ±1 SD about the mean. * symbol indicates no significant difference between species for the same treatment (Student's t-test, $p<0.05$). Letters indicate no significant difference between treatments within each species (one-way ANOVA, $p<0.05$).

Si content normalized to surface area decreased with increasing growth rate for *T. antarctica* (Fig. 4.4). The two high temperature treatments of *P. glacialis* follow the same trend. However, the Si content of the two low temperature treatments of *P. glacialis* appears to be unrelated to growth rate.

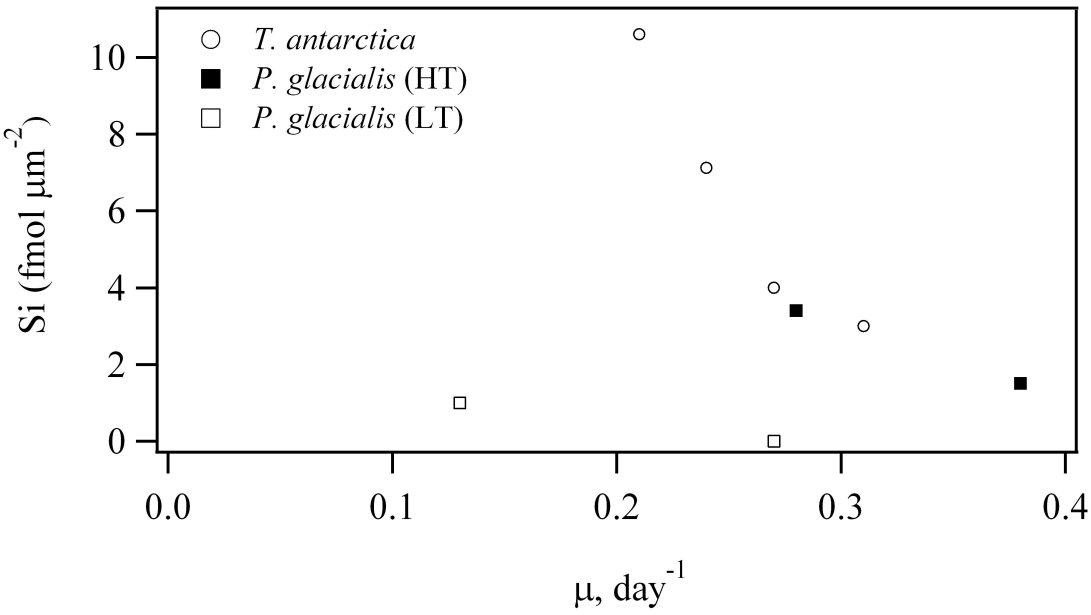

Figure 4.4. Cellular Si content normalized to cell surface area as a function of specific growth rate.

4.3.7 Cellular Stoichiometry

Ratios of cellular content C, N and Si as well as C:chl *a* are displayed in Table 4.3. C:N ratios were consistently below the Redfield ratio of 6.6 (Redfield, 1958). The only exceptions were the low temperature treatments of *P. glacialis.* Si:C ratios ranged from 0.09 to 0.24 for *T. antarctica* and from 0.11 to 0.25 for *P. glacialis*. Si:N ratios were below 1.0 for most of the treatments; exceptions were the LI/HT treatment for both species and the HI/LT treatment for *P. glacialis*. C:Chl *a* ratios ranged from 4.57 to 6.51 for *T. antarctica* and from 8.03 to 13.8 for *P. glacialis*.

Table 4.3. Cellular ratios of C:N, Si:C, Si:N and C:chl *a* for each species under each treatment. Values are the mean of cellular content ratios ± 1 SD of the mean.

		C:N mol:mol	Si:C mol:mol	Si:N mol:mol	C:Chl a mol:μg
HI/HT	*T. antarctica*	5.11±0.43	0.23±0.4	0.17±0.21	6.51±1.29
	P. glacialis	5.01±0.89	0.14±0.03	0.69±0.12	13.8±5.5
HI/LT	*T. antarctica*	5.08±0.26	0.09±0.03	0.47±0.13	6.50±1.42
	P. glacialis	7.19±0.4	0.19±0.05	1.37±0.36	8.03±2.31
LI/HT	*T. antarctica*	5.28±0.25	0.24±0.03	1.26±0.11	5.69±0.79
	P. glacialis	5.34±1.39	0.25±0.06	1.29±0.09	10.5±2.65
LI/LT	*T. antarctica*	5.22±0.18	0.13±0.03	0.70±0.15	4.57±1.11
	P. glacialis	6.93±0.48	0.11±0.02	0.77±0.07	8.53±1.1

4.3.8 Incorporation Rates

4.3.8.1 Comparison between species

Incorporation rates for C, N and Si for each species and under each treatment are displayed in Fig. 4.5. Incorporation rates of C were not significantly different between species, except for the LI/LT treatment (Fig. 4.5A). Significant differences between species were found for N incorporation rates for all treatments except the HI/LT treatments (Fig. 4.5B). No significant differences between species were found for the incorporation rates of Si (Fig. 4.5C) (Student's t-test, $p<0.05$).

4.3.8.2 Comparison between treatments

One-way ANOVA's determined that there were significant differences in the incorporation rates of the three nutrients between treatments for *P. glacialis*, but no

significant differences occurred between incorporation rates for any nutrients for *T. antarctica*. The C incorporation of *P. glacialis* under the LI/LT treatment was significantly lower than the three other treatments. The N incorporation of *P. glacialis* under the HI/LT treatment was significantly higher than the LI/LT and the HI/HT treatments. The Si incorporation of *P. glacialis* for the HI/LT was significantly higher than the other three treatments. The general trend for nutrient incorporation in *P. glacialis* was that the HI/LT treatment resulted in higher incorporation of any nutrient, while for *T. antarctica* no overall trend in nutrient incorporation could be deciphered.

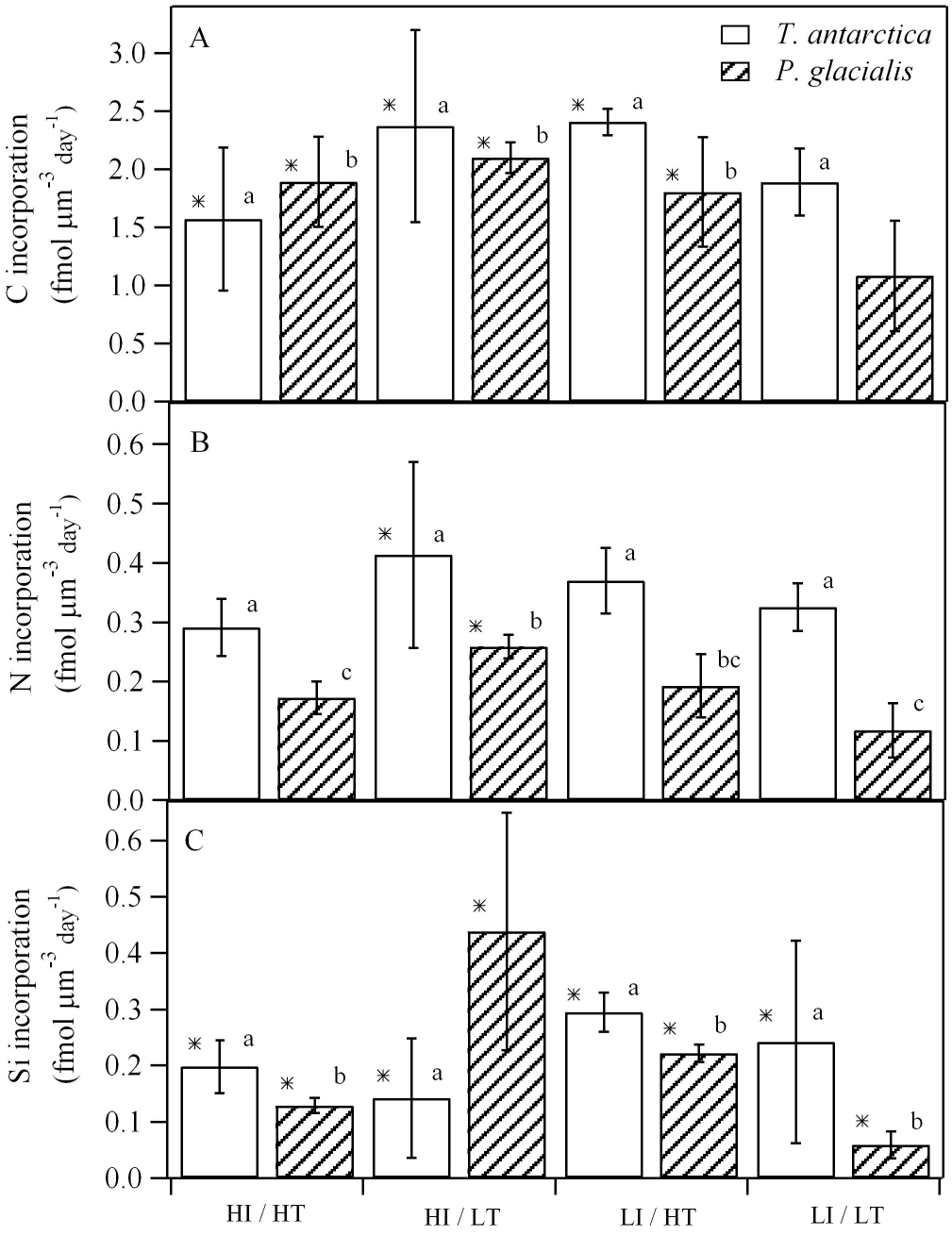

Figure 4.5. Incorporation rates for carbon (A), nitrogen (B) and silicon (C). Error bars represent nutrient incorporation rates ±1 SD of the mean. The * symbol indicates no significant difference between species for the same treatment (Student's t-test, $p<0.05$). Letters indicate no significant difference between treatments within each species (one-way ANOVA, $p<0.05$). Note the different y-axis range for A.

4.4 Discussion

4.4.1.1 Growth Rates

Specific growth rates for both species were low (0.13 – 0.38 day^{-1}) (Table 4.1) in comparison to those found for temperate species (e.g. *Skeletonema costatum* has a growth rate of >1 day^{-1} at optimum temperatures (Suzuki and Takahashi, 1995)). However, they generally agree well with previous estimates of growth rates for polar diatoms (e.g. <0.6 day^{-1} (Jacques, 1983)). The different affect of temperature on the growth rates of *T. antarctica* compared to *P. glacialis* shows that temperature effects are species-specific. Different responses to changes in temperature are predicted by the paradox of the plankton (Hutchinson, 1961), however, the changes are still of interest to community dynamics.

4.4.1.2 Cellular Stoichiometry

Our C:N ratios fall within the range of 3 to 17 reported by Geider and Laroche (2004). Our C:N ratios are not influenced by irradiance, which coincides with what Leonardos and Geider (2004) found for nutrient replete cultures. Most of the Si:C and Si:N particulate ratios reported in this study fall within the range reported for temperate diatoms by Brzezinski (1985). Exceptions are the Si:C ratios of *T. antarctica* at both high temperature treatments and that of *P. glacialis* at the LI/HT treatment. These three treatments exhibited Si:C ratios up to 0.13 above the average 0.12 reported by Brzezinski (1985). Claquin and Martin-Jezequel (2002) report that Si:C and Si:N ratios can increase from 2 to 6-fold when cultures are limited by irradiance. Brzezinski (1985) found that cultures grown under low light had higher Si:C ratios. In our study, the two highest Si:C ratios occurred under low irradiance treatments in agreement with Brzezinski (1985). As

C concentrations did not change with irradiance, changes in these ratios must be Si driven.

4.4.2 Species-specific Effects

Results show that the four different treatments affected the species in different ways. For example, the growth rate of *T. antarctica* increased from the HI/HT to the HI/LT while the growth rate for *P. glacialis* decreased from the HI/HT to the HI/LT treatment; C content decreased from the HI/LT treatment to the LI/LT treatment for both species. The species-specific effects of irradiance and temperature combined indicate that results from experiments conducted on one or two species cannot be generalized to a larger group of polar diatoms. Species-specific effects were expected, based on the paradox of the phytoplankton (Hutchinson, 1961). However, it remains important to determine in what way species adapt differently, and what the potential ecological implications of this are.

Temperature had a stronger effect on growth rates for these two species compared to irradiance. This result agrees with results found by Fialia and Oriol (1990) who determined that temperature was a more important factor than irradiance for seven diatom species tested over a temperature range of 0 to 15°C and an irradiance range of 46-220 μmol quanta m^{-2} s^{-1}. However, Mortain-Bertrand (1989) found that during an experiment with Antarctic diatoms, low growth rates were due to low irradiances rather than low temperatures. The variable influence of temperature and irradiance on the growth rates of polar diatoms indicates species-specific differences in adaptation strategies.

Species-specific effects complicate the prediction of natural phytoplankton assemblage changes due to environmental changes. The response of a phytoplankton

assemblage in terms of nutrient dynamics to changes in environmental conditions would depend on the dominant species within a phytoplankton assemblage. For example, the growth rate of a phytoplankton assemblage dominated by *P. glacialis* may show an increase in growth rate at 10°C if irradiance is increased, while an assemblage dominated by *T. antarctica* might not. Understanding the affects of irradiance and temperature in the natural environment may be better understood if experiments were conducted with different phytoplankton assemblages and the species composition of the assemblages was determined.

4.4.3 Irradiance Adaptations

Studies in the literature differ in their interpretation of phytoplankton adaptation to irradiance. For example, Mortain-Bertrand (1989) found that phytoplankton assemblages in the Southern Ocean were limited by irradiance, while Hoffman et al., (2007) found that phytoplankton assemblages in the Southern ocean were actually photoinhibited by irradiance, as deep as 28 m. This study shows that two polar diatom species, which inhabit the same environment, can be affected differently by irradiance levels. Thus, although a phytoplankton assemblage as a whole may either be limited or photoinhibited, the response of individual species may differ from response of the assemblage, an example of the paradox of the phytoplankton (Hutchinson, 1961). Generalizations of whether a phytoplankton assemblage is irradiance limited or photoinhibited do not take into account the diversity of species adaptations within a phytoplankton assemblage. Species specific responses may help understand dynamics within a natural phytoplankton assemblage, when an assemblage appears to be inhibited by irradiance, yet shows high productivity, such as in the Hoffman et al., (2007) paper.

4.4.4 Growth Rate - Silicon Content Relationship

Our results agree for the most part with those of Claquin and Martin-Jezequel (2002) who found a significant increase in Si per cell and per cell surface area with a decrease in growth rate. A decrease in growth rate allows for the diatom cells to spend relatively more time in the cell wall synthesis phase, allowing for a higher amount of silicification (Martin-Jezequel et al., 2000). The data from this study include two exceptions, however. For the treatments of *T. antarctica*, silicification always increased with a decrease in growth rate. For *P. glacialis*, silicification increased with decreased growth rates at the high temperature. However at the low temperature, silicification did not appear to be related to growth rate for *P. glacialis*. This is not just another example of species-specific effects, but an indication of a unique metabolic difference between *P. glacialis* and *T. antarctica*.

To my knowledge, there is no reason why the relationship between growth rate and silicification should not hold at low temperatures. In previous studies, diatoms grown under limiting conditions such as light (Taylor, 1985), temperature (Paasche, 1980) and ammonium (Martin-Jezequel et al, 2000) all show an increase in silicification with decreased growth rate. The requirement for Si by diatoms is solely for the production of the cell frustule; no other metabolic function is affecting the silicification of this species to my knowledge. It is my suggestion that further work should be conducted to determine the reasons behind deviations from the silicification/growth rate relationship.

4.4.5 Ecological Implications

Competition between two species results in the species with the higher growth rate out-competing the other species. Under low irradiance and low temperature, *T. antarctica* and *P. glacialis* have the same growth rate, however, a competitive advantage may still be awarded in the natural environment if another factor such as low nutrient concentrations becomes limiting. Under high irradiance and low temperature, *T. antarctica* would out-compete *P. glacialis*. Under these conditions, *T. antarctica* had significantly higher chlorophyll a, C and N (but not Si content). *P. glacialis* would out-compete *T. antarctica* at the higher temperature, under both irradiance conditions. Under these conditions, the only difference in cellular quota between the two species was their chlorophyll a levels at the high irradiance/high temperature treatment. On a cellular basis, *P. glacialis* contains lower concentrations of C, N and Si.

Based on the findings of Durbin (1977) and Paasche (1980), as well as the findings in this study, the response of species to changes in temperature and irradiance appear to be species-specific, and the relationship between growth rate and silicification does not always hold. If this is the case, predictions of the affect of changing physical conditions in the Arctic on phytoplankton assemblages remain difficult. The two species in this study respond differently to variations in irradiance and temperature levels. This would explain how these two species are able to coexist in the same environment; conditions *in situ* are constantly fluctuating and irradiance and temperatures, which may favor one species at a given moment can change to favor the other species (Hutchinson, 1961).

Growth rate is specifically controlled by the total light flux per day, not just the intensity of the irradiance (Mortain-Bertrand, 1989). Deep mixing layers in the Southern Ocean would favor diatoms adapted to living under constant light fluctuation; diatoms may be capable of rapidly adapting to available light, taking advantage of the total irradiance they are exposed to, rather then responding to an optimum condition which may be rare (Mortain-Bertrand, 1989). However, along the extensive coastal shelves found in the Arctic, deep mixing is not necessarily a factor and the euphotic zone can reach down to the shelf floor (see Chapter 3). Mortain-Bertrand concluded that a possible combined effect of temperature and irradiance should not be ignored.

Chapter 5

Conclusions

5.1 Accounting for Lithogenic Silica Interference on the Measurement of Biogenic Silica

The study outlined in Chapter 2 showed that linear relationships between BSi and LSi are not necessarily causative. In order to properly account for interference of lithogenic silica on the measurement of biogenic silica, clay sediment composition at the study site should be taken into account. In this study, estimating interference from dissolution characteristics of sediment components resulted in correction factors which fell within the range previously reported in the literature. Although a causative relationship did not exist between BSi and LSi at the study sites examined in this thesis, this does not preclude the relationship occurring at other study sites. Future research should be conducted to validate this method of correction for LSi interference on BSi measurements.

5.2 Carbon, Nitrogen and Silicon Cycling Along a Transect through the NE Pacific Ocean, Bering and Chukchi Seas

Stations sampled in different water masses along a transect from Victoria, Vancouver Island to Barrow, Alaska could be statistically categorized into three regions: the NE Pacific Ocean, the Bering Sea and the Chukchi Sea. ANOVA and Kruskal Wallis analysis showed significant differences between biological parameters in the NE Pacific

Ocean compared to the Bering Sea and the Chukchi Sea. Comparatively, the Bering and Chukchi Sea showed fewer significant differences between them. The similarity between the Bering and Chukchi Sea region could be due to iron replete conditions or to the influence of the Anadyr Stream in the Chukchi Sea. Further research to fully characterize the extent of the Anadyr Stream's influence is needed.

Biogenic silica net incorporation was estimated using an incubation method without the aid of stable or radioactive isotopes. Net incorporation rates calculated from this method agreed well with previous estimates from the literature where they were available. This method provided the first estimates of biogenic silica net incorporation in the Chukchi Sea. Prior to widespread use of this method, however, it should be validated in a study by the dual estimation of BSi net incorporation using this method as well as a stable isotopic method.

Estimates of BSi net incorporation illustrated the opportunity for BSi export in the NE Pacific Ocean. In contrast, in the Bering Sea and the Chukchi Sea, BSi was usually recycled in the upper water column. Estimates in the Bering and Chukchi Seas were limited to five depth profiles. Considering the scarcity of data in this region for BSi dynamics, this region should continue to be characterized by future studies.

5.3 Temperature and Irradiance Effects on Two Polar Diatom Species

Thalassiosira antarctica and *Porosira glacialis* cultured in the lab were treated with four combinations of irradiances and temperatures. Species-specific affects were seen in their cellular stoichiometry and growth rates. The cellular Si content did not always show an inverse relationship to growth rate, as is present in the literature for other diatom species. The deviation of *P. glacialis* from this relationship at the temperature of

6°C warrants further study. Similar studies with a larger number of polar diatom species should be conducted to determine the frequency of this deviation. Also, studies should be conducted to determine what aspect of diatom physiology is responsible for this deviation.

5.4 Silicon:Carbon Ratios in the Laboratory and in Natural Environments

Data from the NE Pacific and Bering and Chukchi Seas show that BSi:PC ratios are higher where the water is lower in temperature. Lab results show that the Si:C ratio of two polar diatom species was relatively high compared to the average found by Brzezinski (1985) for temperate species. The higher Si:C of polar diatoms may be the cause of the high BSi:PC ratio in the natural environment. The increase in cellular Si could be the result of a decrease in growth rate (Martin-Jezequel et al., 2000); this decrease has been shown for growth rate limitation by temperature (Paasche, 1980). As temperatures in the Arctic warm, growth rates of phytoplankton should generally increase. This could result in a decrease in silicification of diatoms at northern latitudes. Changes in silicification of diatoms will result in alterations to the biological Si cycle.

5.4.1 Future studies

There exists little BSi data for the polar areas of the Bering and the Chukchi Seas. Characterization of the silicification of diatoms in natural populations at high latitudes should be conducted to confirm the cause of the high BSi:PC ratios in this area. This could be undertaken by collecting samples for phytoplankton community composition, BSi and temperature data throughout the Bering and Chukchi Sea. Estimates of diatom BSi could be made from the BSi concentrations and diatom cell number data. Such a

study would benefit from the estimation of phytoplankton growth rates *in situ* to accompany the other data. It would be interesting to confirm a relationship between the silicification of the diatoms and either temperature or growth rate in the Bering and Chukchi Seas.

5.5 Acclimation of Natural Phytoplankton Populations to Environmental Changes

Previous studies have found that irradiance levels at high latitudes can be limiting or photoinhibiting to phytoplankton growth (e.g. Mortain-Bertrand; Hoffman et al., 2007). Based on the species-specific nature of the effects of irradiance found in this study, a study on species distribution may help understand the apparent discrepancy in the nature of responses to irradiance in natural environments. In this study, high concentrations of BSi were found at the bottom of the euphotic zone in the Bering and Chukchi Seas. Either productivity is photoinhibited by light levels closer to the surface, or irradiance levels near the surface are ideal, and production which occurs near the surface is simply sinking through the water column. Without species composition of the phytoplankton community coupled with knowledge of the irradiance range of the species present, or specific irradiance measurements, it cannot be said whether phytoplankton in this area are limited or photoinhibited or both. Phytoplankton production would be better understood if irradiance was quantified where phytoplankton production was measured.

5.5.1 Future studies

Few studies outlining the irradiance levels through the water column in the Arctic exist in the literature. Many studies of primary production rely on estimates of irradiance as percentages of surface irradiance, without reporting an actual measurement of surface

irradiance, including this study. Light levels in the Arctic are believed to be generally lower than levels at low latitudes due to the different angle of the sun. Primary production estimates coupled to real time irradiance measurements would help determine the true state of phytoplankton acclimation to light levels *in situ*.

5.6 Phytoplankton Production in the Bering and Chukchi Seas

Discrepancies in production estimates between recent studies and those conducted in the 1980's and 1990's in the Bering and Chukchi Seas indicate that we do not have a clear understanding of the state of primary production in the Arctic. We do not know whether primary production is stable in time, fluctuating on short term cycles or declining over the long term. The state of primary production is important in the Arctic as it is an essential wildlife habitat and productive area for higher trophic levels. Changes in primary production may already be affecting higher trophic levels (Grebmeier et al., 2006). The lab study conducted for this thesis (chapter 4) showed that polar diatom species differ significantly in their responses to concomitant changes in irradiance and temperature. Therefore it is difficult to project whole phytoplankton community changes without more data on individual polar species. Also lacking is a regular sampling program for primary production in the Bering and Chukchi Seas. Production data from this study agreed with the most recent estimates, however, it is still not possible to conclude whether these two studies represent a longer term decline in primary production.

5.6.1 Future studies

In order to determine if low levels of primary production recently measured in the Bering and Chukchi Seas are part of long term decline, a regular sampling program

should be initiated. In order to predict how changing conditions in the environment will affect primary production, it would be interesting to conduct mesoscale grow out experiments with natural phytoplankton assemblages from polar environments, subjecting them to different temperatures and irradiances. This would help account for species-specific responses to changing temperature and irradiance if natural populations were used for these experiments.

References

Aguilar-Islas, A. M., M. P. Hurst, K. N. Buck, B. Sohst, G. J. Smith, M. C. Lohan and K. W. Bruland (2007) Micro- and macronutrients in the southeastern Bering Sea: Insight into iron-replete and iron-depleted regimes. Progress in Oceanography 72(2):99-126

Aizawa, C., M. Tanimoto and R. W. Jordan (2005) Living diatom assemblages from North Pacific and Bering Sea surface waters during summer 1999. Deep-Sea Research II 52: 2186-2205

Bak, Y. S, K. C. Yoo, H. I. Yoon, J. D. Lee and H. Yun (2007) Diatom evidence for Holocene paleoclimatic change in the South Scotia Sea, West Antarctica. Geosciences Journal 11(1):11-22

Banahan, S. and J. J. Goering (1986) The production of biogenic silica and its accumulation on the southeastern Bering Sea shelf. Continental Shelf Research 5(1/2):199-213

Barwell-Clarke, J. and F. Whitney (1996) Institute of Ocean Sciences nutrient methods and analysis. Can. Tech. Rep. Hydrogr. Ocean Sci, pp. 49

Basile-Doelsch, I., J. D. Meunier and C. Parron (2005) Another continental pool in the terrestrial silicon cycle. Nature 433: 399-402

Bates, N. R., M. H. P. Best and D. A. Hansell (2005) Seasonal and spatial distribution of particulate organic matter (POM) in the Chukchi and Beaufort Seas. Deep Sea Research II: 52 (24-26): 3324-3343

Bauer, A. and Berger, G. (1998) Kaolinite and smectite dissolution rate in high molar KOH solutions at 35° and 80°C. Applied Geochemistry 13(7):905-916

Beardall, J. and I. Morris (1976) The concept of light intensity adaptation in marine phytoplankton: Some experiments with *Phaeodactylum tricornutum*. Marine Biology 37(4):377-387

Berges, J. A., D. E. Varela, P. J. Harrison (2002) Effects of temperature on growth rate, cell composition and nitrogen metabolism in the marine diatom *Thalassiosira pseudonana* (Bacillariophyceae) Marine Ecology Progress Series 225:139-146

Bidle, K. D. and Azam, F. (1999) Accelerated dissolution of diatom silica by marine bacterial assemblages. Nature 397 (6719): 508-512

Bidle, K. D and Azam, F. (2001) Bacterial control of silicon regeneration from diatom detritus: Significance of bacterial ectohydrolases and species identity. Limnology and Oceanography 46 (7): 1606-1623

Bidle, K. D., M. Manganelli and F. Azam (2002) Regulation of oceanic silicon and carbon preservation by temperature control on bacteria. Science 298 (5600): 1980-1984

Boyd, P. and P. J. Harrison (1999) Phytoplankton dynamics in the NE subarctic Pacific. Deep-Sea Research Part II-Topical Studies in Oceanography 46(11-12):2405-2432

Boyd, P., J. LaRoche, M. Gall, R. Frew and R. M. I. McKay (1999) Role of iron, light and silicate in controlling algal biomass in subantarctic waters SE of New Zealand. Journal of Geophysical Research 104 C6:13395-13408

Brzezinski, M. A. (1985) The Si:C:N ration of marine diatoms: Interspecific variability and the effect of some environmental variables. Journal of Phycology 21:347-357

Brzezinski, M. A. (1992) Cell-cycle effects on the kinetics of silicic acid uptake and resource competition among diatoms. Journal of Plankton Research 14:1511-1539

Brzezinski, M. A. and D. M. Nelson (1989) Seasonal-changes in the silicon cycle within a gulf-stream warm-core ring. Deep-Sea Research Part A-Oceanography Research Papers 36(7):1009-1030

Brzezinski, M. A. and D. M. Nelson (1995) Tha annual silica cycle in the Sargasso Sea near Bermuda. Deep Sea Research I 42 (2):1215-1237

Brzezinski, M. A., J. L. Jones, K. D. Bidle and F. Azam (2003) The balance between silica production and silica dissolution in the sea: Insights from Monterey Bay, California, applied to the global data set. Limnology and Oceanography 48 (5): 1846-1854

Brzezinski, M. A., M. Dickson, D. M. Nelson and R. Sambrotto (2003) Ratios of Si, C and N uptake by microplankton in the Southern Ocean. Deep-Sea Research II 50:619-633

Bruland, K. W., E. L Rue and G. J. Smith (2001) Iron and macronutrients in California coastal upwelling regimes: Implications for diatom blooms. Limnology and Oceanography 46(7):1661-1674

Carmack, E. and P. Wassmann (2006) Food webs and physical-biological coupling on pan-Arctic shelves: Unifying concepts and comprehensive perspectives. Progress in Oceanography 71:446-477

Claquin, P. and V. Martin-Jezequel (2002) Uncoupling of silicon compared with carbon and nitrogen metabolisms and the role of the cell cycle in continuous cultures of Thalassiosira pseudonana (Bacillariophyceae) under light, nitrogen and phosphorus control. Journal of Phycology 38(5):922-930

Claquin, P., V. Martin-Jezequel, J. C. Kromkamp, M. J. W. Veldhuis and G. W. Kraay (2002) Uncoupling of silicon compared with carbon and nitrogen metabolisms and the role of the cell cycle in continuous cultures of Thalassiosira pseudonana (Bacillariophyceae) under light, nitrogen and phosphorus control. Journal of Phycology 38:922-930

Coachman, L. K., K. Aagaard and R. B. Tripp (1975) Bering Strait: The regional physical oceanography. University of Washington Press 172pp.

Coachman, L. K. (1986) Circulation, water masses, and fluxes on the southeastern Bering Sea shelf. Continental Shelf research 5(1-2):23-108

Codispoti, L. A. et al (2001) The oceanic fixed nitrogen and nitrous oxide budgets: moving targets as we enter the anthropocene? Scientia Marina 65: 85-205

Dauchez, S., L. Legendre and L. Fortier (1995) Assessment of simultaneous uptake of nitrogenous nutrients (15N) and inorganic carbon (13C) by natural phytoplankton populations. Marine Biology 123:651-666

DeMaster, D. J. (2002) The accumulation and cycling of biogenic silica in the Southern Ocean: revisiting the marine silica budget. Deep-Sea research Part II-Topical Studies in Oceanography 49(16):3155-3167

Ducklow, H. W., D. K. Steinberg, K. O. Buesseler (2001) Upper ocean export and biological pump. Oceanography JGOFS special issue

Dugdale, R. C. and J. J. Goering (1967) Uptake of new and regenerated forms of nitrogen in primary productivity. Limnology and Oceanography 12(2):196-206

Dugdalde, R. C. and F. P. Wilkerson (1986) The use of 15N to measure nitrogen uptake in eutrophic oceans; experimental considerations. Limnology and Oceanography 31(4):673-689

Dugdale, R. C. and F. P. Wilkerson (1998) Silicate regulation of new production in the equatorial Pacific upwelling. Nature 391:270-273

Dugdale, R. C., F. P. Wilkerson and H. J. Minas (1995) The role of a silicate pump in driving new production. Deep-Sea Research Part 1 – Oceanographic Research Papers 42 (5): 697-719

Durbin, E. G. (1977) Studies of the autoecology of the marine diatom Thalssiosira nordenskioeldii II. The influence of cell size on growth rate and carbon, nitrogen, chlorophyll a and silicon content. Journal of Phycology 13:150

Dytham, C. (2003) Choosing and using statistics A biologists guide. Blackwell Publishing 248pp.

Elrifi, I. R. and D. H. Turpin (1985) Steady-state luxury consumption and the concept of optimum nutrient ratios – A study with phosphate and nitrate limited Selenastrum minutum (Chlorophyta). Journal of Phycology 21(4):592-602

Eppley, R. W. (1972) Temperature and phytoplankton growth in the sea. Fishery Bulletin 70(4):1063-1085

Falkowski, P. G. (2000) Rationalizing elemental ratios in unicellular algae. Journal of Phycology 36:3-6

Favorite, F., A. J. Dodimead and K. Nasu (1976) Oceanography of the Subarctic Pacific region, 1960-1971. Bulletin of the International North Pacific Fishery Commission 33:1-187

Fiala, M. and L. Oriol (1990) Light-temperature interactions on the growth of Antarctic diatoms. Polar Biology 10:629-636

Flynn, K. F. and V. Martin-Jezequel (2000) Modelling Si-N-limited growth of diatoms. Journal of Plankton Research 22:447-472

Franck, V. M., M. A. Brzezinski, K. H. Coale and D. M. Nelson (2000) Iron and silicic acid concentrations regulate Si uptake north and south of the Polar Frontal Zone in

the Pacific Sector of the Southern Ocean. Deep-Sea Research Part II-Topical Studies in Oceanography 47(15-16):3315-3338

Fry, B. and S. C. Wainright (1991) Diatom sources of ^{13}C-rich carbon in marine food webs. Marine Ecology Progress Series 76(149-157)

Furnas, M. (1978) Influence of temperature and cell size on the division rate and chemical content of the diatom *Chaetoceros curvisetum* Cleve. Journal of Experimental Biology and Ecology 34:97-109

Geider, R. J. and J. La Roche (2002) Redfield revisited: variability of C:N:P in marine microalgae and its biochemical basis. European Journal of Phycology 37:1-17

Gosselin, M., L. Legendre, J. C. Therriault and S. Demers (1990) Light and nutrient limitation of sea-ice microalgae (Hudson-Bay, Canadian Arctic) Journal of Phycology 26(2):220-232

Grebmeier, J. M., L. W. Cooper, H. M. Feder and B. I. Sirenko (2006) Ecosystem dynamics of the Pacific-influenced Northern Bering and Chukchi Seas in the Amerasian Arctic. Progress in Oceanography 71:331-361

Grebmeier, J. M., J. E. Overland, S. E. Moore, E. V. Farley, E. C. Carmack, L. W. Cooper, K. E. Frey, J. H. Helle, F. A. McLaughlin and S. L. McNutt (2005) A major ecosystem shift in the Northern Bering Sea. Science 311:1461-1464

Guillard, R. R. L. (1975) Culture of phytoplankton for feeding marine invertebrates. In Smith, W. L. and M. H. Chanley (eds.) Culture of Marine Invertebrate Animals. Plenum Press, New York pp. 26-60

Guillard, R. R. and J. H. Ryther (1962) Studies of marine planktonic diatoms, I. Cyclotella nana Hustedt, and Detonula confervacea (cleve). Canadian Journal of Microbiology 8:229-239

Hardin, G. (1960) The competitive exclusion principle. Science 131(3409):1292-1297

Harrison, P. J., P. W. Boyd, D. E. Varela, S. Takeda, A. Shiomoto and T. Odate (1999) Comparison of factors controlling phytoplankton productivity in the NE and NW subarctic Pacific gyres. Progress in Oceanography 43: 205-234

Harrison, P. J., R. E. Waters and F. J. R. Taylor (1980) A broad spectrum artificial seawater medium for coastal and open ocean phytoplankton. Journal of Phycology 16:28-35

Herbert, R. A. (1999) Nitrogen cycling in coastal marine ecosystems. FEMS Microbiological Reviews 23(5):563-590

Hoffman, L. J., I. Peeken and K. Lochte (2007) Co-limitation by iron, silicate, and light of three Southern Ocean diatom species. Biogeosciences Discussions 4:209-247

Hoffman, L. J., I. Peeken and K. Lochte (1997) Effects of iron on the elemental stoichiometry during EIFEX and in the diatoms Fragilariopsis kerguelensis and Chaetoceros dichaeta. Biogeosciences 4:569-579

Hood, D. W. (1983) The Bering Sea in Estuaries and Enclosed Seas edited by Ketchum, B. H. Elsevier Scientific Publishing Company pgs 337-370

Hulth, S., R. C. Allen, D. E. Canfield, T. DAlsgaard, P. Engstrom, F. Gilbert, K. Sundback, B. Thamdrup (2005) Nitrogen removal in marine environments: recent findings and future research challenges. Marine Chemistry 94: 125-145

Hunt, G. L., P. Stabeno, G. Walters, E. Sinclair, R. D. Brodeur, J. M. Napp and N. A. Bond (2002) Climate change and control of the southeastern Bering Sea pelagic ecosystem. Deep-sea research II 49:5821-5853

Hutchins, D. A. and K. W. Bruland (1998) Iron-limited diatom growth and Si:N uptake ratios in a coastal upwelling regime. Nature 393(6685):561-564

Hutchinson, G. E. (1961) The paradox of the plankton. The American Naturalist XCV(882): 137-145

Intergovernmental Panel on Climate Change, 2007. Fourth Assessment Report, Climate Change 2007: Synthesis Report. The Core Writing Team IPCC, Geneva Switzerland, 52pp.

Jacques, G. (1983) Some ecophysiological aspects of the Antarctic phytoplankton. Polar Biology 2:27-33

Johannessen, O. M., L. Bengtssen, M. W. Mills, S. I. Kuzmina, V. A. Semenov, G. V. A. Lekseev, A. P. Nagurnyi, V. F. Zakharov, L. P. Bobylev, L. H. Pettersson, K. Hasselmann, H. P. Cattle (2004) Arctic climate change: observed and modeled temperature and sea-ice variability. Tellus A 56(4):328-341 doi:10.1111/j.1600-0870.2004.00060.x

Kamatani, A. (1982) Dissolution rates of silica from diatoms decomposing at various temperatures. Marine Biology 68 (1): 91-96

Kamatani, A. and Riley, J. P. (1979) Rate of dissolution of diatom silica walls in seawater. Marine Biology 55 (1): 29-35

Karcher, M. J., R. Gerdes, F. Kauker and C. Koberle (2003) Arctic warming: Evolution and spreading of the 1990's warm event in the Nordic Seas and the Arctic Ocean. Journal of Geophysical Research 108 C2 3034 doi:10.1029/2001JC001265

Kiorboe, T. and J. L. S. Hansen (1993) Phytoplankton aggregate formation: pbservations of patterns and mechanisms of cell sticking and the significance of exopolymeric material. Journal of Plankton Resrach 15(9):993-1018

Kirst, G. O and C. Wiencke (1995) Ecophysiology of polar algae. Journal of Phycology 31:181-199

Klausmeier, C. A., E. Litchman, T. Daufresne and S. A. Levin (2004) Optimal nitrogen-to-phosphorus stoichiometry of phytoplankton. Nature 429:171-174

Krausse, G. L., C. L. Schelske and C. O. Davis (1983) Comparison of three wet-alkaline methods of digestion of biogenic silica in water. Freshwater Biology 13 73-81

Leblanc, K., C. E. Hare, P. W. Boyd, K. W. Bruland, B. Sohst, S. Pickmere, M. C. Lohan, K. Buck, M. Ellwood and D. A. Hutchins (2005) Iron and zinc effects on the silicon cycle and diatom community structure in two contrasting high and low silicate HNLC areas. Deep Sea Research Part I 52(10): 1842-1864

LeBlanc, K, B. Queguiner, N. Garcia, P. Rimmelin and P. Raimbault (2003) Silicon cycle in the NW Mediterranean Sea: seasonal study of a coastal oligotrophic site. Oceanologica Acta 26(4):339-355

Lee, S. H., T. E. Whitledge, S-H. Kang (2007) Recent carbon and nitrogen uptake rates of phytoplankton in the Bering Strait and Chukchi Sea. Continental Shelf Research 27:2231-2349

Leonardos, N. and R. J. Geider. (2004) Effects of nitrate:phosphate supply ratio and irradiance on the C:N:P stoichiometry of *Chaetoceros muellri*. European Journal of Phycology 39:173-180

Leu, E. S. Wanberg, A. Wilff, S. Falk-Petersen, J. B. Orbael and D. O. Hessen (2006) Effects of changes in ambient PAR and UV radiation on the nutritional quality of an Arctic diatom (*Thalassiosira antarctica* var. *borealis*). Journal of Experimental marine Biology and Ecology 337:65-81

Levitus, S. (1982) Climatological Atlas of the World Ocean. U.S. Dept of Commerce, National Oceanic and Atmospheric Administration, 173pp.

Lewin, J. C. (1961) The dissolution of silica from diatom walls. Geochimica et Cosmochimica Acta 21:182-198

Lewin, J. C. (1962) Silification *In* Lewin, R. A. [Ed] Physiology and Biochemistry of Algae. Academic Press, pp. 445-455

MacIsaac, J. J, R. C. Dugdale, R. T. Barber, D. Blasco and T. T. Packard (1985) Primary production cycle in an upwelling center. Deep-sea Research 32(5A):503-529

Maddison, E. J. et al (2006) Post-glacial seasonal diatom record of the Mertz Glacier Polynya, East Antarctica. Marine Micropaleontology 60 (1): 66-88

Martin, J. H. and S. Fitzwater (1988) Iron deficiency limits phytoplankton growth in the north-east Pacific subarctic. Nature 331:341-343

Martin-Jezequel, V., M. Hildebrand and M. A. Brzezinski (2000) Silicon metabolism in diatoms: implications for growth. Journal of Phycology 36: 821-840

Massana, R. Pedrosalio (1994) A method to determine predation in stratified waters. Limnology and Oceanography 39:248-262

Moore, S. E., J. M. Grebmeier and J. R. Davies (2003) Gray whale distribution relative to forage habitat in the northern Bering Sea: current conditions and retrospective summary. Canadian Journal of Zoology 81(4):734-742

Mortain-Bertrand, A. (1989) Effects of light fluctuations on the growth and productivity of Antarctic diatoms in culture. Polar Biology 9:245-252

Naidu, A. S., J. S. Creager and T. C. Mowatt (1982) Clay mineral dispersal patterns in the North Bering and Chukchi Seas. Marine Geology 47:1-15

Naidu, A. S. and T. C. Mowatt (1983) Sources and dispersal patterns of clay minerals in surface sediments from the continental-shelf areas off Alaska. Geological Society of American Bulletin 94:841-854

Naidu, A. S., M. W. Han, T. C. Mowatt, and W. Wajda (1995) Clay minerals as indicators of sources of terrigenous sediments, their transportation and deposition: Bering Basin, Russian-Alaskan Arctic. Marine Geology 127:87-104

Nelson, D. M., P. Treguer, M. A. Brzezinski, A. Leynaert and B. Queguiner (1995) Production and dissolution of biogenic silica in the ocean: Revised global estimates, comparison with regional data and relationship to biogenic sedimentation. Global Biogeochemical Cycles 9 (3): 359-372

Nihoul, J. C. J, P. Adam, P. Brasseur, E. Deleersnijder, S. Djenidi and J. Haus (1993) Three-dimensional general circulation model of the northern Bering Sea's summer ecohydrodynamics. Continental Shelf Research 13(5/6):509-542

Paasche, E. (1980) Silicon content of five marine plankton diatom species measured with a raptor filter method. Limnology and Oceanography 25(3):474-480

Parsons, T. R., Y. Maita, and C. M. Lalli (1984) A Manual of Chemical and Biological Methods for Seawater Analysis. Pergamom Press pp 3-28

Pena, M. A. and D. E. Varela (2007) Seasonal and interannual variability in phytoplankton and nutrient dynamics along Line P in the NE subarctic Pacific. Progress in Oceanography 75:200-222

Ragueneau, O. and P. Treguer (1994) Determination of biogenic silica in coastal waters: applicability and limits of the alkaline digestion method. Marine Chemistry 45: 43-51

Raven, J. A and R. J. Geider (1988) Temperature and algal growth. New Phytologist 110(4):441-461

Redfield, A. C. (1958) The biological control of chemical factors in the environment. American Scientific 46:205-221

Ryther, J. H and D. W. Dunstan (1971) Nitrogen, phosphorus and eutrophication in the marine environment. Science 171(3975):1008-1013

Sakshaug, E. and D. Slagstad (1991) Light and productivity of phytoplankton in polar marine ecosystems: a physiological view. *In* Proceedings of the Pro Mare Symposium on Polar Marine Ecology. Sakshaug, E., C. C. E. Hopkins and N. A. Oritsland (eds.) Pp. 69-85

Sambrotto, R. N., G. Savidge, C. Robinson, P. Boyd, T. Takahashi, D. M. Karl, C. Langdon, D. Chipman, J. Marra and L. Codispoti (1993) Elevated consumption of carbon relative to nitrogen in the surface ocean. Nature 363:248-250

Schandelmeier, L. and V. Alexander (1981) An analysis of the influence of ice on spring phytoplankton population-structure in the Southeast Bering Sea. Limnology and Oceanography 26(5):935-943

Schell, D. M. (2000) Declining carrying capacity in the Bering Sea: isotopic evidence from baleen whale. Limnology and Oceanography 45(2):459-462

Serreze, M. C., J. A. Maslanik, T. A. Scambos, F. Fetterer, J. Stroeve, K. Knowles, C. Fowler, S. Drobot, R. G. Barry and T. M. Haran (2003) A record minimum arctic

sea ice extent and area in 2002. Geophysical Research Letters 30:3, 1110, doi:10.1029/2002GL016406

Shipe, R. F. and M. A. Brzezinski (2003) Siliceous plankton dominate rimary and new productivity during the onset of El Nino conditions in Santa Barbara Basin, California. Journal of Marine Systems 42:127-143

Shuter, B. (1979) A model of physiological adaptation in unicellular algae. Journal of Theoretical Biology 78(4):519-552

Smith, R. E., P. Clement and E. Head (1989) Biosynthesis and photosynthate allocation patterns of Arctic ice algae. Limnology and Oceanography 34(3):591-605

Springer, A. M. and C. P. McRoy (1993) The paradox of pelagic food webs in the northern Bering Sea – III. Patterns of primary production. Continental Shelf Research 13 (5/6): 575-599

Springer, A. M., C. P. McRoy and M. V. Flint (1996) The Bering Sea green belt: shelf-edge processes and ecosystem production. Fisheries Oceanography 5(3/4):205-223

Stickley, C. E., J. Pike and A. Leventer (2005) Deglacial ocean and climate seasonality in laminated diatom sediments, Mac. Robertson Shelf, Antarctica. Palaeogeography Palaeoclimatology Palaeoecology 227(4):290-310

Stroeve, J. C., M. C. Serreze, F. Fetterer, T. Arbetter, W. Meier, J. Maslanik and K. Knowles (2005) Tracking the Arctic's shrinking ice cover: Another extreme September minimum in 2004. Geophysical Research Letters 32:L04501 doi:10.1029/2004GL021810

Sukhanova, I. N., M. V. Flint, T. E. Whitledge, D. A. Stockwell and T. K. Rho (2006) Mass development of the planktonic diatom *Proboscia alata* over the Bering Sea shelf in the summer season. Oceanology 46(2):200-216

Sun, J. and D. Y. Liu (2003) Geometric models for calculating cell biovolume and surface area for phytoplankton. Journal of Palnkton Research 25(11):1331-1346

Suzuki, Y. and M. Takahashi (1995) Growth responses of several diatom species isolated from various environments to temperature. Journal of Phycology 31 (6): 880-888

Takeda, S. (1998) Influence of iron availability on nutrient consumption ratio of diatoms in oceanic waters. Nature 393(6687):774-777

Taylor, N. J. (1985) Silica incorporation in the diatom Coscinodiscus granii as affected by light intensity. Br. Phycology Journal 20:365-374

Thompson, P. (1999) The response of growth and biochemical composition to variations in daylength, temperature, and irradiance in the marine diatom *Thalassiosira pseudonana* (Bacillariophyceae). Journal of Phycology 35:1215-1223

Treguer, P., D. M. Nelson, A. J. Vanbennekom, D. J. Demaster, A. Leynaert and B. Queguiner (1995) The silica balance in the world ocean – a reestimate. Science 268(5209):375-379

Tsunogai, S., M. Kusakabe, H. Iizumi, I. Koike and A. Hattori (1979) Hydrographic features of the deep water of the Bering Sea, the sea of silica. Deep-Sea Research 26A:641-659

Varela, D. E. and P. J. Harrison (1999) Seasonal variability in nitrogenous nutrition of phytoplankton assemblages in the northeastern subarctic Pacific Ocean. Deep-Sea Research II 46:2505-2538

Villareal, T. A. and G. A. Fryxell (1983) Temperature effects on the valve structure of the bipolar diatoms *Thalassiosira antarctica* and *Porosira glacialis*. Polar Biology 2:163-169

Von Quillfeldt, C. H. (2000) Common diatom species in arctic blooms: their distribution and abundance. Botanica Marina 43(6):499-516

Viscosi-Shirley, C. K Mammone, N. Pisias and J. Dymond (2003) Clay mineralogy and multi-element chemistry of surface sediments on the Siberian-Arctic shelf: implications for sediment provenance and grain size sorting. Continental Shelf Research 23 (11-12):1175-1200

Walsh, J. J., C. P. McRoy, L. K. Coachman, J. J. Goering, J. J. Nihoul, T. E. Whitledge, T. H. Blackburn, P. L. Parker, C. D. Wrick, P. G. Shuert, J. M. Grebmeier, A. M. Springer, R. D. Tripp, D. A. Hansell, S. Djenidi, E. Deleersnuder, K. Henriksen, B. A. Lund, P. Anderse,. F. E. Muller-Karger and K. Dean (1989) Carbon and nitrogen cycling within the Bering/Chukchi Seas: Source regions for organic matter effecting AOU demands of the Arctic Ocean. Progress in Oceanography 22:277-339

Ward, B. B. (2000) Nitrification and the marine nitrogen cycle. In: Kirchman, D. L. (Ed.), Microbial Ecology of the Oceans. Wiley-Liss, New York, pp. 427-453

Whitledge, T. E., W. S. Reeburgh and J. J. Walsh (1986) Seasonal inorganic nitrogen distributions and dynamics in the South Eastern Bering Sea. Continental Shelf Research 5 (1-2):109-132

Whitney, F. A. and H. J. Freeland (1999) Variability in upper-ocean water properties in the NE Pacific Ocean. Deep-Sea Research II 46:2351-2370

Whitney, F. A., D. W. Crawford and T. Yoshimura (2005) The uptake and export of silicon and nitrogen in HNLC waters of the NE Pacific Ocean. Deep-Sea Research II 52:1055-1067

Wong C. S., N. A. D. Waser, Y. Nojiri, F. A. Whitney, J. S. Page and J. Zeng (2002) Seasonal cycles of nutrients and dissolved inorganic carbon at high and mid latitudes in the North Pacific Ocean during the Skaugran cruises: determination of new production and nutrient uptake ratios. Deep Sea Research II 49: 5317-5338

Wong, C. S. and Matear, R. J. (1999) Sporadic silicon limitation of phytoplankton productivity in the subarctic North Eastern pacific Ocean. Deep Sea Research Part II 46(11-12): 2539-2555

Woodgate, R. (2006) Applied Physics Laboratory, University of Washington. personal communication

Zehr, J. P. and Ward, B. B. (2002) nitrogen cycling in the ocean: new perspectives on processes and paradigms. Applied and Environmental Microbiology 68: 1015-1024

Zielinkski, U. and R. Gersonde (1997) Diatom distribution in Southern Ocean surface sediments (Atlantic sector): Implications for palaeoenvironmental reconstructions. Palaeogeography Palaeoclimatology Palaeoecology 129(3-4):213-250

Appendix

Table 7.1 Latitude, longitude and depth of stations sampled as part of a surface transect leading up to Unimak Pass.

Station	Latitude (N)	Longitude (W)	Depth (m)
UN8	53° 38.35’	163° 47.991’	>1000
UN7	53° 43.9857’	163° 55.934’	>1000
UN6	53° 48.446’	164° 3.722’	91
UN5	53° 53.03’	164° 11.64’	81
UN4	53° 57.57’	164° 20.148’	110
UN3	54° 25.09’	164° 27.998’	110
UN2	54° 6.874’	164° 35.774’	88
UN1	54° 11.405’	164° 43.827’	69

Table 7.2 Biological parameters for the stations heading up to Unimak Pass. All samples were collected at 1 m depth. ND means no data.

Station	chl a (μg L^{-1})	PC (μmol L^{-1})	PN (μmol L^{-1})	Bsi (μmol L^{-1})	Lsi (μmol L^{-1})	C incorporation (μmol L^{-1} day^{-1})	N incorporation (μmol L^{-1} day^{-1})	Bsi net incorporation (μmol L^{-1} day^{-1})	Nitrate (μmol L^{-1})	Phosphate (μmol L^{-1})	Silicic acid (μmol L^{-1})
8	9.36	6.64	1.15	0.84	0.02	0.97	0.07	0.26	9.51	2.96	15.71
7	1.18	13.82	2.50	1.84	0.02	2.78	0.35	0.48	1.17	1.44	8.05
6	1.36	14.67	2.63	5.98	0.01	2.41	0.07	-1.14	0.00	1.28	3.94
5	3.23	14.59	2.78	0.56	0.04	3.76	0.07	0.11	0.00	1.24	12.77
4	0.71	8.44	1.44	0.13	0.02	0.86	0.03	0.03	0.00	1.02	14.33
3	0.52	8.07	1.41	ND	ND	1.25	0.07	ND	0.00	1.08	13.66
2	0.49	8.25	1.64	0.17	0.02	1.72	0.04	0.08	0.00	1.25	14.81
1	0.94	9.99	2.15	0.46	0.04	2.67	0.07	0.32	0.64	1.68	15.74

Table 7.3 Latitude, longitude and depth of stations sampled as part of a surface transect from the deep Bering Sea basin to the Bering Sea Shelf

Station	Latitude (N)	Longitude (W)	Bottom Depth (m)
BS1	56° 18.680’	172° 49.520’	1715
BS2	56° 25.025’	172° 47.873’	1356
BS3	56° 28.502’	172° 46.90’	800
BS4	56° 32.659’	172° 45.510’	248
BS5	56° 38.711’	172° 43.821’	133

Table 7.4 Biological parameters for the stations leading from the deep Bering Sea basin to the Bering Sea shelf. All samples were collected at 1 m depth.

Station	chl a (μg L^{-1})	PC (μmol L^{-1})	PN (μmol L^{-1})	Bsi (μmol L^{-1})	Lsi (μmol L^{-1})	C incorporation (μmol L^{-1} day^{-1})	N incorporation (μmol L^{-1} day^{-1})	Bsi net incorporation (μmol L^{-1} day^{-1})	Nitrate (μmol L^{-1})	Phosphate (μmol L^{-1})	Silicic acid (μmol L^{-1})
1	0.58	9.42	1.84	1.12	0.02	1.19	0.04	0.09	3.78	0.96	5.24
2	0.62	9.34	1.83	1.24	0.04	1.27	0.03	0.05	3.60	0.83	4.25
3	0.82	10.96	2.21	1.33	0.03	1.82	0.07	-0.01	4.37	1.11	4.66
4	1.24	12.62	2.50	1.53	0.03	2.20	0.10	0.11	3.40	0.97	4.93
5	1.40	10.62	2.44	0.99	0.01	1.99	0.05	0.28	0.38	0.59	8.94